

9651

NATIONAL LIBRARY  
OTTAWA



BIBLIOTHÈQUE NATIONALE  
OTTAWA

NAME OF AUTHOR... *Kunihiko Takagi* .....

TITLE OF THESIS... *Thermolysis of Azoalkanes* .....

.....

UNIVERSITY... *University of Alberta* .....

DEGREE FOR WHICH THESIS WAS PRESENTED... *Ph.D.* .....

YEAR THIS DEGREE GRANTED... *1971* .....

Permission is hereby granted to THE NATIONAL LIBRARY  
OF CANADA to microfilm this thesis and to lend or sell copies  
of the film.

The author reserves other publication rights, and  
neither the thesis nor extensive extracts from it may be  
printed or otherwise reproduced without the author's  
written permission.

(Signed) *Kunihiko Takagi*

PERMANENT ADDRESS:

*6-2 Kikuzocho*  
*Sho-wa-ku, Nagoya*  
*Japan*

DATED... *July 13* ..... 1971

THE UNIVERSITY OF ALBERTA

THERMOLYSIS OF AZOALKANES

BY



KUNIHICO TAKAGI

A THESIS

SUBMITTED TO THE FACULTY OF GRADUATE STUDIES  
IN PARTIAL FULFILMENT OF THE REQUIREMENTS FOR THE  
DEGREE OF DOCTOR OF PHILOSOPHY

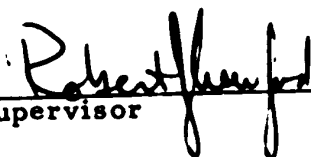
DEPARTMENT OF CHEMISTRY

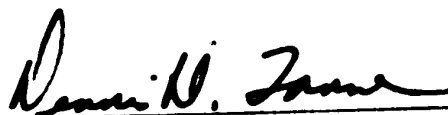
EDMONTON, ALBERTA

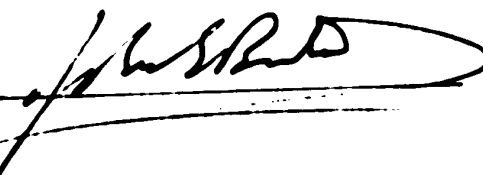
FALL 1971

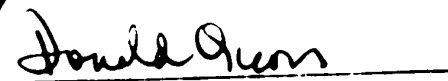
THE UNIVERSITY OF ALBERTA  
FACULTY OF GRADUATE STUDIES


The undersigned certify that they have read, and recommend  
to the Faculty of Graduate Studies for acceptance, a thesis entitled  
THERMOLYSIS OF AZOALKANES  
submitted by Kunihiko Takagi, in partial fulfilment of the requirements  
for the degree of Doctor of Philosophy.

  
Supervisor

  
\_\_\_\_\_

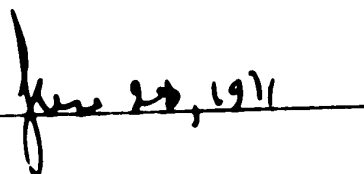
  
\_\_\_\_\_

  
\_\_\_\_\_

  
\_\_\_\_\_

  
External Examiner

Date

  
\_\_\_\_\_

---

**TO MY PARENTS**

## ACKNOWLEDGMENT

The author would like to express his sincere appreciation and gratitude to Dr. Robert J. Crawford, who conceived this research problem, and who gave invaluable guidance and counselling throughout the course of this work.

The author wishes to express his sincere gratitude and appreciation to:

Mr. A. Jodhan for his help with the kinetic apparatus;

Messrs. R. Swindlehurst, J. Hoyle, D. J. Gifford and G. Bigam and Mrs. D. Formanski and M. Tychkowsky for their services in the spectroscopy laboratory;

Mrs. D. Mahlow and A. Dunn for performing the microanalysis;

Dr. A. Hogg and Messrs. A. Budd, D. Morgan and J. Olekszyk for their help with the mass spectrometry;

the technical staff of the Department for various services;

Mrs. G. Conway for her excellent preparation of this manuscript;

the University of Alberta for the financial support;

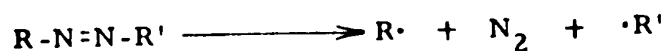
Unitika Co., Ltd. for providing the opportunity to study in the

Faculty of Graduate Studies of the University of Alberta.

## ABSTRACT

Two mechanisms, Scheme A and Scheme B, have been proposed for the thermolysis of azoalkanes.

Scheme A (Concerted cleavage of both carbon-nitrogen bonds)



Scheme B (Two step process)



The unsymmetrical azo compounds, methylazo-3-propene (36), 1-propylazo-3-propene (46) and tert-butylazo-3-propene (47) were studied to decide between the two schemes.

The thermolysis of methylazo-3-propene (36) exhibited the characteristics of a radical chain induced decomposition. Nitric oxide was found to suppress the radical chains and to eliminate methane formation and to decrease the rate of thermolysis. The rate increased slightly with the increasing pressure of nitric oxide, but experiments with  $^{15}\text{NO}$  indicated that ca. 5% of the nitrogen produced came from the nitric oxide. The rate constant was found to be unchanged after correcting for the nitric oxide.

Rate studies of the thermolysis of methylazo-3-propene (36) and 1-propylazo-3-propene (46) were carried out in the optimum nitric oxide to the azo compound ratio of 0.15 to 0.20 where the total nitrogen formed can be used directly to calculate the rates with very little loss of precision. The activation energy and frequency factors were found to be 35.5 kcal mole<sup>-1</sup>,  $10^{14.36}$  sec<sup>-1</sup> for 36

and  $35.6 \text{ kcal mole}^{-1}$ ,  $10^{14.80} \text{ sec}^{-1}$  for 46.

Criteria were proposed to make a choice between Scheme A and Scheme B from the known data for the symmetrical azo compounds and taking steric factors into consideration.

The ratio of the rate constant for 46 to that for 3,3'-azo-1-propene (52) is only 2.96, close to the statistical factor of 2, we may conclude that both compounds are proceeding via the same sequential mechanism. Because of the rather good Polanyi plot observed by Al-Sader and Crawford (6) it also implies that all gas-phase azo compounds thermolyze via the two step sequential mechanism (Scheme B).

Comparing the activation energies found for methylazo-3-propene (36), 1-propylazo-3'-propene (46) and 3,3'-azo-1-propene (52) with that of azoethane the decrease in activation energy,  $12.4 - 13.0 \text{ kcal mole}^{-1}$ , is attributed to a contribution from the allylic resonance energy which is comparable to the values generally accepted.

The secondary deuterium kinetic isotope effect was determined for methylazo-3-propene-3,3-d<sub>2</sub>. The value obtained,  $k_H/k_D = 1.27 - 1.28$  at  $126.00^\circ$  ( $\Delta G^\ddagger = 95 - 98 \text{ cal mole}^{-1}$ ), is consistent with the one bond cleavage mechanism where the transition of the fragmentation occurs late of the reaction coordinate.

## TABLE OF CONTENTS

ACKNOWLEDGMENT	iii
ABSTRACT	iv
LIST OF TABLES	viii
LIST OF FIGURES	xii
INTRODUCTION	1
HISTORICAL	2
RESEARCH OBJECTIVES	52
EXPERIMENTAL	57
(A) Apparatus	58
(B) Procedure	58
(a) Preparation of Samples	58
(b) Reaction Bath	65
(c) Method of Analysis of Products	66
(C) Syntheses	70
(a) Methylazo-3-propene	70
(b) 1-Propylazo-3'-propene	80
(c) <u>tert</u> -Butylazo-3-propene	83
(D) Control Experiments	92
RESULTS AND DISCUSSION	96
(A) Syntheses	96
(B) Products of the Non-inhibited Thermolysis of Methylazo-3-propene and <u>tert</u> -Butylazo-3-propene	102
(C) Kinetics of the Non-inhibited Reactions	117



**Table of Contents - Continued**

<b>(D) Inhibition by Nitric Oxide</b>	<b>124</b>
<b>(E) Allylic Resonance Energy</b>	<b>158</b>
<b>(F) Secondary Deuterium Kinetic Isotope Effects</b>	<b>158</b>
<b>CONCLUSIONS</b>	<b>165</b>
<b>REFERENCES</b>	<b>166</b>
<b>VITA</b>	<b>176</b>

## LIST OF TABLES

Table I	Kinetic parameters for the thermolysis of some azoalkanes.	3
Table II	Rate constants for the thermolysis of bicycloalkyl and tricycloalkyl azo compounds at 300° in benzene (30).	10
Table III	Rate constants of the thermolysis of unsymmetrical azoalkanes R-N=N-R' in benzene at 300° (31).	11
Table IV	Values of $\Delta G^\ddagger$ for the thermolysis of bridgehead azoalkanes compared with predicted values (kcal mole <sup>-1</sup> ).	12
Table V	Rate constants for the thermolysis of azo nitriles, RR'(CN)-N=N-C(CN)RR', in toluene at 80.2° (32, 33, 35).	14
Table VI	Thermolysis rate constants of 1-azo-bis-1-phenylalkanes C <sub>6</sub> H <sub>5</sub> CHR-N=N-CHRC <sub>6</sub> H <sub>5</sub> at 100.4° (34).	15
Table VII	Rate constants for the thermolysis of $\alpha$ -alkyl- and dialkylazoalkanes, C <sub>6</sub> H <sub>5</sub> RR'C-N=N-CRR'C <sub>6</sub> H <sub>5</sub> in diphenyl ether at 120° (20).	16
Table VIII	Comparison of rate constants for <u>meso</u> - and <u>rac</u> -azoalkanes, R-N=N-R.	20
Table IX	Longest wavelength absorption bands for <u>trans</u> -azoalkanes R-N=N-R (40).	21
Table X	Limiting rates for different inhibitors in some thermolysis processes (53).	27

## List of Tables - Continued

Table XI	Radical deuterium isotope effects.	35
Table XII	Allylic resonance energies obtained from thermolyses of vinyl-substituted compounds.	44
Table XIII	Allylic resonance energies (ARE) obtained from the heat of formation of the allyl radical $\Delta H_f^\circ$ (allyl).	51
Table XIV	Prediction of relative rates using mechanistic criteria.	54
Table XV	Calibration of the volume of the manifold.	60
Table XVI	Calibration of the volume of the Bourdon gauge.	60
Table XVII	Calibration of the pressure of the Bourdon gauge.	61
Table XVIII	Relative retention time data.	71
Table XIX	Mass spectrometric analyses of some control experiments.	93
Table XX	Reaction of 1-butene with nitric oxide.	94
Table XXI	Product composition in the thermolysis of methylazo-3-propene ( <u>36</u> ) (57 torr) at 131.6°.	103
Table XXII	Mass spectral data of the thermolysis products of methylazo-3-propene ( <u>36</u> ).	105
Table XXIII	Product composition in the thermolysis of methylazo-3-propene ( <u>36</u> ) in the presence of xenon at 131.6°.	110
Table XXIV	Product composition in the thermolysis of <u>tert</u> -butylazo-3-propene ( <u>47</u> ) at 122.3°.	113

## List of Tables - Continued

Table XXV	Mass spectral data of the thermolysis products of <u>tert</u> -butylazo-3-propene (47).	115
Table XXVI	Rate constants and activation parameters for the thermolysis of methylazo-3-propene (36).	121
Table XXVII	Rate measurement of the thermolysis of methylazo-3-propene (36) at 131.6°.	122
Table XXVIII	Rate measurement of the thermolysis of methylazo-3-propene (36) in the presence of xenon at 131.6°. $Xe/[36]^0 = 4.8$ .	123
Table XXIX	Rate measurement of the thermolysis of <u>tert</u> -butylazo-3-propene (47) at 122.3°.	125
Table XXX	Recovery of unreacted methylazo-3-propene (36).	128
Table XXXI	Mass spectrometric analysis from the runs of methylazo-3-propene (36) with $^{15}NO$ at 126.35° for 90 minutes.	130
Table XXXII	Surface effects on the inhibited thermolysis of methylazo-3-propene (36) at 126.00° for 90 minutes. $^{15}NO/[36]^0 = 0.170$ .	136
Table XXXIII	Rate constants for the inhibited thermolysis of methylazo-3-propene (36) at various total pressures at 129.29°.	137
Table XXXIV	Inhibited thermolysis of methylazo-3-propene (36).	139
Table XXXV	Rate constants and activation parameters for the thermolysis of methylazo-3-propene (36) in the presence of nitric oxide. Pressure range 50-60 torr.	142

## List of Tables - Continued

Table XXXVI	Inhibited thermolysis of 1-propylazo-3'-propene ( <u>46</u> ).	143
Table XXXVII	Rate constants and activation parameters for the thermolysis of 1-propylazo-3'-propene ( <u>46</u> ) in the presence of nitric oxide. Pressure range 50-60 torr.	145
Table XXXVIII	Mass spectrometric analysis of nitrogen produced during the thermolysis of 1-propyl-azo-3'-propene ( <u>46</u> ) with $^{15}\text{NO}$ .	146
Table XXXIX	Rate constants for the thermolysis of 3,3'-azo-1-propene ( <u>52</u> ) at $100.73^\circ$ .	147
Table XL	Inhibited thermolysis of <u>tert</u> -butylazo-3-propene ( <u>47</u> ).	150
Table XLI	Rate constants and activation parameters for the thermolysis of <u>tert</u> -butylazo-3-propene ( <u>47</u> ) in the presence of nitric oxide. Pressure range 50-60 torr.	151
Table XLII	Reaction of 2-methyl-2-nitrosopropane ( $7.22\mu\text{moles}$ ) with $^{15}\text{NO}$ ( $29.2\mu\text{moles}$ ).	152
Table XLIII	Kinetic parameters for azoalkane thermolysis.	155
Table XLIV	Inhibited thermolysis with $^{15}\text{NO}$ of methylazo-3-propene ( <u>36</u> ) and methylazo-3-propene- <u>3,3-d</u> <sub>2</sub> ( <u>43</u> ) at $126.00^\circ$ .	160
Table XLV	Secondary kinetic isotope effects for $\alpha$ -deuterated methylazo-3-propene at $126.00^\circ$ .	163

## LIST OF FIGURES

Figure 1	Dependence of the rate of formation of cyclic carbonium ions and radicals on the ring size (2, 36).	17
Figure 2	Linear relation between free energies of thermolysis and solvolysis of bridgehead compounds. Thermolysis of R-N=N-R at 300° in benzene. Solvolysis of RBr in 80% ethanol at 25° (2).	18
Figure 3	Characteristic inhibition curves (53).	25
Figure 4	Inhibition curves for 100 mm n-pentane at 560° (52).	25
Figure 5	Graphical representation of the basis for making the decision between Scheme A and Scheme B.	56
Figure 6	Schematic diagram of the vacuum rack.	59
Figure 7	Break-seal connected to a glass tube for thermolysis.	64
Figure 8	Break-seal for mass spectrometric analysis of nitrogen.	64
Figure 9	Nmr spectrum of diethyl N-allylbicarbamate (38).	73
Figure 10	Nmr spectrum of diethyl N-methylbicarbamate (39).	73
Figure 11	Nmr spectrum of diethyl N allyl-N'-methylbicarbamate (37).	73
Figure 12	Nmr spectrum of methylazo-3-propene (36).	77
Figure 13	Nmr spectrum of 1-allyl-2-methylhydrazine hydrochloride.	77

## List of Figures - Continued

Figure 14	Nmr spectrum of diethyl N-(allyl- <u>1,1-d<sub>2</sub></u> )-N'-methylbicarbamate (44).	77
Figure 15	Nmr spectrum of methylazo-3-propene- <u>3,3-d<sub>2</sub></u> (43).	81
Figure 16	Nmr spectrum of diethyl N-allyl-N'-(1-propyl)-bicarbamate (45).	81
Figure 17	Nmr spectrum of 1-propylazo-3'-propene (46).	81
Figure 18	Nmr spectrum of <u>tert</u> -butyl hydrazine hydrochloride.	85
Figure 19	Nmr spectrum of dimethyl N- <u>tert</u> -butylbicarbamate.	85
Figure 20	Nmr spectrum of 1- <u>tert</u> -butyl-2-carbomethoxyhydrazine.	85
Figure 21	Nmr spectrum of dimethyl N-allyl-N'- <u>tert</u> -butylbicarbamate (49).	88
Figure 22	Nmr spectrum of 1-allyl-2- <u>tert</u> -butylhydrazine hydrochloride.	88
Figure 23	Nmr spectrum of <u>tert</u> -butylazo-3-propene (47).	88
Figure 24	Temperature dependence of the peak corresponding to the ester methyl in dimethyl N-allyl-N'- <u>tert</u> -butyl-bicarbamate (49) in dimethyl sulfoxide.	89
Figure 25	100 Mc nmr spectrum of methylazo-3-propene- <u>3,3-d<sub>2</sub></u> (43) recovered after the inhibited thermolysis with <sup>15</sup> NO.	95
Figure 26	Product composition from the thermolysis of methylazo-3-propene (36), 57 torr at 131.6°.	104

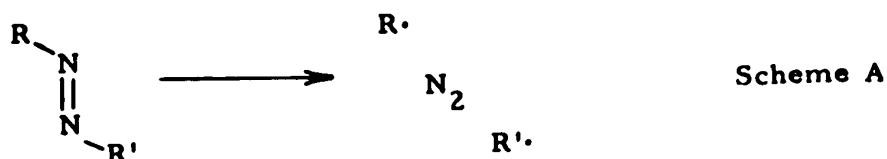
## List of Figures - Continued

- Figure 27 Product composition from the thermolysis of methylazo-3-propene (36), 9 torr in the presence of xenon, 46 torr at  $131.6^{\circ}$ . 111
- Figure 28 Product composition from the thermolysis of tert-butylazo-3-propene (47), 46 torr at  $122.3^{\circ}$ . 114
- Figure 29 Plot of  $\log (E_{\infty} - E_t)$  versus time for the thermolysis of methylazo-3-propene (36) at  $182.8^{\circ}$ . 119
- Figure 30 Inhibited thermolysis of methylazo-3-propene (36) with nitric oxide at  $125.9^{\circ}$  for 100 minutes. 127
- Figure 31 Plot of  $10^6 k_1^{\text{tot}}$  versus  $[^{15}\text{NO}]^{\circ} / [36]^{\circ}$  showing the best line from least square data. 133
- Figure 32 Plot of  $-\log (1 - N_2 / [36]^{\circ})$  versus time for the inhibited thermolysis of methylazo-3-propene (36) at  $129.52^{\circ}$ . 141
- Figure 33 Plot of  $-\log (1 - \frac{[^{15}\text{N}_2]}{[N_2]} \frac{[N_2^{\text{tot}}]}{[47]})$  versus time for the inhibited thermolysis of tert-butylazo-3-propene (47) at  $90.90^{\circ}$ . 148
- Figure 34 Choice between Scheme A and Scheme B. 157
- Figure 35 Nitric oxide inhibited thermolysis of 36 and 43. 162

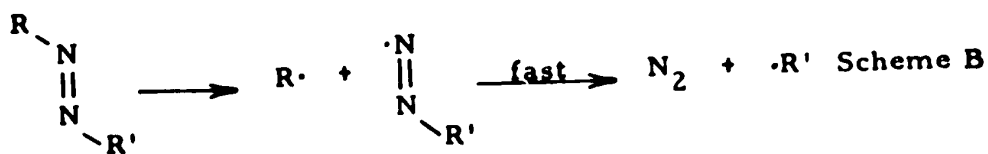


## INTRODUCTION

Azoalkanes have been used for many years as a convenient source of alkyl radicals, and for almost as many years chemists have pondered the details of the initial reaction (1). Two schemes have outlasted all others, and the choice between these has been made by many but proven by few. A review, presenting a strong case for the simultaneous cleavage of both carbon-nitrogen bonds in the rate determining step (Scheme A), has recently appeared (2).



Almost simultaneously the alternative two-step process (Scheme B) has been supported in the literature (3) by an analysis of the existing kinetic and thermodynamic data. Even more



recently there has appeared a communication (4) wherein the authors claim to have trapped the hitherto elusive intermediate  $\text{R}'\text{-N}=\text{N}\cdot$ . In the first chapter of this thesis we hope to examine critically the more cogent arguments for both mechanisms, and to briefly review the mechanistic relevance of some of the techniques used. While criticism tends to be negative and eroding we attempt in later chapters to construct systems and evidence to support a choice between Schemes A and B.

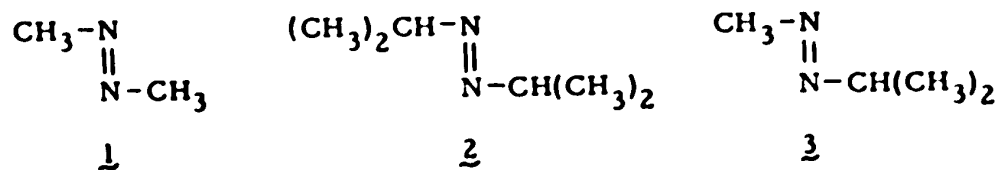
## HISTORICAL

Azomethane, the simplest of the azoalkanes, is a relatively stable material which decomposes at elevated temperatures (ca 300°) to produce nitrogen and a variety of hydrocarbons (5). When  $\alpha$ -substituents, capable of stabilizing the resulting radicals, are introduced the homolytic cleavage occurs more rapidly. This is quantitatively exemplified by a good Polanyi plot for the thermolysis of azoalkanes (6). The activation energy, from the thermolysis of symmetrical azoalkanes,  $R-N=N-R$ , correlates with the bond dissociation energy,  $D(R-H)$ , of the corresponding alkane,  $R-H$ .

$$E_a = 0.996 D(R-H) - 48.4 \text{ kcal mole}^{-1}$$

Although the near unity value of the slope in the aforementioned Polanyi plot makes the interpretation of a single bond cleavage reaction, Scheme B, attractive it proves nothing since slopes varying from 0.49 to 1.1 have been observed for various hydrogen atom abstraction processes (7).

The earliest kinetic work addressed directly to deciding between Scheme A and Scheme B is that of H. C. Ramsperger (8) who in 1929 compared the activation parameters for 1, 2 and 3, and



as seen from data in Table I was led to conclude that: "The heat of activation of the new compound (3) is intermediate between that

Table 1. Kinetic parameters for the thermalolysis of some azalanes.

Compound	Solvent	Inhibitor	$E_a$ kcal mole <sup>-1</sup>	$\log A$ at 120°	$\Delta S^\ddagger$ e.u. <sup>a</sup>	$k$ , sec <sup>-1</sup>	$k$ , sec <sup>-1</sup> at 120°	Reference
1. CH <sub>3</sub> -N=N-CH <sub>3</sub>	Gas phase	None	51.2	16.0	12.1	$4.6 \times 10^{-5}$ (275.9°)	$2 \times 10^{-13}$	9
2. CH <sub>3</sub> -N=N-CH <sub>3</sub>	Gas phase	None	50.2	15.9	11.7		$8 \times 10^{-13}$	9b
3. CH <sub>3</sub> -N=N-CH <sub>3</sub>	Gas phase	CH <sub>3</sub> CH=CH <sub>2</sub>	51.2	15.7	10.0	$2.2 \times 10^{-5}$ (276.3°)	$1 \times 10^{-13}$	10a
4. CH <sub>3</sub> -N=N-CH <sub>3</sub>	Gas phase	NO	55.5	17.2	19.0	$1.51 \times 10^{-5}$ (275.9°)	$2 \times 10^{-14}$	11
		CH <sub>3</sub> CH=CH <sub>2</sub>				$2.25 \times 10^{-5}$ (275.9°)		
		CH <sub>2</sub> =CH <sub>2</sub>				$2.55 \times 10^{-5}$ (275.9°)		
5. CD <sub>3</sub> -N=N-CD <sub>3</sub>	Gas phase	NO	50.7	15.99	9.0	$1.50 \times 10^{-5}$ (275.6°)	$2 \times 10^{-13}$	12
6. CH <sub>3</sub> CH <sub>2</sub> -N=N-CH <sub>2</sub> CH <sub>3</sub>	Gas phase	Toluene	48.5	15.0	11.2		$6 \times 10^{-12}$	13
7. CH <sub>3</sub> CH <sub>2</sub> -N=N-CH <sub>2</sub> CH <sub>3</sub>	Gas phase	None	47.2	15.11	0.0		$6 \times 10^{-12}$	14
8. (CH <sub>3</sub> ) <sub>2</sub> CH-N=N-CH <sub>3</sub>	Gas phase	None	47.5	15.45	12.6		$1 \times 10^{-11}$	8
9. CH <sub>3</sub> CH <sub>2</sub> CH <sub>2</sub> -N=N-CH <sub>2</sub> CH <sub>2</sub> CH <sub>3</sub>	Gas phase	None	45.7	14.60	5.7		$2 \times 10^{-11}$	15
	Flow system	None	47.7	15.00	9.4		$0 \times 10^{-12}$	15
10. (CH <sub>3</sub> ) <sub>2</sub> CH-N=N-CH(CH <sub>3</sub> ) <sub>2</sub>	Gas phase	None	40.0	13.60	1.3		$1 \times 10^{-9}$	15
	Flow system	None	40.9	13.09	2.5		$1 \times 10^{-9}$	15
11. (CH <sub>3</sub> ) <sub>2</sub> CH-N=N-CH(CH <sub>3</sub> ) <sub>2</sub>	Gas phase	None	40.9	13.75	1.0	$1.07 \times 10^{-3}$ (190°)	$3 \times 10^{-8}$	16
12. (CH <sub>3</sub> ) <sub>2</sub> C=N-N-C(CH <sub>3</sub> ) <sub>3</sub>	Gas phase	None	42.0	16.34	13.7	$1.19 \times 10^{-3}$ (190°)		17
13. C <sub>6</sub> H <sub>5</sub> -CH <sub>2</sub> -N=N-CH <sub>2</sub> -C <sub>6</sub> H <sub>5</sub>	Gas phase	None	39.0	14.09	3.3		$4.2 \times 10^{-6}$	18
14. C <sub>6</sub> H <sub>5</sub> -CH(CH <sub>3</sub> )-N=N-CH(CH <sub>3</sub> )-C <sub>6</sub> H <sub>5</sub>	Diphenyl ether	None	36.5	15.36	9.2		$1.1 \times 10^{-5}$	19
15. C <sub>6</sub> H <sub>5</sub> -CH(CH <sub>3</sub> )-N=N-CH(CH <sub>3</sub> )-C <sub>6</sub> H <sub>5</sub>	Ethylbenzene	None	32.6	14.08	7.0		$5.6 \times 10^{-4}$	21
16. (C <sub>6</sub> H <sub>5</sub> ) <sub>2</sub> CH-N=N-C <sub>6</sub> H <sub>5</sub>	Decalin	None	34.0	14.22	4.0		$2.0 \times 10^{-5}$	21
17. (C <sub>6</sub> H <sub>5</sub> ) <sub>2</sub> C=N-N-C <sub>6</sub> H <sub>5</sub>	Toluene	None	27.0	14.45	3.0		$2.0 \times 10^{-1}$	22
18. (C <sub>6</sub> H <sub>5</sub> ) <sub>2</sub> C=N-N-C <sub>6</sub> H <sub>5</sub>	Toluene	None	27.4	14.72	6.3		$3.1 \times 10^{-1}$	23
19. (C <sub>6</sub> H <sub>5</sub> ) <sub>2</sub> CH-N=N-CH(C <sub>6</sub> H <sub>5</sub> ) <sub>2</sub>	Toluene	None	24.6	13.77	1.9		$9.3 \times 10^{-2}$	24

<sup>a</sup>  $\Delta S^\ddagger$  are calculated according to the following equation.

$$\Delta S^\ddagger = 2.303 R \log \frac{A \cdot h}{h' \cdot T_0} = 0.576 (\log A - 10.3271 - \log T - 0.0503)$$

$$= 0.976 (\log A - 13.35)$$

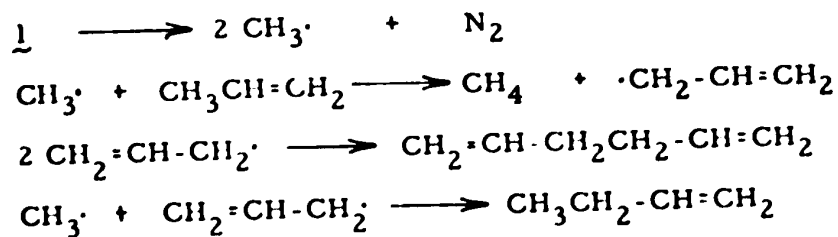
<sup>b</sup>  $k$ 's are calculated according to the following equation.

$$\log h = \log A - \frac{E_a}{2.303 R T} = \log A - \frac{E_a}{1.799}$$

for dimethyl diimide (1) and di-isopropyl diimide (2) . . . .

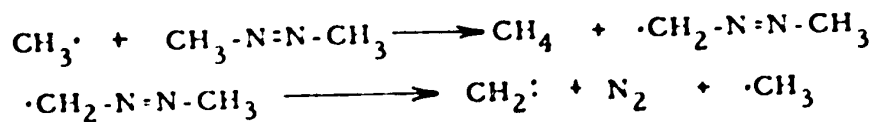
If the reaction occurs by the simultaneous rupture of both bonds, then we may expect an intermediate heat of activation, and this is the experimental result " , the value  $47.7 \text{ kcal mole}^{-1}$ , for 3, being slightly larger than the arithmetic mean of the then accepted values of  $51.2$  and  $40.9 \text{ kcal mole}^{-1}$  for 1 and 2.

Azomethane proved to be an attractive molecule to gas-phase kineticists and further studies upon it were undertaken (9). The advent of gas chromatography made available detailed product studies and with these the realization that the earlier studies on 1 had a contribution from a chain induced decomposition (10). Propylene has been used as an inhibitor of the chain induced decomposition. The initially produced methyl radicals abstract an allylic hydrogen and the much less reactive allyl radicals dimerize



to form 1,5,-hexadiene or react with methyl radicals to give 1-butene (10a).

Forst has recently completed a study of the uninhibited azomethane decomposition (5) and suggests that the chain propagating reactions are:



The formation of methylene is a major factor complicating the product mixture. Saturated and unsaturated hydrocarbons having 1, 2 and 3 carbons are produced along with hydrazines and higher molecular weight azo compounds. Forst and Rice (11) have used nitric oxide gas as an inhibitor of the azomethane chain. The nitric oxide gas traps the initially produced methyl radicals,



and while this has the advantage that the failure to produce methane will indicate the efficiency of the scavenger, disadvantages arise from complications of the nitrosomethane (see subsequent discussion on the use of nitric oxide). Inhibitor addition has shown that the earlier rate studies were in error, e.g. in Table I we see that the rate constant for uninhibited azomethane decomposition is three times larger, at 275.9°, than the rate constant measured in the presence of nitric oxide. The earlier reaction parameters tended to be too low for  $E_a$  and  $\log A$ . A good value for azomethane seems difficult to select since Chang and Rice have studied azomethane- $d_6$  (12) and have repeated some of the experiments of Forst and Rice (11) but prefer an activation energy of 50 kcal mole<sup>-1</sup>. It would appear that most azoalkane studies suffer from chain induced decomposition reactions and that only a few e.g. 2,2'-azoisobutane (no  $\alpha$ -hydrogens) (17) and azoethane (13, 14) because it was obtained to low conversion are likely to be reliable for further interpretation. Systems such as azoisopropane, which Ramsperger (16) studied have  $\alpha$ -hydrogens that are tertiary in nature and would be expected

to be very sensitive to chain induced decomposition, and thus it seems probable that Ramsperger's arguments for a simultaneous rupture of both carbon-nitrogen bonds in azoalkane were made using faulty data.

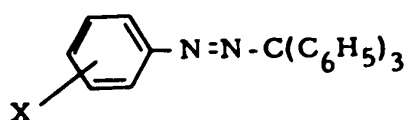
Substitution upon the  $\alpha$ -carbon stabilizes the radicals produced and brings about a decrease in activation energy. The phenyl group is particularly significant in this regard for if we compare azotoluene ( $E_a = 35.0 \text{ kcal mole}^{-1}$ ) (18) with azoethane ( $E_a = 48 \text{ kcal mole}^{-1}$ ) we see that the activation energy decreases  $13 \text{ kcal mole}^{-1}$ . If Scheme A is the true mechanism we have a decrease in activation energy ( $\delta E_a$ ) of  $6.5 \text{ kcal mole}^{-1}$  per phenyl. If Scheme B is the true representation then  $\delta E_a$  is  $13 \text{ kcal mole}^{-1}$  per phenyl since only one phenyl group is intimately involved. Temperature, vapor pressure and the practical limits upon the ease of measurement of rates have forced the majority of large azoalkane thermolysis rates to be measured in solution. For an unimolecular reaction the rate constants should be about the same in the gas and solution (25).

Overberger and DiGiulio (20) have argued on the basis of the comparison of entries 14, 15 and 11 in Table I that the replacement of a methyl by a phenyl resulted in a  $4 \text{ kcal mole}^{-1}$  decrease in  $E_a$ , and that subsequent replacement of a pair of methyls by a pair of phenyls (compare 11 and 15) produced  $8 \text{ kcal mole}^{-1}$  decrease, an additivity effect, and hence Scheme A. The authors did not discuss their value of  $4 \text{ kcal mole}^{-1}$  relative to that observed above of



of the interdependency by carrying out deuterium kinetic isotope effect studies. These studies support their conclusion that 6 is cleaved by Scheme A and 4 by Scheme B (see later section secondary deuterium kinetic isotope effects).

Cohen and coworkers (23, 27) determined the rates of thermolysis of a series of m- and p-substituted phenylazotriphenylmethanes.



X = p-H, CH<sub>3</sub>, NO<sub>2</sub>, HO, CH<sub>3</sub>O,  
CH<sub>3</sub>CONH

and X = m-CH<sub>3</sub>, Br and NO<sub>2</sub>

All substituents listed, except methyl, caused thermolysis to occur more slowly than the parent compound. They concluded that Scheme A was applicable and discussed the substituent effects in terms of the resonance stabilization of the reactants and destabilization of the phenyl radicals by electron withdrawal. David, Hay and Williams (22) discussed the same series in terms of Scheme B and concluded that the formation of the phenylazo and triphenylmethyl radical was rate determining and discussed the substituent effects in terms of resonance and solvation phenomena. Recently Pryor and Smith (29) provided evidence that p-nitrophenylazotriphenylmethane decomposes by the scission of one carbon-nitrogen bond at a time. This they achieved by studying the rate-viscosity relationship of homolytic process and concluded that the unsymmetrical azo compound displayed "internal radical return".



Rüchardt and Oberlinger (30) studied the thermolysis of bridgehead linked bicyclo- and tricycloalkylazo compounds. As is shown in Table II the ring system has less influence on the thermolysis of tricycloalkylazo-tert-butanes 14 to 16 than the corresponding symmetrical azo compounds 8 to 12 in agreement with simultaneous but non-uniform cleavage of both C-N bonds in the course of thermolysis. The cleavage of the N-tert-butyl bond is certainly much advanced than that of the other C-N bond in the transition state. Further studies of series of unsymmetrical bridgeheads azoalkanes (Table III) have indicated that the homolytic azo-fragmentation is becoming less and less symmetrical when the two attached groups have different C-N bond energies (31). It is of particular interest to note that the free energy of activation,  $\Delta G^\ddagger$ , for the mixed azo compound R-N=N-R' is close to the arithmetic mean of R-N=N-R and R'-N=N-R' (Table IV). Ideally one should compare  $\Delta H^\ddagger$  values but the rates have been reported at only one temperature.

#### Steric Effects Upon Azoalkane Thermolysis

Steric factors play an important role in the thermolysis of hindered and cyclic azo compounds. The steric effects on the thermolysis rate were first demonstrated by Overberger and co-workers (32, 33, 35) utilizing a series of azonitriles with the structure

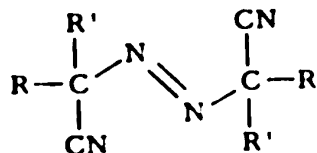




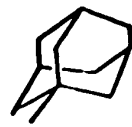


Table II. Rate constants for the thermolysis of bicycloalkyl and tricycloalkyl azo compounds at 300° in benzene (30).

R	R-N=N-R *		R-N=N-C(CH <sub>3</sub> ) <sub>3</sub>	
	No.	k <sub>1</sub> (rel.)	No.	k <sub>1</sub> (rel.)
(CH <sub>3</sub> ) <sub>3</sub> C-	(7)	1	(13)	1
	(8)	1.98 x 10 <sup>-6</sup>	(14)	4.64 x 10 <sup>-3</sup>
	(9)	3.51 x 10 <sup>-5</sup>		
	(10)	3.67 x 10 <sup>-5</sup>		
	(11)	5.06 x 10 <sup>-5</sup>	(15)	2.04 x 10 <sup>-2</sup>
	(12)	4.02 x 10 <sup>-4</sup>	(16)	4.36 x 10 <sup>-2</sup>

\* While all of the acyclic azo compounds are considered to have the trans configuration there is no evidence for, or against, the involvement of cis azo compound in the thermolysis reaction.

**Table III.** Rate constants of thermolysis of unsymmetrical bridgehead azoalkanes  $R-N=N-R'$  in benzene at  $300^\circ \cdot 10^4$  ( $\text{sec}^{-1}$ ) (31).













$R'$ \ $R$	$(\text{CH}_3)_3\text{C}-$			
$(\text{CH}_3)_3\text{C}-$	15715	687	321	73
		623		0.28
			0.80	0.128
				0.031

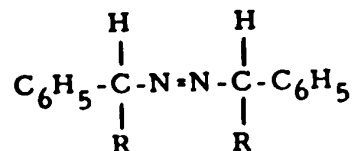
Table IV. Values of  $\Delta G^\ddagger$  for the thermolysis of bridgehead azoalkanes compared with predicted values (kcal mole<sup>-1</sup>).

		R			
R'		$(\text{CH}_3)_3\text{C}-$			
$(\text{CH}_3)_3\text{C}-$		33.7	37.3 (38.2)	38.1 (39.4)	39.9 (41.2)
			42.7	-----	46.2 (45.7)
				45.0	47.1 (46.9)
					48.7

The values in brackets are those obtained as an average from the two symmetrical azoalkanes (see text).

where R and R' are alkyl substituents. When R and R' were methyl, ethyl, isopropyl or tert-butyl similar rates were observed, indicating there was probably no change in the transition state. However, when branching was introduced on carbon  $\gamma$  - to the azo linkage (R and/or R' are isobutyl or neopentyl), a striking rate enhancement was observed (Table V). This effect was attributed to frontal or "F" strain, since models show considerable interaction between the two halves of the molecules in the more stable trans configuration.

In the series



where R = methyl, ethyl and isobutyl, the size of R groups had only a small but noticeable effect on the rate of decomposition (34) (Table VI). Some further examples of steric factors are exemplified in Table VII. While the difference between entry 1 and 2 may be rationalized on an electromeric basis a difference of the same magnitude exists between 2 and 4 and this would be difficult to attribute to electromeric effects (20). Further examples of steric factors contributing to thermolysis rates are exemplified in Figures 1 and 2 (36, 2), and are compared graphically with processes known to be effected by steric parameters.

Steric effects on the thermolysis rate recently have been demonstrated in the azonorborene system. Hinz and Ruchardt (37)

Table V. Rate constants for the thermolysis of azo nitriles,  $RR'(CN)C-N=N-C(CN)RR'$ , in toluene at  $80.2^\circ$  (32, 33, 35).

R	R'	$10^4 k$ (sec $^{-1}$ )	R	R'	$10^4 k$ (sec $^{-1}$ )
CH <sub>3</sub>	CH <sub>3</sub>	1.72 - 1.60	CH <sub>3</sub>	C <sub>2</sub> H <sub>5</sub>	1.72
C <sub>2</sub> H <sub>5</sub>	C <sub>2</sub> H <sub>5</sub>	0.94 - 0.80	CH <sub>3</sub>	n-C <sub>3</sub> H <sub>7</sub>	0.94
n-C <sub>3</sub> H <sub>7</sub>	n-C <sub>3</sub> H <sub>7</sub>	1.74 - 1.65	CH <sub>3</sub>	iso-C <sub>3</sub> H <sub>7</sub>	1.03
iso-C <sub>3</sub> H <sub>7</sub>	iso-C <sub>3</sub> H <sub>7</sub>	1.25	CH <sub>3</sub>	n-C <sub>4</sub> H <sub>9</sub>	1.58
n-C <sub>4</sub> H <sub>9</sub>	n-C <sub>4</sub> H <sub>9</sub>	1.58	CH <sub>3</sub>	<u>tert</u> -C <sub>4</sub> H <sub>9</sub>	0.77
iso-C <sub>4</sub> H <sub>9</sub>	iso-C <sub>4</sub> H <sub>9</sub>	49.5	CH <sub>3</sub>	iso-C <sub>4</sub> H <sub>9</sub>	10.0
iso-C <sub>3</sub> H <sub>5</sub>	C <sub>2</sub> H <sub>5</sub>	0.95	CH <sub>3</sub>	n-C <sub>4</sub> H <sub>9</sub>	1.63
			CH <sub>3</sub>	CH <sub>2</sub> -C(CH <sub>3</sub> ) <sub>3</sub> <sup>a</sup>	158
			CH <sub>3</sub>	CH <sub>2</sub> -C(CH <sub>3</sub> ) <sub>3</sub> <sup>a</sup>	136

<sup>a</sup> stereo isomers

Table VI. Thermolysis rate constants of 1-azo-bis-1-phenylalkanes  $C_6H_5CHR-N=N-CHRC_6H_5$  in ethylbenzene at  $100.4^\circ$  (34).

R	$10^5 k$ (sec <sup>-1</sup> )
CH <sub>3</sub>	5.45
C <sub>2</sub> H <sub>5</sub>	2.35
iso-C <sub>4</sub> H <sub>9</sub>	7.6

Table VII. Rate constants for the thermolysis of  $\alpha$ -alkyl- and dialkylazoalkanes,  $C_6H_5RR'C-N=N-CRR'C_6H_5$  in diphenyl ether at  $120^\circ$  (20).

	R	R'	$10^4 k$ (sec <sup>-1</sup> )	Rel. Rate
1	CH <sub>3</sub> -	H	0.132	0.125
2	CH <sub>3</sub> -	CH <sub>3</sub> -	1.06	1.00
3	C <sub>2</sub> H <sub>5</sub> -	C <sub>2</sub> H <sub>5</sub> -	0.78	0.73
4	CH <sub>3</sub> -	(CH <sub>3</sub> ) <sub>2</sub> CH-CH <sub>2</sub> -	8.51	8.03



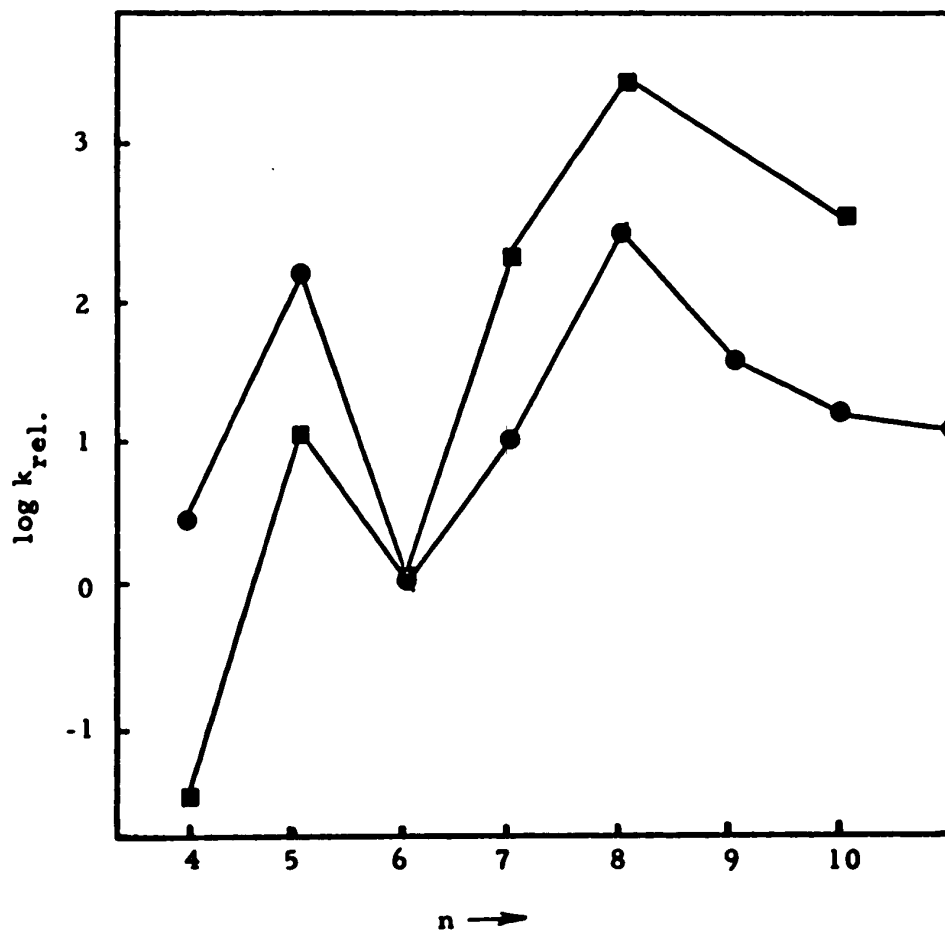
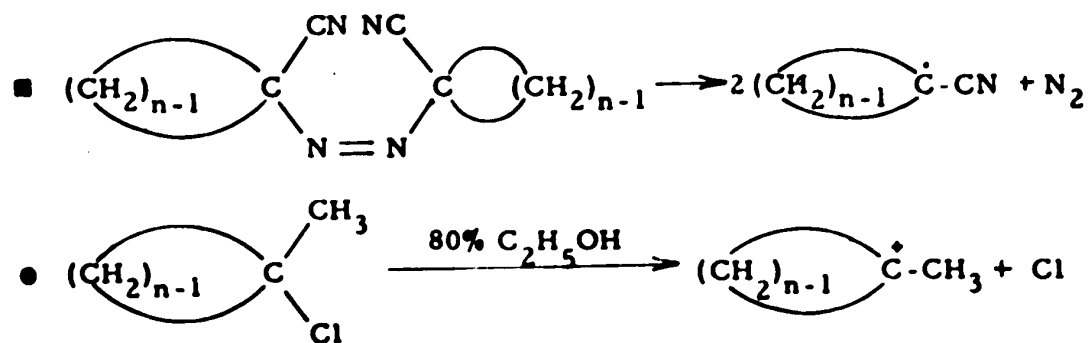


Figure 1. Dependence of the rate of formation of cyclic carbonium ions and radicals on the ring size.  $n$ : number of ring members (2, 36).



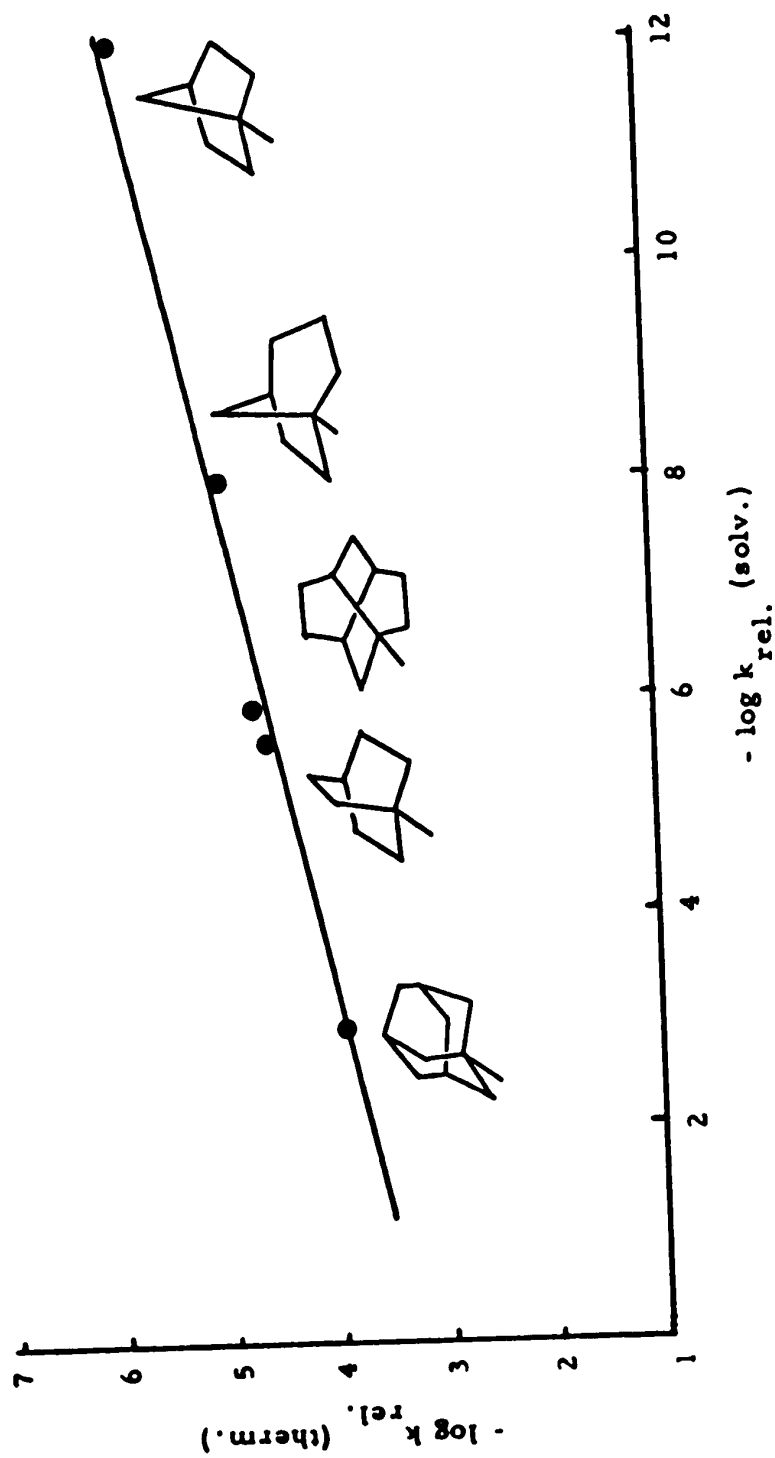
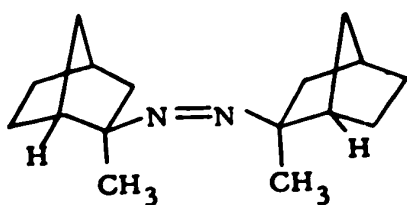
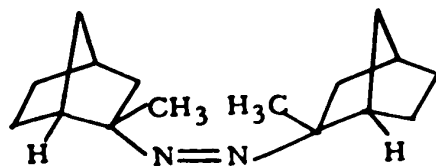


Figure 2. Linear relation between free energies of thermolysis and solvolysis of bridgehead compounds. Thermolysis of R-N=N-R at 300°C in benzene. Solvolysis of RBr in 80% ethanol at 25° (2).

synthesized and thermolyzed exo- and endo-2,2'-dimethyl-2-azonorbornane. They found that 17 thermolyzed 68 times as rapidly as 18. They suggested that difference in the rates comes from the torsional strain required to allow the methyl group in 18 to swing into the planar arrangement for the thermolysis transition state.



17



18

A subtle form of steric effects that has been observed on these occasions is the difference in the rate of stereoisomers. Table VIII lists the rate comparisons observed for meso and rac-azoalkanes.

Severn and Kosower have studied the ultraviolet spectra of several azo compounds, Table IX, and have attributed the different values of the  $n - \pi^*$  transition to steric hindrance in the ground state (40).

Table VIII. Comparison of rate constants for meso- and rac-azoalkanes, R-N=N-R.

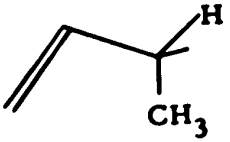
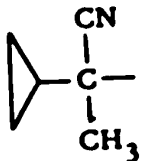
R	T <sup>o</sup>	Ratio of rates	Reference
$\begin{array}{c} \text{C}_6\text{H}_5 \\   \\ \text{C}_6\text{H}_5\text{CH}_2-\text{C}- \\   \\ \text{H} \end{array}$	106	1.17	38
$\begin{array}{c} \text{CH}_3 \\   \\ (\text{CH}_3)_3\text{C}-\text{CH}_2-\text{C}- \\   \\ \text{CN} \end{array}$	80.2	1.16	35
	125	1.2	39
$\begin{array}{c} \text{CN} \\   \\ (\text{CH}_3)_3\text{C}-\text{C}- \\   \\ \text{CH}_3 \end{array}$	79.9	1.42	33
	44.2	1.12	33
$\begin{array}{c} \text{CN} \\   \\ (\text{CH}_3)_2\text{CH}-\text{CH}_2-\text{C}- \\   \\ \text{CH}_3 \end{array}$	69.9	1.46	33

Table IX. Longest wavelength absorption bands for trans-azoalkanes R-N=N-R (40).

R	Solvent	$\lambda_{\max}$	$\epsilon_{\text{mn}}$
CH <sub>3</sub> -	gas	340	5
	water	343	2
CH <sub>3</sub> , C <sub>2</sub> H <sub>5</sub>	gas	346	6.4
	water	356	15
(CH <sub>3</sub> ) <sub>3</sub> CH-	gas	356	8
(CH <sub>3</sub> ) <sub>3</sub> C-	isooctane	367	13.5
C <sub>6</sub> H <sub>5</sub> C(CH <sub>3</sub> )(C <sub>2</sub> H <sub>5</sub> )	isooctane	376	36
C <sub>6</sub> H <sub>11</sub> <sup>a</sup> C(CH <sub>3</sub> )(C <sub>2</sub> H <sub>5</sub> )	isooctane	380	22
1-C <sub>10</sub> H <sub>15</sub> <sup>b</sup> -	isooctane	368	16

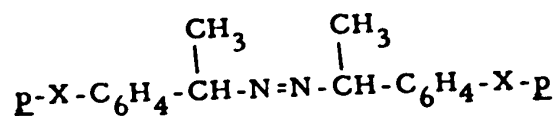
<sup>a</sup> Cyclohexyl.

<sup>b</sup> 1-adamantyl.

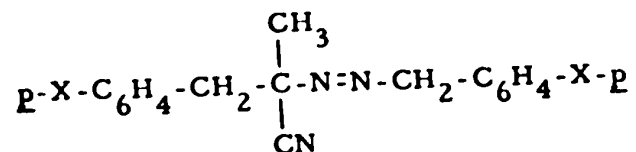
### Polar Effects

It is well known that polar factors play an important role in the decomposition of peroxides (41 - 44). However, little is known about polar effects on the decomposition of azo compounds.

In the decomposition of 1-azo-bis-1-phenylethane (34)

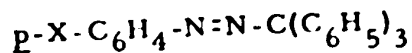


the substituents methyl and methoxy led to small (ca. 8 and 30%) increases in rate, indicating that the radicals are stabilized by electron donation which tends toward completion of an octet. The substituents chlorine and nitro led to a small decrease (ca. 24 and 14%) in the rates of thermolysis of azo compounds of structure



in agreement with the known poor transmission of electronic effects by methylene groups (45).

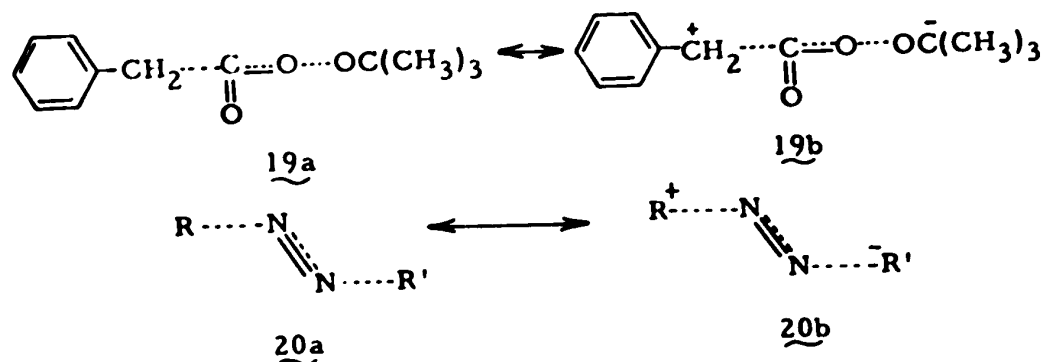
In the decomposition of phenylazo-triphenylmethanes (23)



both electron-donating and electron-attracting substituents led to decreases in the rates of thermolysis. It was pointed out that both types of substituents could increase the resonance stabilization of the ground state by increasing the conjugation to the phenyl and azo groups and strengthening the phenyl-nitrogen bond. However in view of Pryor and Smith's (29) conclusion that *p*-nitrophenylazotriphenylmethane and phenylazotriphenylmethane proved Scheme B,

and that there is a reasonable amount of reversibility associated with the first step we can only conclude that we are not dealing with substituent effects on a one step process, but substituent effects upon dissociation to a radical pair and upon the homolysis of the arylidazine radical  $\text{Ar-N=N}\cdot$ .

While there is no well defined information pertaining to polar, or resonance, effects in azo thermolysis reaction we cannot out of hand dismiss it. Just as Bartlett and Rüchardt (41) were able to ascribe the Hammett  $\rho$ -value of  $-1.09$  in tert-butyl phenylperacetate decomposition to polar contribution to the transition state such as  $19a \leftrightarrow 19b$  then the equivalent type of resonance

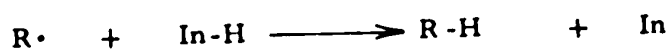


contribution,  $20a \leftrightarrow 20b$  may be of importance in considering the possibility of the two bond synchronous mechanism (Scheme A) of azoalkane homolysis, particularly when the azoalkanes are unsymmetrical.

### The Inhibition Radical Reaction with Nitric Oxide

A major turn in azoalkane chemistry occurred when Forst and Rice (11) demonstrated that the presence of nitric oxide in

the thermolysis of azomethane suppressed methane formation and lead to a decreased rate of formation of nitrogen. The vast majority of gas phase inhibitors act as hydrogen donors e.g.



and the same alkane is produced that one expects as a product from chain induced decomposition. By using nitric oxide one can claim to have suppressed the usual chain induced decomposition when alkanes, R-H, are no longer produced.

Nitric oxide has been used as an inhibitor of gaseous free-radical chain reactions such as the decomposition of alkanes (46), ethers (47), peroxides (48) and azoalkanes (11, 12, 17). The general effect of the addition of inhibitors on reaction rate is shown in Figure 3. A method of describing the figure is to refer to region (a) as the region of inhibition, (b) the maximally inhibited region, and (c) as the region of induced reaction. It should be noted that region (b) may be very small (as in curve II, in Figure 3). The basic assumptions made for inhibited decompositions are (i) the inhibitors reduce the rate to a limit which corresponds to a molecular, non-chain, decomposition of the substrate; (ii) as a corollary to (i), different inhibitors reduce the rate to the same minimum limiting rate, although different amounts of inhibitor may be necessary; at any chosen temperature this will be independent of surface condition, surface:volume ratio and reactant pressure; (iii) there is consumption of the inhibitor in the maximally inhibited region, such consumption being small, and the products arising



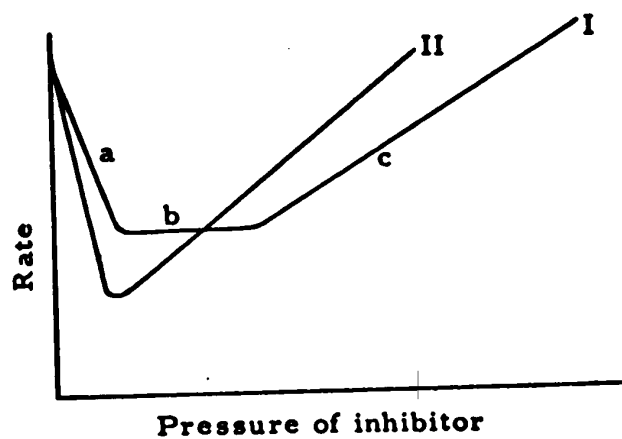


Figure 3. Characteristic inhibition curves (53).

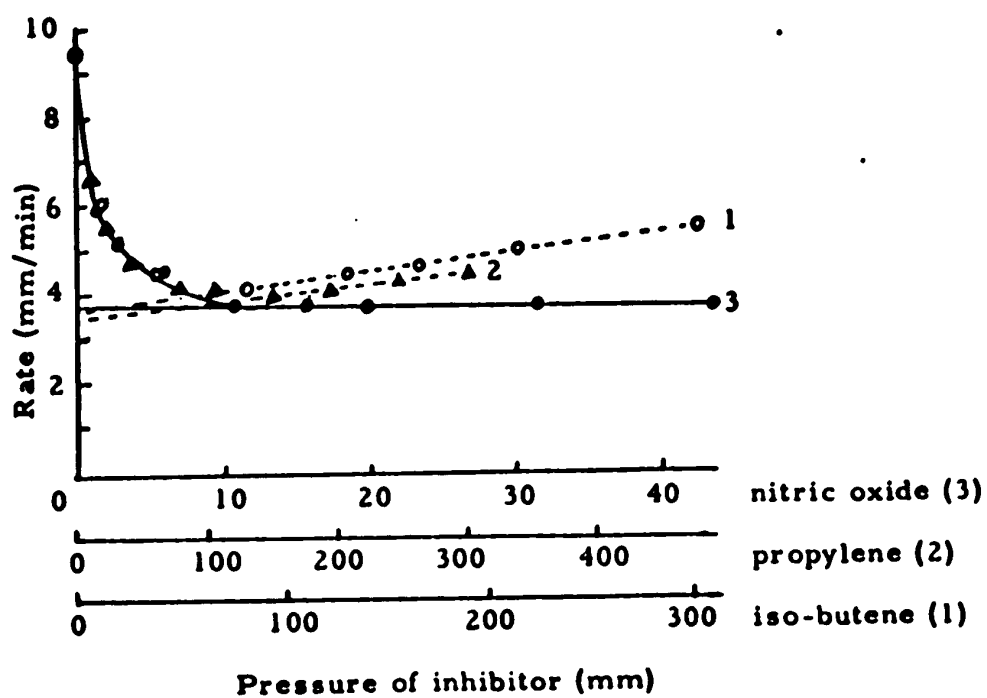
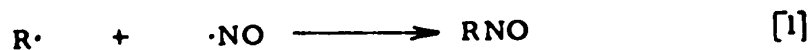


Figure 4. Inhibition curves for 100 mm n-pentane at 560°.

1, iso-butene; 2, propylene; 3, nitric oxide (52).

therefrom having no effect upon the reaction rate or an effect that can be readily measured. The Table X summarizes the evidence for the frequent assumption that the maximally inhibited rate is the same for propene as for nitric oxide. See also Figure 4. However in the case of the thermolysis of azomethane (11) ethene and propene were found unsuitable, and the addition of nitric oxide reduced the rate to a minimum which was lower than that with added propene or ethene. Further addition of nitric oxide increases the rate, giving a curve similar to curve II in Figure 3.

It has been generally accepted that the primary reaction in the nitric oxide inhibition is removal of free radicals,  $R\cdot$ , by reaction 1 to form a nitrosoalkane (53, 54).



The subsequent reactions of nitrosoalkanes are complex and are not fully understood. Generally, there are four possible reactions for initially formed products, 1) dimerization leading to the formation of the stable solid alkyl nitroso dimers (reaction 2), 2) isomerization to the corresponding oxime (reaction 3), 3) further reaction with nitric oxide (reaction 4), 4) further reaction with radicals (reaction 5).

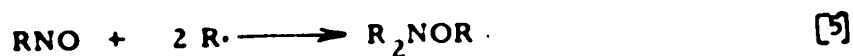
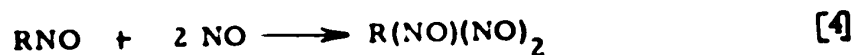
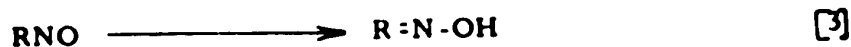
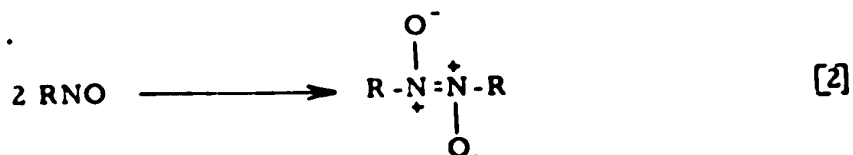


Table X. Limiting rates for different inhibitors in some thermolysis processes (53).

Substrate	Temp. °C	NO rate <sup>a</sup>	C <sub>3</sub> H <sub>6</sub> rate	iso-C <sub>4</sub> H <sub>8</sub> rate	Ref.
(C <sub>2</sub> H <sub>5</sub> ) <sub>2</sub> O	550	1.91 x 10 <sup>-3</sup>	2.02 x 10 <sup>-3</sup>	-	49
C <sub>2</sub> H <sub>5</sub> CHO	550	3.96 x 10 <sup>-3</sup>	4.44 x 10 <sup>-3</sup>	-	49
(CH <sub>3</sub> ) <sub>2</sub> CO	570	1.40 x 10 <sup>-3</sup> <sup>b</sup>	0.55 x 10 <sup>-3</sup>	-	50
n-C <sub>5</sub> H <sub>12</sub>	530	0.58	0.58	-	51
	560	3.7	3.9	4.0	52
iso-C <sub>5</sub> H <sub>12</sub>	560	5.0	4.6	4.8	52
iso-C <sub>4</sub> H <sub>10</sub>	560	1.8	1.9	2.0	52

<sup>a</sup> Hydrocarbon rates in mm/min, others in sec<sup>-1</sup>.

<sup>b</sup> Some catalysis by nitric oxide.

### Reaction 2: Dimerization

Calvert, Thomas and Hanst (55) determined the rate of formation and decay of nitrosomethane, formed in the photolysis of azomethane-nitric oxide mixture at 25° by infrared absorption spectroscopy. The rate-determining step in the decay of nitrosomethane monomer in the dark was found to be a homogeneous gas phase reaction which was second order in nitrosomethane. The only measurable final product of methyl radical-nitric oxide reaction at 25° was the dimer of nitrosomethane.

Gowenlock and Key (56) argued that the dimerization would be of little importance at higher temperature because reactions of this type have a low activation energy (6 kcal mole<sup>-1</sup>) and a large negative entropy of activation. Christie (57) found that the nitrosomethane formed in an irradiated mixture of methyl iodide and nitric oxide disappeared in absence of excess nitric oxide at room temperature. She suggested that this second order reaction ( $k_2 = 1.2 \text{ mole}^{-1} \text{ ml sec}^{-1}$ ) was most likely a heterogeneous dimerization to either the cis or trans dimer.

Chilton and Gowenlock (58) studied the reaction products of the pyrolysis of diisopropylmercury in a flow system with nitrogen and nitric oxide as carrier gases in the temperature range 230-280°. Absorption spectra and chemical tests showed that the dimer of 2-nitrosopropane was formed along with acetone oxime. They found that the monomer-dimer transition took place in the region 85-95°.

Gowenlock and Trotman (59) prepared dimeric nitrosomethane by photolysis or pyrolysis in a flow system at 330-390°. They found monomeric nitrosomethane was converted to the dimer at room temperature in the dark and that dimer to monomer conversion took place at 350°.

Reaction 3: Isomerization to oximes

The isomerization to the oxime was confirmed by the work of Gowenlock and coworkers. Chilton and Gowenlock (58) found acetone oxime in the reaction products of pyrolysis of diisopropylmercury in a flow system with nitrogen and nitric oxide as carrier gases.

Gowenlock and Trotman (59) found that monomeric nitrosomethane could undergo isomerization to formaldoxime in various solvents at room temperature. However little formaldoxime was obtained in the pyrolysis of tert-butyl nitrite or trans dimeric nitrosomethane.

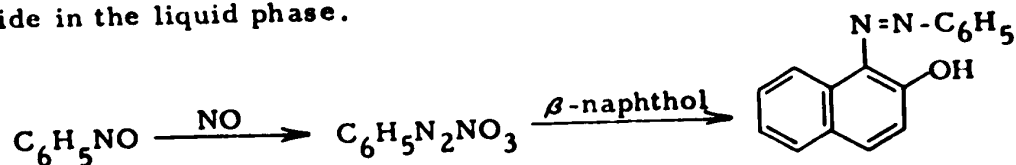
Batt and Gowenlock (60) found that the isomerization of nitrosomethane to formaldoxime has an activation energy of 40 kcal mole<sup>-1</sup> for the homogeneous gas-phase process, but proceeds rapidly in the presence of an active surface with an activation energy of 10 - 14 kcal mole<sup>-1</sup>.

Pratt and Purnell (61) studied the reactions of ethyl radicals generated by the photolysis of tetraethyllead with nitric oxide in the temperature range 233-267°. The most important reaction was the formation of acetaldoxime which decomposes

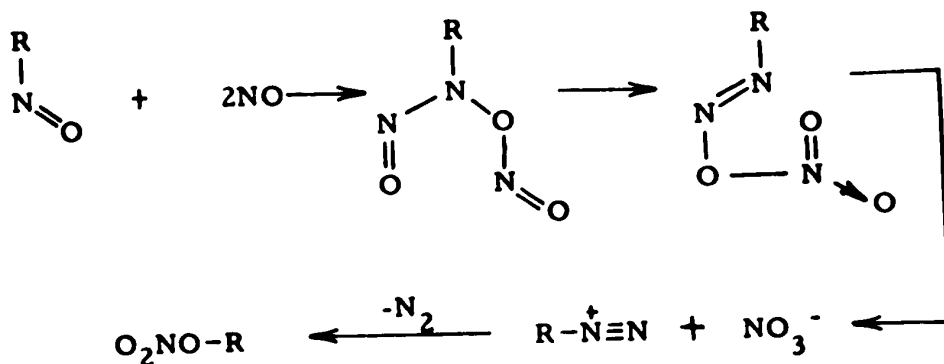
heterogeneously to acetonitrile.

Reaction 4: Further reaction with nitric oxide

Reaction 4 was first shown by Bomberger (62) who obtained phenyldiazonium nitrate from nitrosobenzene and nitric oxide in the liquid phase.



Brown (63) studied a number of reactions involving isobutylene and nitric oxide. He proposed that the reaction occurs via a diazonium nitrate, the formation of which can be visualized as:



Christie (57, 64) found that nitrosomethane reacted with nitric oxide in the ratio of 1:2 to give a product which was stable in the gas phase at room temperature, but decomposed on freezing and rewarming.

Forst and Rice (11) studied the thermal decomposition of azomethane in the presence of the isotopic nitric oxide,  $^{15}\text{NO}$ , and found that nitrogen was produced from the nitric oxide. The ratio of the nitric oxide consumed to nitrogen produced increased with increasing the nitric oxide pressure and reached the vicinity of

two at about the same pressure as when the rate of formation of nitrogen was minimum. Beyond this point the amount of nitric oxide consumed continued to increase slowly.

Gowenlock and Healey (65) have recently studied the pyrolysis of 2-methyl-2-nitrosopropane over the temperature range 140 to 220°. They obtained nitrogen, nitric oxide and isobutane as the major reaction products. They found that small amount of nitrogen (0.05% decomposition) could be produced at temperatures as low as 70°.

#### Reaction 5: Further reaction with radicals

Gingras and Waters (66) found that 2-cyano-2-propyl radicals added to nitric oxide and aromatic nitroso compounds to give trisubstituted hydroxyamines.

Bromberger and Phillips (67) observed the formation of trimethylhydroxylamine via the successive addition of methyl radicals to nitrosomethane.

Hoare (68) found that in the photolysis of acetone-nitric oxide mixture at 200° the number of radicals scavenged per nitric oxide molecule is between two and three, but no products were identified.

Maschke, Shapiro and Lampe (69) studied the photolysis of azomethane- $d_6$ -nitric oxide mixtures. In the photolysis of a mixture of 11.8 torr of azomethane- $d_6$  and 0.2 torr of nitric oxide,  $CD_3NO$  forms immediately and goes through a maximum. This maximum occurs at about the same time that essentially complete

depletion of nitric oxide is observed and at the same time as the occurrence of a very marked increase in  $(\text{CD}_3)_2\text{NOCD}_3$  concentration. They calculated that nitric oxide is only 15 times more effective than nitrosomethane in scavenging methyl radicals.

### Secondary Deuterium Kinetic Isotopic Effect Studies

Secondary deuterium kinetic isotopic effect studies have proven useful in examining reaction mechanisms. Measureable force constant changes are observed when the isotopically labelled center changes hybridization.

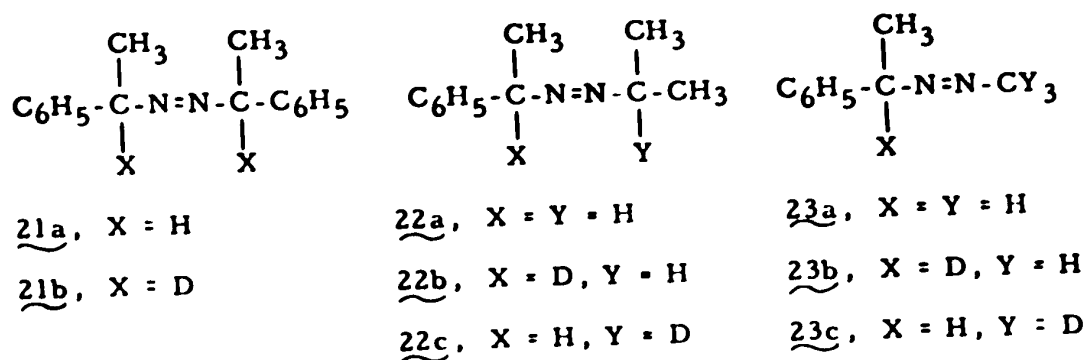
Seltzer and a coworker (19, 70) have used secondary kinetic isotope effects to evaluate the bond-breaking that occurs in the transition state during the thermolysis of various symmetrical and unsymmetrical azo compounds. They found, on comparing azo-bis- $\alpha$ -phenylethane (21a) with azo-bis- $\alpha$ -phenylethane- $\alpha, \alpha$ -d<sub>2</sub> (21b), an isotope effect,  $k_{21a}/k_{21b} = 1.27 \pm 0.03$ . By comparison with numerous other reactions they formulated criteria that if a center is changing from  $sp^3$  in the ground state to  $sp^2$  in the transition state that the change in force constants result in a 12-14% decrease in rate per  $\alpha$ -deuterium substitution at the reaction site (at 105°). Halevi has reviewed secondary isotope effects (71) and using equation:

$$\log k_{\text{H}}/k_{\text{D}} = n \delta \Delta G^\ddagger / 2.303 R T$$

where  $n$  is the number of deuteriums undergoing change of hybridization and  $\delta \Delta G^\ddagger$  is the free energy change per isotopic substitution has suggested that the values commonly found for

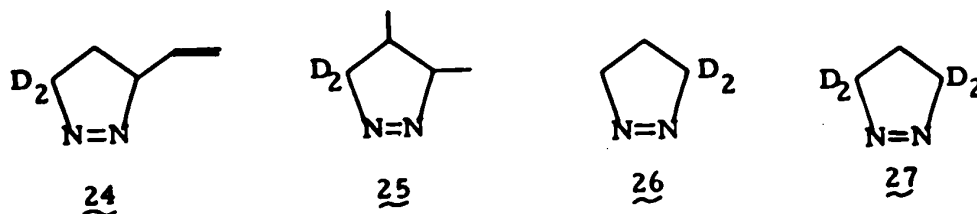


$\alpha$ -deuterium kinetic effects are in the order of 80 - 115 cal mole<sup>-1</sup>. Table XI lists some of the values presented in the literature. Thus the value obtained by Seltzer provides good evidence for the simultaneous rupture of both carbon-nitrogen bonds, Scheme A, p. 1. Thermolysis of  $\alpha$ -phenylazo-2-propane (22) presented a somewhat different picture. The secondary effects,  $k_{22a} / k_{22b} = 1.16$  and  $k_{22a} / k_{22c} = 1.04$ , led to the conclusion that here too, both carbon-nitrogen bonds stretch in the transition state but to unequal degrees.



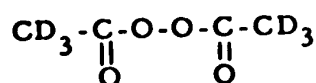
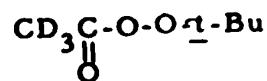
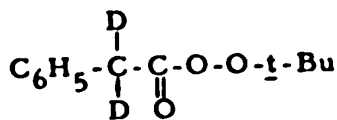
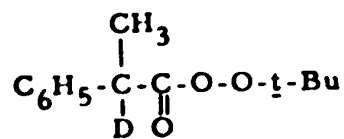
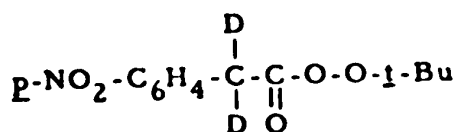
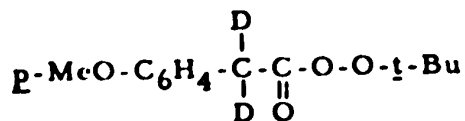
In a third and less symmetrical case,  $\alpha$ -phenylethylazomethane ( $\underline{23a}$ ),  $\alpha$ -phenylethyl- $\alpha$ -d<sub>1</sub>-azomethane ( $\underline{23b}$ ) and  $\alpha$ -phenylazomethane-d<sub>3</sub> ( $\underline{23c}$ ) were thermolyzed. A comparison of rate constants,  $k_{23a} / k_{23b} = 1.13$  and  $k_{23a} / k_{23c} = 0.97$ , led to the conclusion that the slow step involved rupture of only the  $\alpha$ -phenylethyl carbon-nitrogen bond. Rupture of the methyl-carbon bond had to occur in a subsequent step.

Crawford and coworkers (73 - 75) have measured  $\alpha$ -deuterium kinetic effects on the thermolysis of 1-pyrazolines  $\underline{24}$ ,  $\underline{25}$ ,  $\underline{26}$ , and  $\underline{27}$ .



The observed  $\delta \Delta G^\ddagger$  values of 77 - 93 cal per deuterium were interpreted as suggesting that both carbon-nitrogen bonds are being cleaved in the rate-determining step (see Table XI).

Koenig and coworkers (76 - 78) have studied the  $\alpha$ -deuterium secondary kinetic isotope effects on the thermal decomposition of acetyl peroxide 28, tert-butyl peracetate 29 and tert-butyl-phenyl peracetates 30 - 33 (see Table XI).

282930313233

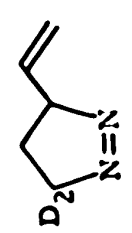
The very small values of the isotope effects observed for 28 and 29 were interpreted in terms of a non-concerted process.

Table XI. Radical  $\alpha$ -deuterium isotope effects

Reaction	Solvent	T°C	$k_H/k_D$	$\delta\Delta G^\ddagger_a$ (cal)	Reference
1. Thermolysis of $\begin{array}{c} \text{CH}_3 \quad \text{CH}_3 \\   \quad   \\ \text{C}_6\text{H}_5-\text{C}-\text{N}=\text{N}-\text{C}-\text{C}_6\text{H}_5 \\   \quad   \\ \text{D} \quad \text{D} \end{array}$ $\text{21b}$	Ethylbenzene	105	1.27	$89 \pm 6$	70
2. Thermolysis of $\begin{array}{c} \text{CH}_3 \quad \text{CH}_3 \\   \quad   \\ \text{C}_6\text{H}_5-\text{C}-\text{N}=\text{N}-\text{C}-\text{CH}_3 \\   \quad   \\ \text{D} \quad \text{H} \end{array}$ $\text{22b}$	Diphenylether- benzoquinone solution	143.2	1.148	$114 \pm 10$	70
3. Thermolysis of $\begin{array}{c} \text{CH}_3 \\   \\ \text{C}_6\text{H}_5-\text{C}-\text{N}=\text{N}-\text{CH}_3 \\   \\ \text{D} \end{array}$ $\text{23b}$	Diphenylether- benzoquinone solution	161.0	1.13	$105 \pm 8$	19




Continued

Table XI. - Continued

Reaction	Solvent	T°C	k <sub>H</sub> /k <sub>D</sub>	ΔG‡ <sup>a</sup> (cal)	Reference
<p>4. Thermolysis of</p> $  \begin{array}{c}  \text{H} \quad \text{C}_6\text{H}_5 \\    \quad   \\  \text{C}_6\text{H}_5\text{-C-C-N=N-C-C-C}_6\text{H}_5 \\    \quad   \quad   \quad   \\  \text{H} \quad \text{D} \quad \text{D} \quad \text{H}  \end{array}  $ <p>meso- dl-</p>	Ethylbenzene Ethylbenzene	106.47 106.47	1.221 1.202	75 ± 10 69 ± 10	38 38
<p>5. β-scission of</p> $  \begin{array}{c}  \text{CH}_3 \\    \\  \text{C}_6\text{H}_5\text{-C-O}\cdot \\    \\  \text{CD}_3  \end{array}  $	Carbontetrachloride- cyclohexane	75	1.12	78 ± 10	72
<p>6. Thermolysis of</p> 	Gas phase	134.5	1.21	77 ± 7	73

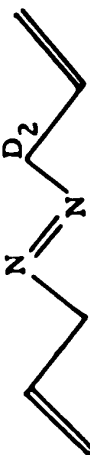
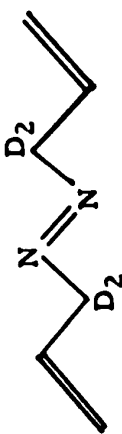
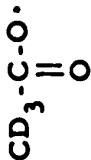
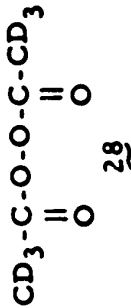
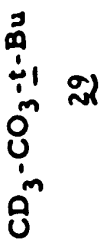
Continued

Table XI. - Continued

Reaction	Solvent	T°C	$k_H/k_D$	$\delta\Delta G^\ddagger$ (cal)	Reference
7. Thermolysis of					
					
<u>25</u>					
<u>cis-</u>	Gas phase	220.9	1.19	86	74
<u>trans-</u>	Gas phase	220.9	1.21	93	74
8. Thermolysis of					
					
<u>26</u>	Gas phase	229.4	1.19	86	75
9. Thermolysis of					
	Gas phase	229.4	1.40	84	75

Continued

Table XI. - Continued


Reaction	Solvent	T°C	k <sub>H</sub> /k <sub>D</sub>	ΔG‡ <sup>a</sup> (cal)	Reference
10. Thermolysis of 	Gas phase	161.7	1.15	62	6
11. Thermolysis of 	Gas phase	161.7	1.13	62	6
12. Decarboxylation of 	Isooctane	74.8	1.09	20	76
13. Thermolysis of 	Isooctane Paraffin oil	74.8 74.8	1.039 1.056	4 6	76 76
14. Thermolysis of 	Isooctane Oil	130.1 130.1	1.00 1.02	0 5	78 78

Continued

Table XI. - Continued

Reaction	Solvent	T°C	k <sub>H</sub> /k <sub>D</sub>	ΔG <sup>‡</sup> <sub>a</sub> (cal)	Reference
15. Thermolysis of $\begin{array}{c} \text{D} \\   \\ \text{C}_6\text{H}_5-\text{C}-\text{CO}_3-\text{t-Bu} \\   \\ \text{D} \end{array}$ $\underline{30}$	Chlorobenzene Isooctane Paraffin oil	84.98 84.98 84.98	1.11 1.13 1.12	34 43 40	77 77 77
16. Thermolysis of $\begin{array}{c} \text{CH}_3 \\   \\ \text{C}_6\text{H}_5-\text{C}-\text{CO}_3-\text{t-Bu} \\   \\ \text{D} \end{array}$ $\underline{31}$	Isooctane	73.99	1.046	31	77
17. Thermolysis of $\begin{array}{c} \text{D} \\   \\ \text{p-NO}_2\text{C}_6\text{H}_4-\text{C}-\text{CO}_3-\text{t-Bu} \\   \\ \text{D} \end{array}$ $\underline{32}$	Chlorobenzene Nujol	85.10 85.10	1.10 1.09	34 31	78 78

Table XI. - Continued

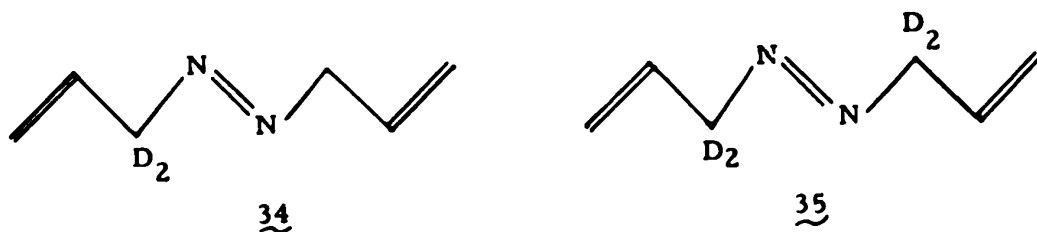
Reaction	Solvent	T °C	k <sub>H</sub> /k <sub>D</sub>	ΔG <sup>‡</sup> <sup>a</sup> (cal)	Reference
18. Thermolysis of $\begin{array}{c} \text{D} \\   \\ \text{P-MeOC}_6\text{H}_4\text{-C-CO}_3\text{-t-Bu} \\   \\ \text{D} \end{array}$	Isooctane Nujol	60.46 60.46	1.07 1.05	22 16	78 78
19. Cope rearrangement of $\begin{array}{c} \text{Et} \\   \\ \text{NC} \quad \text{Me} \\   \quad / \\ \text{NC} \quad \text{C} \\   \quad   \\ \text{D} \quad \text{D} \end{array}$	n-Decane	90.0 - 93.9	1.19	63	79
20. Rearrangement of $\begin{array}{c} \text{S} \\    \\ \text{C}_6\text{H}_5\text{-C-O-C-CH=CH}_2 \\   \\ \text{D} \end{array}$	Acetonitrile	70 - 100	1.122	39 - 42	80
21. Retro Diels-Alder reaction of 	Isooctane	49.6	1.08	49	81

<sup>a</sup>ΔG<sup>‡</sup> are calculated according to the equation,  $\log k_{\text{H}}/k_{\text{D}} = n \Delta G^{\ddagger} / 2.303 R T$



while the relatively large isotope effects observed for 30 - 33 were rationalized by a concerted mechanism leading directly to decarboxylated radical, carbon dioxide and tert-butoxy radical in single step with no intervening intermediate. The lower values of  $\alpha$ -effects on the thermolysis of the peroxy esters compared with those of the azo compounds indicate that the transition state of the fragmentation of the peroxy esters occurs early on the reaction coordinate in relation to carbon-carbon cleavage.

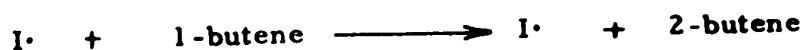
The values of  $\delta\Delta G^\ddagger$  obtained for the azo compounds 34 and 35, even when maximized for possible error from scrambling, are smaller than those normally encountered (6)



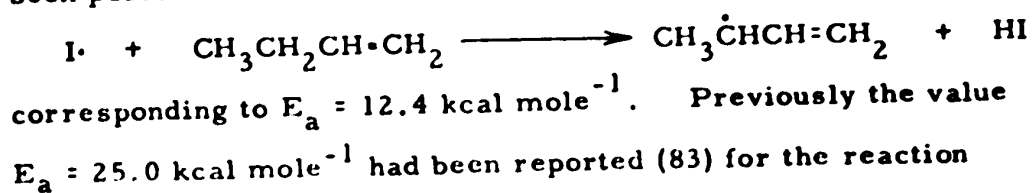
being  $65 \pm 10$  cal mole<sup>-1</sup>. If a non-maximum correction for scrambling were applied the values would be  $62 \pm 10$  cal mole<sup>-1</sup> when interpreted by Scheme A wherein both allylic center are being altered. Application of Scheme B gives value of  $124 \pm 15$  cal mole<sup>-1</sup> a value which though in the maximum range generally encountered is not unreasonable since for azo compounds the transition state occurs late on the reaction coordinate (see section 3.3 of reference 2). The authors were concerned about the low value for the allylic resonance energy that was implied from a mechanism following Scheme A. Whereas Scheme B gave a value which did not seem unreasonable.

### Allylic Resonance Energy (ARE)

The allylic resonance energy is defined as the difference in dissociation energies between a C-H bond conjugated with a double bond and the similar bond in a saturated paraffin at the same temperature. The most reliable value of the allylic resonance energy\* has been determined by Egger, Golden and Benson (82) from a study of the iodine-catalyzed isomerization of 1-butene. The overall reaction is



and by a steady-state treatment of the detailed mechanism it has been possible to obtain an activation energy for the step



which was identified with the activation energy for the analogous reaction with n-butane, since  $D(\text{i-C}_3\text{H}_7\text{-H}) \cong D(\text{sec-C}_4\text{H}_9\text{-H})$ . It follows that the resonance energy is given by  $25.0 - 12.4 = 12.6 \text{ kcal mole}^{-1}$ . The uncertainty in the allylic resonance energy has been claimed to be less than  $1 \text{ kcal mole}^{-1}$ . The value reported previously by Benson, Bose and Nangia (84) in a preliminary kinetic study of the iodine-catalyzed isomerization of 1-butene was

---

\* Some of these values are butenyl resonance energies however it is generally assumed that there is little difference between the allylic resonance energy value and the butenyl resonance energy value (103).

$13.3 \pm 1.3 \text{ kcal mole}^{-1}$ . These values are in excellent agreement with the values obtained from the thermal rearrangement of vinyl-substituted cyclobutanes and cyclopropanes.

Hammond and DeBoer (85) have reported an activation enthalpy of  $\Delta H^\ddagger = 34.0 \text{ kcal mole}^{-1}$  for the first-order cleavage of the carbon bond between the substituents in trans-divinylcyclobutane. At a mean temperature of  $448^\circ\text{K}$  it can be calculated  $E_a = \Delta H^\ddagger + RT = 34.0 + 0.9 = 34.9 \text{ kcal mole}^{-1}$ . This value is to be compared with the activation energy of  $61.3 \text{ kcal mole}^{-1}$  for the cleavage of the same bond in 1,2-dimethylcyclobutane, as reported by Gerberich and Walters (86). This leads to an allylic resonance energy of  $(61.3 - 34.9)/2 = 13.2 \text{ kcal mole}^{-1}$ .

Ellis and Frey (87), comparing the activation energies for the isomerization of 1,1-dimethylcyclopropane to methylbutene (62.6 kcal) and 1-methyl-1-vinylcyclopropane to 1-methylcyclopentene (49.4 kcal), deduced a value for the allylic resonance energy of 13.2 kcal. Other values of the allylic resonance energy obtained from the thermal rearrangement of vinyl-substituted cyclobutanes and cyclopropanes are listed in Table XII.

The bond dissociation energy  $D(\text{allyl-H})$  is given by the expression

$$D(\text{allyl-H}) = \Delta H_f^\circ(\text{allyl}) + \Delta H_f^\circ(\text{H}) - \Delta H_f^\circ(\text{propene})$$

where  $\Delta H_f^\circ(\text{allyl})$ ,  $\Delta H_f^\circ(\text{H})$  and  $\Delta H_f^\circ(\text{propene})$  are the heat of formation of the allyl radical, hydrogen and propene at  $298^\circ\text{K}$  respectively. From the existing thermochemical data,

Table XII. Allylic resonance energies obtained from thermolyses of vinyl-substituted compounds  
(see footnote page 42 ).


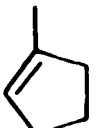



Reaction	Activation energy kcal/mole	Allylic resonance energy kcal/allyl	Reference
$\text{CH}_3\text{CH}_2\text{CH}=\text{CH}_2 + \text{I} \longrightarrow \text{CH}_3\dot{\text{C}}\text{HCH}=\text{CH}_2 + \text{HI}$	12.4	12.6	82
$\text{CH}_3\text{CH}_2\text{CH}_3 + \text{I} \longrightarrow \text{CH}_3\dot{\text{C}}\text{HCH}_3 + \text{HI}$	25.0		83
$\text{CH}_3\text{CH}_2\text{CH}=\text{CH}_2 + \text{I} \longrightarrow \text{CH}_3\dot{\text{C}}\text{HCH}=\text{CH}_2 + \text{HI}$	13.2	11.8	84
$\text{CH}_3\text{CH}_2\text{CH}_3 + \text{I} \longrightarrow \text{CH}_3\dot{\text{C}}\text{HCH}_3 + \text{HI}$	25.0		83
 $\longrightarrow$ 	49.4		87
 $\longrightarrow$  + 	62.6	13.2	88

Table XII. - Continued

Reaction	Activation energy kcal/mole	Allylic resonance energy kcal/allyl	Reference
	32.1	16.5	89
	48.6		92
	60.5	13.4	90
	47.1		91
	48.6	11.9	92
	60.5		93

Table XII. - Continued






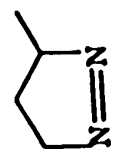
Reaction	Activation energy kcal/mole	Allylic resonance energy kcal/allyl	Reference
	34.9 <sup>a</sup>		85
		13.2	
	61.3		86
	44.2	~13 <sup>b</sup>	94
 $D(\text{CH}_3\text{CH}_2 - \text{CH}_2\text{CH}_3)$	78 - 80		95
	32.2		73
	41.0	8.8	96
			46

Table XII. - Continued

a Calculated from an activation enthalpy  $\Delta H^\ddagger = 34.4$  kcal.

b Corrections have been made for the bond weakening effect of two additional alkyl groups ( $\sim 2 \times 3$  kcal) plus the difference in strain energy between the ground state and the transition state ( $3 \sim 4$  kcal).

$\Delta H_f^\circ(\text{propene}) = 4.88 \text{ kcal mole}^{-1}$  and  $\Delta H_f^\circ(\text{H}) = 51.2 \text{ kcal mole}^{-1}$

(7), this leads to

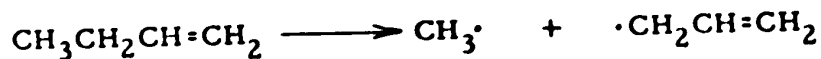
$$\begin{aligned} D(\text{allyl-H}) &= \Delta H_f^\circ(\text{allyl}) + 52.1 + 4.88 \\ &= \Delta H_f^\circ(\text{allyl}) + 47.2 \end{aligned}$$

and since

$$\begin{aligned} \text{ARE} &= D(\text{CH}_3\text{CH}_2\text{CH}_2\text{-H}) - D(\text{allyl-H}) \\ \text{and } D(\text{CH}_3\text{CH}_2\text{CH}_2\text{-H}) &= 98 \text{ kcal mole}^{-1} \text{ (7), this leads to} \end{aligned}$$

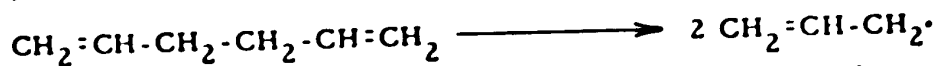
$$\text{ARE} = 51 - \Delta H_f^\circ(\text{allyl})$$

therefore ARE can be calculated knowing  $\Delta H_f^\circ(\text{allyl})$ .  $\Delta H_f^\circ(\text{allyl})$  was first obtained from the thermolysis of 1-butene by the toluene-carrier technique (97),



corresponding to  $E_a = 66.2 \text{ kcal mole}^{-1}$ . The known thermochemical data lead to  $\Delta H_f^\circ(\text{allyl}) = 30.2 \text{ kcal mole}^{-1}$ . A reinvestigation of the thermolysis of 1-butene using the aniline carrier technique (98) showed that first-order rate constants were measured in the pressure-sensitive region, and hence the experimental activation energy was considerably less than the limiting pressure value.

The very low heat of formation of allyl radical (32 kcal mole<sup>-1</sup>) was also observed in the studies of 1,5-hexadiene thermolysis by Homer and Lossing (99).

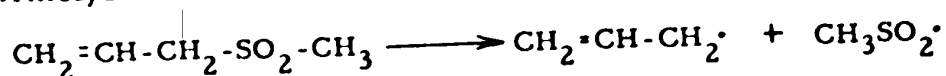


while Akers and Throssell (104) later obtained 37 kcal mole<sup>-1</sup> for the same thermolysis. The origin of the discrepancy is not



obvious but it is known that a major complication arises from a radical chain decomposition of 1,5-hexadiene (100).

Results on the thermolysis of allyl methyl sulfone by toluene-carrier technique can also be used to obtain  $\Delta H_f^\circ(\text{allyl})$ . Besfield and Ivin (101) have determined  $E_a = 47.7 \text{ kcal mole}^{-1}$  for the thermolysis reaction

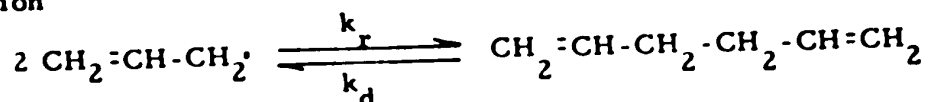


and thus

$$\Delta H_f^\circ(\text{allyl}) = D(\text{C}_3\text{H}_5-\text{SO}_2\text{CH}_3) - \Delta H_f^\circ(\text{SO}_2\text{CH}_3) + \Delta H_f^\circ(\text{C}_3\text{H}_5\text{SOCH}_3)$$

$\Delta H_f^\circ(\text{C}_3\text{H}_5\text{SOCH}_3)$  has been shown to be as  $-73.5 \text{ kcal mole}^{-1}$  and  $\Delta H_f^\circ(\text{SO}_2\text{CH}_3)$  can be estimated as  $-63.2 \text{ kcal mole}^{-1}$  so that  $\Delta H_f^\circ(\text{allyl})$  is  $37.4 \text{ kcal mole}^{-1}$  corresponding to  $D(\text{allyl-H}) = 94.6 \text{ kcal mole}^{-1}$ .

Golden, Gac and Benson (102) have recently reported the direct measurement of the equilibrium constant  $K_{r,d}$  for the reaction

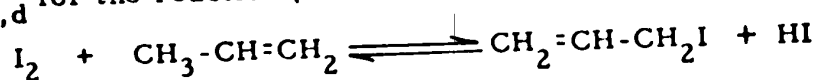


and, thereby, a direct measurement of ARE.  $K_{r,d}$  was measured by determining both  $k_r$  and  $k_d$  under exactly the same condition. The  $k_r$  and  $k_d$  was measured by observing the decomposition of diallyl oxalate and of 1,5-hexadiene. Diallyl oxalate decomposes to give 2 allyl radicals and  $\text{CO}_2$  and the allyl radicals combine to yield 1,5-hexadiene. The values of  $K_{r,d}$  determined at two different temperatures yielded the enthalpy change  $\Delta H_{r,d}^\circ = -62.2 \text{ kcal mole}^{-1}$ .

Since

$$\Delta H_{r,d}^{\circ} = \Delta H_f^{\circ}(1,5\text{-hexadiene}) - 2\Delta H_f^{\circ}(\text{allyl})$$

and since  $\Delta H_f^{\circ}(1,5\text{-hexadiene}) = 20.2 \text{ kcal mole}^{-1}$ , this leads to  $\Delta H_f^{\circ}(\text{allyl}) = 41.2 \text{ kcal mole}^{-1}$ . This value is in agreement with the value  $\Delta H_f^{\circ}(\text{allyl}) = 41.4 \text{ kcal mole}^{-1}$  obtained by the measurement of  $K_{r,d}$  for the reaction (103)



The value of  $\Delta H_f^{\circ}(\text{allyl}) = 41.2 \text{ kcal mole}^{-1}$  yields  $D(\text{allyl-H}) = 99.4 \text{ kcal mole}^{-1}$  and  $ARE = 9.6 \text{ kcal mole}^{-1}$ . They have stated that the value of  $9.6 \text{ kcal mole}^{-1}$  may be uncertain by as much as 2 or 3  $\text{kcal mole}^{-1}$  but it must surely lay to rest any thought that  $ARE$  is much greater than  $12 \text{ kcal mole}^{-1}$ . Table XIII summarizes the allylic resonance energies obtained by the studies of  $\Delta H_f^{\circ}(\text{allyl})$ . We shall adopt  $12 \text{ kcal mole}^{-1}$  as a reasonable value for the allylic resonance energy.

Utilizing the azoethane activation energy of  $48.5 \text{ kcal mole}^{-1}$  Al-Sader (6) estimated the allylic resonance energy contribution to the transition state for a two bond homolysis (Scheme A) mechanism to be  $6.2 \text{ kcal mole}^{-1}$  whereas a single carbon-nitrogen bond cleavage (Scheme B) implies an allylic resonance energy of  $12.4 \text{ kcal mole}^{-1}$ . The authors were reluctant to decide in favour of Scheme B because of the possibility that the transition state is now more like the reactant (Hammond's postulate) and consequently all of the allylic resonance energies from both allyl groups may not be manifested in the activation energy.

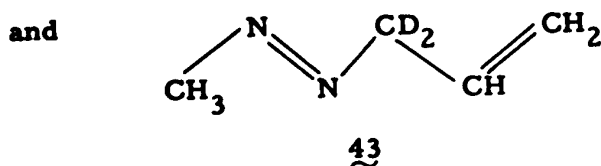
Table XIII. Allylic resonance energies (ARE) obtained from the heat of formation of the allyl radical

Reaction	$\Delta H_f^\circ(\text{allyl})$ kcal mole <sup>-1</sup>	D(allyl-H) <sup>a</sup> kcal mole <sup>-1</sup>	ARE <sup>b</sup> kcal mole <sup>-1</sup>	Reference
$\text{CH}_3\text{CH}_2\text{CH}=\text{CH}_2 \longrightarrow \text{CH}_3^\cdot + \cdot\text{CH}_2\text{CH}=\text{CH}_2$	30.2	77.4	20.6	97
$\text{CH}_2=\text{CHCH}_2\text{CH}_2\text{CH}=\text{CH}_2 \longrightarrow 2 \cdot\text{CH}_2\text{CH}=\text{CH}_2$	33.0	80.2	17.8	99
$\text{CH}_2=\text{CHCH}_2\text{CH}_2\text{CH}=\text{CH}_2 \longrightarrow 2 \cdot\text{CH}_2\text{CH}=\text{CH}_2$	36.9	84.1	13.9	104
$\text{CH}_2=\text{CHCH}_2\text{Br} \longrightarrow \text{CH}_2=\text{CHCH}_2^\cdot + \text{Br}^\cdot$	32.9	80.1	17.9	105
$\text{CH}_2=\text{CHCH}_2\text{SO}_2\text{CH}_3 \longrightarrow \text{CH}_2=\text{CHCH}_2^\cdot + \cdot\text{SO}_2\text{CH}_3$	37.4	84.6	13.4	101
$2 \cdot\text{CH}_2\text{CH}=\text{CH}_2 \rightleftharpoons \text{CH}_2=\text{CHCH}_2\text{CH}_2\text{CH}=\text{CH}_2$	41.2	88.4	9.6	102
$\text{CH}_3\text{CH}=\text{CH}_2 + \text{I}_2 \rightleftharpoons \text{CH}_2=\text{CHCH}_2\text{I} + \text{HI}$	41.4	88.6	9.4	103

<sup>a</sup> D(allyl-H) =  $\Delta H_f^\circ(\text{allyl}) + 47.2$

<sup>b</sup> ARE =  $51 - \Delta H_f^\circ(\text{allyl})$





What differences can we predict for Scheme A and Scheme B in comparing the set 36, 46, 47, and 52? Ramsperger (9) has suggested and Rüchardt (2) has supplied supportive evidence for the criteria for Scheme A that the activation energy for the unsymmetrical compounds will be the mean of the activation energies for the corresponding two symmetrical compounds. Using our knowledge of 52 (6) and the data from Table I we can thus predict rate constants at 120° for 36, 46, and 47. Since some of the azoalkanes have a multiplicity of values we have made our predictions using both the extrapolated maximum and minimum rate constants from Table I, e.g. for 36 the data of Forst and Rice (11) predicts the smallest rate constant for azomethane at 120°, thus taking the mean of the activation energies and log A values gives for 36

$$\log A = \frac{1}{2}(17.2 + 15.5) = 16.3$$

$$E_a = \frac{1}{2}(55.5 + 36.1) = 45.8 \text{ kcal mole}^{-1},$$

using these data at 120° we calculate a rate constant for 36 of  $k = 6.3 \times 10^{-10} \text{ sec}^{-1}$ . The data of Rice and Sickman (9b) gives the largest extrapolated rate constant for azomethane at 120°, and using it we get the activation parameters  $\log A = 15.7$ ,  $E_a = 43.2 \text{ kcal mole}^{-1}$ . These data predict a rate constant for 36 of  $5.0 \times 10^{-9} \text{ sec}^{-1}$  at 120°. The rate constants calculated in the analogous manner for 46 and 47 are shown in Table XIV.

Table XIV. Prediction of relative rates using mechanistic criteria.

$k_n / k_{52}$ at 120°				
n	Scheme A		Scheme B	
	min.	max.	min.	max.
<u>36</u>	$2.5 \times 10^{-5}$	$2.0 \times 10^{-4}$	$5 \times 10^{-2}$	5.0
<u>46</u>	$6.4 \times 10^{-4}$	$1.0 \times 10^{-3}$	$5 \times 10^{-2}$	5.0
<u>47</u>	$3.2 \times 10^{-2}$		$5 \times 10^{-2}$	5.0

If Scheme B is appropriate to the mechanism of azoalkane thermolysis then we expect the first step to be rate determining\* and for the set of compounds 36, 46 and 47 we would expect the allyl-nitrogen bond to be most readily cleaved. To a first approximation then these compounds should be 0.5 times the rate of 52. That steric effects may play a role in making the values different from 0.5 times that of 52 has been documented in the historical section (see Table VII and VIII). It seems unlikely however that the steric effects would change the rate by more than one power of 10. Thus we can predict that if Scheme B is representative of the true mechanism then the rates of 36, 46 and 47 will be in the range  $5 \times 10^{-2} k_{52}$  to  $5 k_{52}$ , and that if the relief of steric

\* Benson (3) has shown that the second step  $R-N_2 \cdot \longrightarrow R \cdot + N_2$  would be very exothermic and thus reasonably expected to be very fast relative to the first step of Scheme B.

compression is playing a role, as has been suggested (32 - 35), then  $k_{47} > k_{46} > k_{36}$  and  $k_{47} \not\gg 100k_{36}$ . The criteria for deciding between Scheme A and B as representative of the azoalkane gas phase thermolysis mechanism are outlined in Table XIV and is shown graphically in Figure 5 (including an allowance for steric effects).



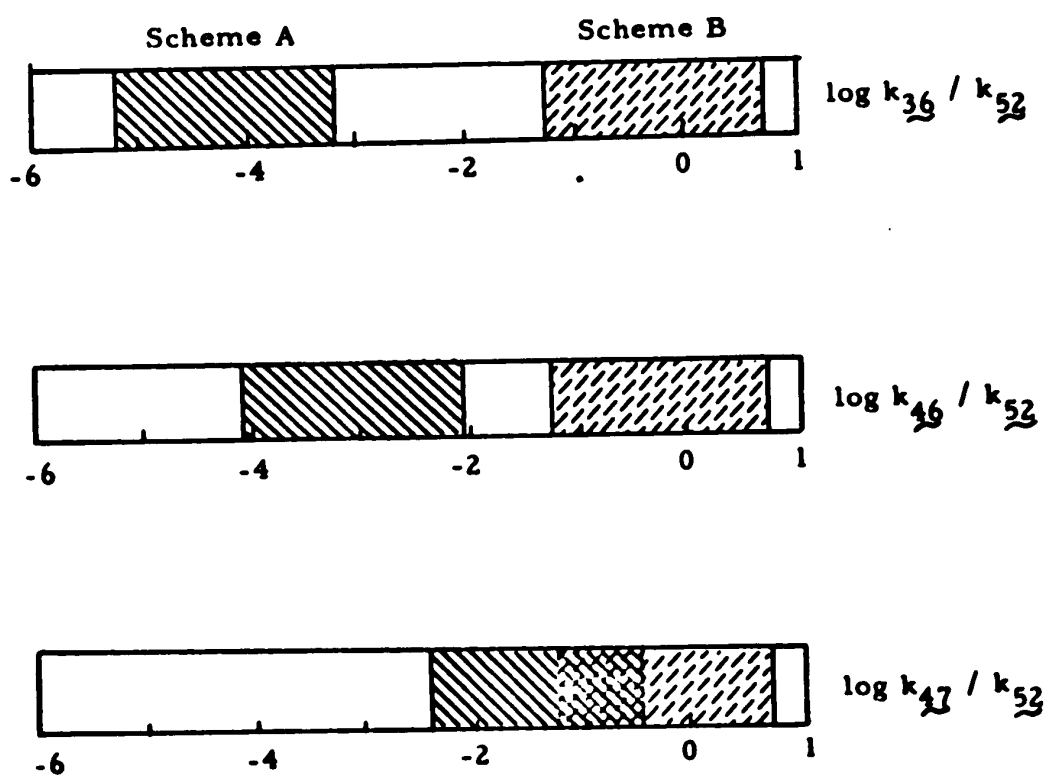
In Figure 5 if the value of  $\log k_n - \log k_{52}$  falls in the lined region  then the mechanism is best represented by Scheme A; if it falls in the dashed region  then Scheme B. Values above and below those areas seem very unlikely and values in the intermediate blank and overlapping regions do not permit a clear cut decision as to mechanism.

Figure 5. Graphical representation of the basis for making the decision between Scheme A and Scheme B.





## EXPERIMENTAL

All boiling points and melting points are uncorrected.

The ultraviolet spectra were obtained on a Jasco Model ORD/UV-5 spectrophotometer. The nuclear magnetic resonance spectra were obtained using a Varian A-60 and HR-100 spectrometer.

The exact masses of the azo compounds were obtained on an A.E.I. MS-9 mass spectrometer (70 eV, room temperature inlet). Products analyses were carried out on an A.E.I. MS-12 mass spectrometer, of which the ion source was coupled by means of a Watson-Biemann helium separator directly to an Aerograph Model 1200 Hy-Fi gas chromatograph. Isotope ratio measurements of nitrogen were carried out on a C.E.C. 21-614 mass spectrometer. Microanalyses were carried out in the Microanalytical Laboratory of the Department of Chemistry, University of Alberta.

Gas chromatography was carried out with an F and M Model 500 programmed temperature gas chromatograph and a Varian Aerograph Series 1200 programmed temperature gas chromatograph. Sample purifications and product analyses were carried out on a gas chromatograph consisting of a Gow-Mac Model TR-2-B,W thermal conductivity cell with a Gow-Mac Model 40-50 power supply in conjunction with a Sargent Model SR recorder.

(A) Apparatus

A schematic diagram of the vacuum rack used for the preparation of samples and analysis of products is shown in Figure 6.

The gas buret was calibrated by filling with mercury and weighing. The volume of the manifold surrounded by valves  $H_1 - H_8$ ,  $N_8$  and  $N_4$  and calibration mark 2 was measured by filling with carbon dioxide which was transferred to the gas buret (Table XV). The volume,  $V$ , of the round flask surrounded by valves  $N_2$  and  $N_3$ , calibration mark 1 and the Bourdon gauge was measured by filling with carbon dioxide and transferring this to the previously calibrated manifold (Table XVI). The Bourdon gauge was calibrated by filling with carbon dioxide, reading the pressure and transferring the carbon dioxide to the gas buret. The pressure in the gas buret was divided by the ratio of the volume  $V$  to that of the gas buret (Table XVII).

(B) Procedure

(a) Preparation of Samples

Valve  $N_4$  and mercury cut MCl were closed. Several break-seals were glassblown to the ends of the valves by blowing through valve  $N_8$  and then pumped overnight for conditioning. The volume of the manifold and the combined volumes of each of the break-seals and the dead volumes in the valves were measured in the following way. A carbon dioxide container was attached at valve  $N_1$ , valves  $F_1$ ,  $N_2$ ,  $F_3$ ,  $F_4$  and  $N_8$  and mercury cut MCl

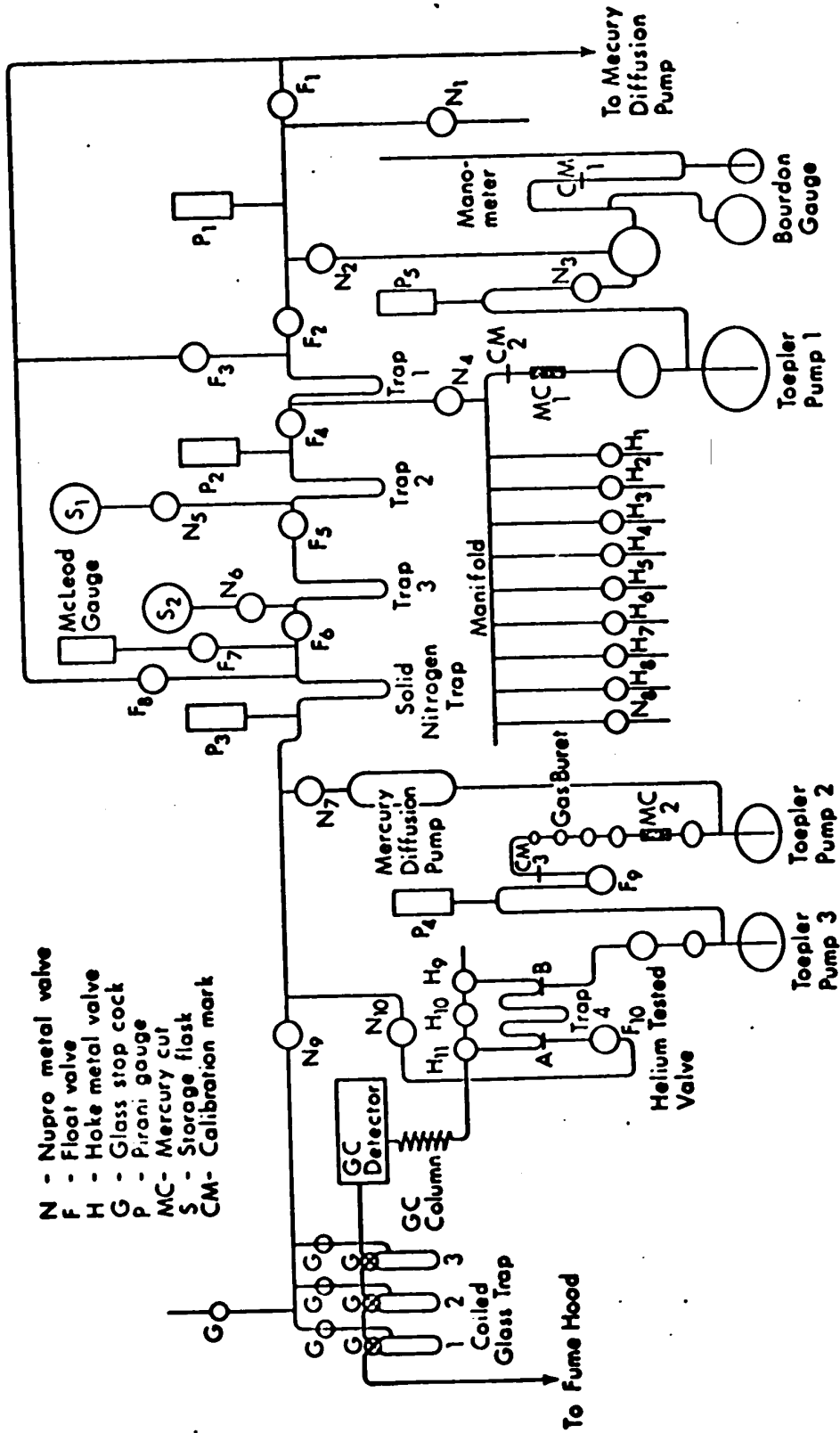


Figure 6. Schematic diagram of the vacuum rack.

Table XV. Calibration of the volume of the manifold.

Pressure in the manifold	Pressure in 51.7 ml buret	Volume in the manifold
57.6 torr	135.4 torr	121.7 ml
47.7	113.0	122.5
73.5	172.1	121.0
		Av. 121.7

Table XVI. Calibration of the volume of the Bourdon gauge.

Pressure in the Bourdon gauge	Pressure in the 121.7 ml manifold	Volume of Bourdon gauge
25.7 torr	165.5 torr	783 ml
33.5	214.0	778
31.4	202.1	782
		Av. 781

Table XVII. Calibration of the pressure of the Bourdon gauge.

Gauge reading torr	Gas buret reading ml	torr	Corrected value torr	Error torr
19.89	51.7	287.5	19.02	-0.87
16.86	51.7	245.6	16.25	-0.61
11.40	51.7	167.1	11.06	-0.34
6.81	25.4	204.7	6.65	-0.17
4.44	25.4	135.2	4.40	-0.04
2.55	11.23	176.0	2.53	-0.02
1.00	11.23	77.2	1.10	+0.10

were closed, then valves  $N_1$ ,  $F_2$ ,  $N_4$  and  $H_1 - H_8$  were opened. Carbon dioxide was transferred to one of the break-seals by freezing at liquid nitrogen temperature. Valve  $N_4$  was closed and the carbon dioxide was expanded to the manifold and break-seals. The mercury in Toepler pump 1 was brought to calibration mark CM2, then the pressure was read by a cathetometer. In order to transfer the carbon dioxide in the manifold into the gas buret, the mercury in valve  $F_9$  was brought to calibration mark CM3, valves  $F_4$ ,  $F_5$ ,  $F_6$  and  $N_7$  were opened, valves  $F_2$ ,  $N_5$ ,  $N_6$ ,  $F_7$ ,  $F_8$ ,  $N_9$  and  $N_{10}$  closed, then valve  $N_4$  was opened. The carbon dioxide was frozen on the surface of the thermowell in Toepler pump 2 which contained liquid nitrogen, the mercury was lifted up above the arm of Toepler pump 2, then the liquid nitrogen was blown off by air. The mercury was brought to one of the calibration marks of the gas buret and the pressure was read by a cathetometer. The combined volume of each of the break-seals and the dead volume in the Hoke valves were measured in this manner.

The azo compound was transferred from storage valve  $S_1$  to one of the break-seals by freezing at liquid nitrogen temperature, valve  $N_4$  was closed, then the azo compound was expanded to the manifold and the break-seals. The mercury in Toepler pump 1 was brought to the calibration mark CM2, then the pressure was read. Samples attached at valves  $H_1 - H_8$  were cooled down to liquid nitrogen temperature and sealed one by one. The break-seals were connected to the glass tubes for thermolysis (see

Figure 7).

In an experiment with a foreign gas such as nitric oxide or xenon, the azo compound was quantified in the above mentioned manner and frozen in one of the break-seals. A foreign gas was transferred and frozen in one of the break-seals and expanded to the manifold and the break-seals (the appropriate number of the break-seals could be used depending on the ratio of the foreign gas to the azo compound), then the gas in the manifold was taken back to a storage bulb. The valves of the break-seals which contained the azo compound and the foreign gas were opened and both gases were thoroughly mixed by raising and lowering ten times the mercury in Toepler pump 1. The mercury was then brought to calibration mark CMI and the pressure was again read. This was always found to be within an experimental error of the calculated value. For example, methylazo-3-propene was expanded to the manifold and eight break-seals (total volume =  $121.7 + 19.2 + 17.9 + 18.6 + 19.3 + 18.9 + 18.5 + 19.0 + 19.2 = 272.3$  ml). The pressure read 31.0 torr. Nitric oxide was measured in one of the break-seals (71.0 torr in 19.3 ml). Methylazo-3-propene and nitric oxide were thoroughly mixed, then the pressure was read 36.1 torr (calculated value,  $31.0 + \frac{19.3}{272.3} \times 71.0 = 31.0 + 5.0 = 36.0$  torr). The ratio of nitric oxide to methylazo-3-propene was calculated  $5.0/31.0 = 0.161$ . The amounts of the azo compound in the break-seals were calculated according to Boyle's law. For example, the 19.2 ml break-seal contained  $31.2 \mu\text{moles}$  of the azo compound at  $27^\circ$ .

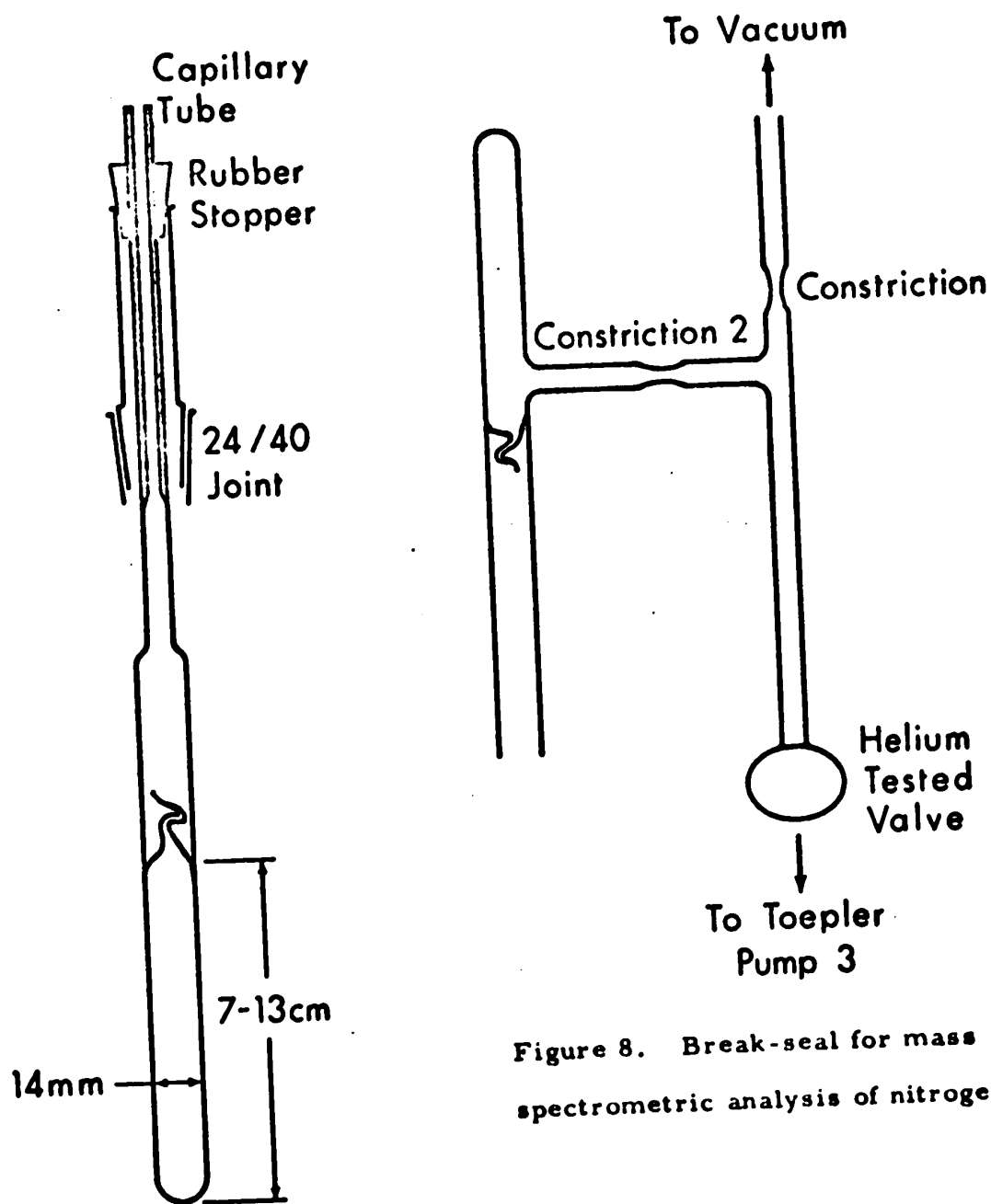


Figure 7. Break-seal connected to a glass tube for thermolysis.

Figure 8. Break-seal for mass spectrometric analysis of nitrogen.



The procedure was modified in the following manner for the azo compounds which have a low vapour pressure. Several 200 ml bulbs were glassblown to the ends of the bulbs. After conditioning overnight, the combined volumes of each of the break-seals and the dead volumes (the bulbs) were measured in the same manner as described above. The azo compound was transferred from a storage cylinder connected to the end of valve  $N_1$  to the bulb attached the Bourdon gauge. The pressure was read, then the azo compound was frozen onto the surface of the thermowell in Toepler pump 1 using liquid nitrogen. The mercury was then lifted up above the side arm of Toepler pump 1, and the liquid nitrogen was blown off. The azo compound was then expanded into the break-seals, the dead volumes and the side arms by lifting the mercury up to calibration mark 2. The subsequent procedure was the same as that described for the more volatile samples.

(b) Reaction Bath

The reaction was carried out in a well insulated covered oil bath. The temperature was controlled by a Melabs proportional temperature controller, and was measured with a four junction iron-constantan thermocouple, using a reference ice bath, and calibrated with a Hewlett-Packard 2801A (NBS) quartz thermometer. Readings were taken with a Leeds & Northrup Type K potentiometer. The oil bath temperature was maintained within  $\pm 0.02^\circ$ .

(c) Method of Analysis of Products

i) Thermolysis products of methylazo-3-propene (36).

After the reaction the break-seals were again connected to the manifold for analysis and then pumped overnight for conditioning. In an experiment without any foreign gas, valves  $H_1 - H_8$ ,  $N_8$ ,  $F_2$ ,  $F_3$ ,  $N_5$ ,  $N_6$ ,  $F_6$ ,  $F_7$ ,  $F_8$ ,  $N_7$ ,  $N_9$  and  $N_{10}$ , and MCl were closed, the mercury in valve  $F_9$  was brought to calibration mark CM3 and traps 2 and 3 were cooled in liquid nitrogen. One of the break-seals was broken by a piece of magnet covered with glass, then the valve  $H_n$  was opened. After 5 minutes  $F_6$  was opened. When the pressure was constant in Pirani gauge  $P_3$ ,  $N_7$  was opened and non-condensable gases (nitrogen and methane) were pumped out by means of Toepler pump 3 until the pressure on Pirani gauge 3 remained constant. The mercury was brought to the calibration mark of the gas buret and the pressure was read. The mercury in valve  $F_{10}$  was brought to point A, valve  $F_9$  was opened, then the non-condensable gases in the gas buret were transferred to trap 4 by means of Toepler pump 3. The mercury in Toepler pump 3 was brought to point B and the non-condensable gases were injected onto a gc column by closing valve  $H_{10}$  and opening valves  $H_9$  and  $H_{11}$ . After the non-condensable gases were analyzed by gc, valves  $H_9$  and  $H_{11}$  were closed,  $H_{10}$  opened, then  $F_{10}$  opened carefully. After ten minutes,  $F_6$  was closed,  $F_8$  and  $N_{10}$  opened and the helium was pumped out. Valves  $F_8$  and  $N_7$  were closed and the mercury in the Toepler pump 3 was brought to point B. Trap 4 was cooled in

liquid nitrogen, valve  $F_6$  was opened, then liquid nitrogen was removed from traps 2 and 3. After the condensable gases were transferred to trap 4, the mercury in valve  $F_{10}$  was brought to point A. The liquid nitrogen was removed from trap 4, then the condensable gases were injected onto a gc column (10 ft dimethylsulfolane column).

ii) Thermolysis products of tert-butylazo-3-propene (49).

The procedures were essentially the same as those for methylazo-3-propene except that trap 2 was cooled in an n-pentane slurry ( $-130^\circ$ ) and trap 3 in liquid nitrogen. The  $C_4$  components trapped in trap 3 were analyzed using a 10 ft dimethylsulfolane column and then the  $C_{6-8}$  components trapped in trap 2 were analyzed by using a 3 ft dimethylsulfolane column.

iii) Nitric oxide and xenon experiments.

When nitric oxide or xenon was present as a foreign gas, solid nitrogen was produced in the solid nitrogen trap ( $-210^\circ$ ) and valve  $F_6$  was opened. After the pressure caused by the non-condensable gases was constant on Pirani gauge 3 the valve  $N_7$  was opened. The non-condensable gases were then pumped out, measured in the gas buret, and then injected onto a gc column.

The nitric oxide trapped in the solid nitrogen trap was pumped out, and the xenon trapped in the liquid nitrogen traps was pumped out at liquid argon temperature ( $-186^\circ$ ). Condensable gases were analyzed by gc in the aforementioned manner. Ethane,

the most volatile condensable gas was not found to be pumped off at the liquid argon temperature.

Nitric oxide and isotopic nitric oxide  $^{15}\text{NO}$  were purified by sublimation from a trap immersed in liquid argon to a trap immersed in liquid nitrogen. The  $\text{N}_2\text{O}$  content was thus reduced to 0.05%.

For mass-spectrometric analysis of nitrogen the nitrogen collected in the gas buret was transferred to a break-seal in the following manner: a break-seal with constricted side arms was connected on the top of Toepler pump 3 (Figure 8). (The helium tested valve should be closed during the glass-blowing operation.) Constriction 1 was sealed while being pumped by a low vacuum pump. The helium tested valve, valves  $F_8$ ,  $F_9$  and  $N_7$  and mercury cut MC2 were opened for conditioning overnight. After the nitrogen was measured by the gas buret, float valve 9 was opened. The nitrogen was then transferred to the break-seal by means of Toepler pump 3, by lifting the mercury up to the side-arm, then constriction 2 was sealed.

#### iv) Gas chromatography.

The non-condensable fraction (methane and nitrogen) was analysed on a 5 ft, 1/4 in. glass column filled with 40-60 mesh high activity charcoal (Burrell). The column was calibrated for nitrogen and methane by injecting a known amount of each gas onto the column and measuring the corresponding peak area. Peak areas were measured by multiplying the peak height by the width at half height.

Seven calibration points were obtained for nitrogen, spaced over the range 16-67  $\mu$  moles, nine calibration points were obtained for methane, over the range 1.4-10  $\mu$  moles. The calibration was linear over the entire range and calibration factors determined by the method of least squares show a standard deviation of 2.6% for nitrogen and 4.9% for methane. The ratio of calibration factors (= ratio of sensitivity) for nitrogen and methane was 1.12, in good agreement with the figure 1.14 determined by Forst and Rice (11).

Condensable gases obtained in the thermolysis of methyl-azo-3-propene were analyzed on a 10-ft, 1/4 in. glass column filled with 20% dimethylsulfolane on 30-60 mesh Chromosorb P (Johns-Manville). The column was calibrated for 1-butene, 1,5-hexadiene and azomethane at room temperature. The ratios of sensitivities of 1-butene to 1,5-hexadiene, and 1-butene to azomethane were 0.83 and 1.11. This column was capable of separating ethane, carbon dioxide, propene, cyclopropane, 1-butene, allene, n-pentane, azomethane, 1,5-hexadiene and methylazo-3-propene, but not ethene- or carbon dioxide-nitrous oxide mixtures at room temperature. The ethane-ethene mixture was separated using an activated aluminum column at 0°. A 6 ft, 1/4 in. glass column filled with 30-60 mesh silica-gel (Hewlett-Packard) was capable of separating small amounts of ethane from xenon.

The C<sub>4</sub> components (isobutane and isobutene) obtained in the thermolysis of tert-butylazo-3-propene were analyzed on a 10 ft, 1/4 in. glass column filled with 20% dimethylsulfolane (F and M Scientific) on 30-60 Chromosorb P (Johns Manville). The C<sub>6</sub>

to C<sub>8</sub> components (1,5-hexadiene, 4,4-dimethyl-1-pentene and 2,2,3,3-tetramethylbutane) were analyzed on a 3 ft, 1/4 in. glass column filled with 20% dimethylsulfolane (F and M Scientific) on 30-60 mesh Chromosorb P (Johns Manville). This column was capable of separating 1,5-hexadiene, 2,2'-azoisobutane and tert-butylazo-3-propene. The relative retention times are recorded in Table XVIII.

(C) Syntheses

(a) Methylazo-3-propene (36)

Preparation of diethyl N-allylbicarbamate (38).

Sodium hydride (19.0 g of a 53.8% slurry, 0.425 mole) was added to a well stirred solution of diethyl bicarbamate (170 g, 0.985 mole) in 800 ml dimethoxyethane (dried by distillation from lithium aluminum hydride) using a protective atmosphere of nitrogen. Upon completion of addition the reaction mixture was stirred for an additional three hours. Allyl bromide (68 g, 0.56 mole) was then added and the solution stirred for an additional four hours.

After standing overnight the reaction mixture was treated with ice and water and the bicarbamate extracted with benzene. The benzene solution was dried over potassium carbonate and the excess benzene removed by evaporation.

The excess ethyl bicarbamate was removed by filtration. The filtrate was then separated into two layers, the upper layer (mineral oil from sodium hydride) was discarded, and

Table XVIII. Relative retention time data.

Column	Column temp. °C	Helium flow rate ml min <sup>-1</sup>	Relative retention time
10' Dimethylsulfolane on Chromosorb P	27	86	Air (0), ethane (0.15), ethene (0.15), carbon dioxide (0.29), nitrous oxide (0.29), propane (0.29), propene (0.42), cyclopropane (0.81), 1-butene (1.00), allene (1.15), n-pentane (1.62), azomethane (2.78), 1,5-hexadiene (9.3), methyl-azo-3-propene (24.5).
	27	86	Isobutane (1.00), isobutene (1.5).
10' Activated alumina	0	46	Air (0), ethane (1.0), ethene (1.5).
5' Activated charcoal	27	60	Start (0), nitrogen (1.0), methane (2.3).
6' Silica gel	27	60	Start (0), xenon (1.0), ethane (1.8).
3' Dimethylsulfolane on Chromosorb P	27	60	Air (0), 2,2-dimethyl-1-pentene (1.00), 1,5-hexadiene (1.30), 2,2,3,3-tetramethylbutane (1.90), 2,2'-azoisobutane (2.26), <u>tert-butylazo-3-propene</u> (8.72).

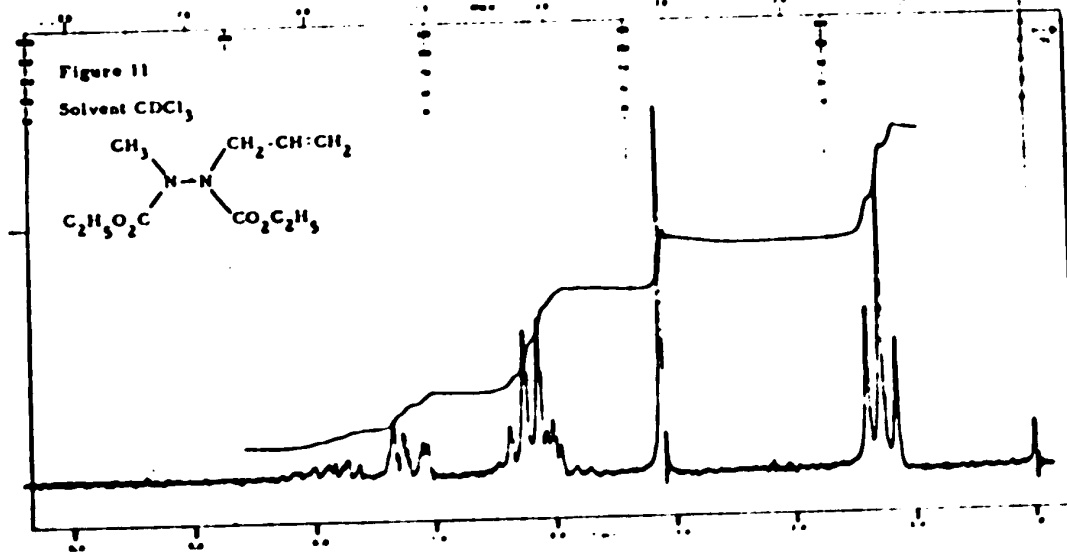
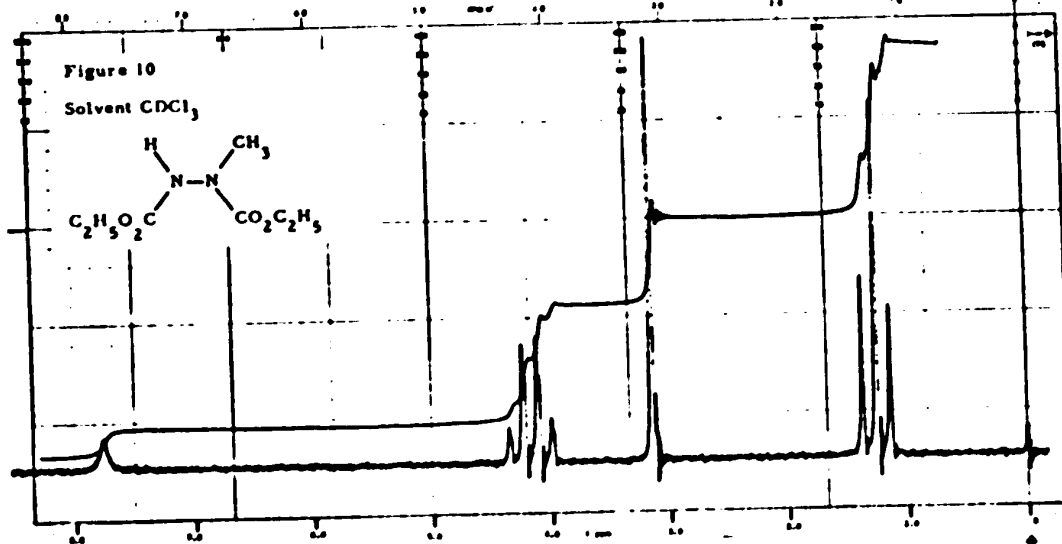
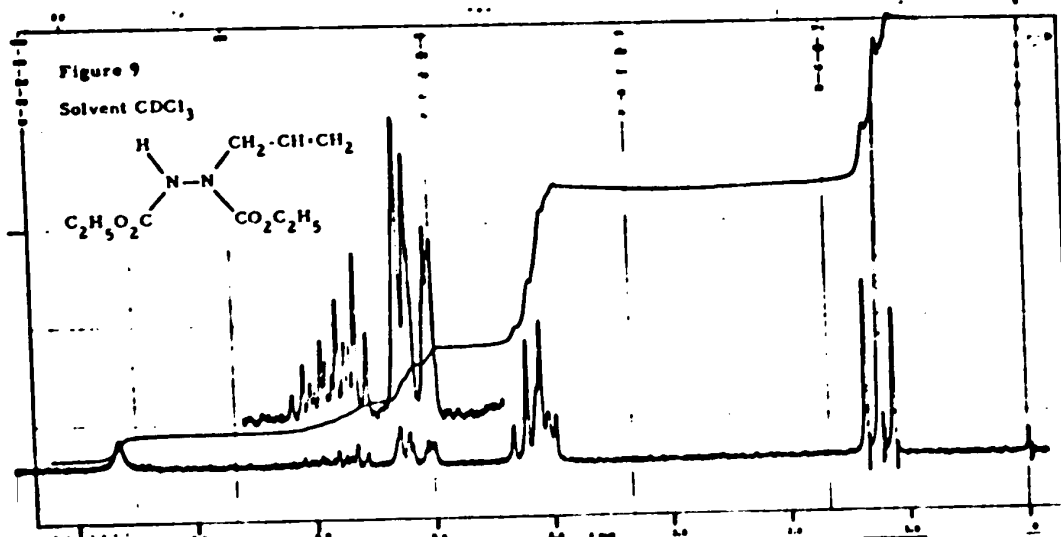
the lower layer was vacuum distilled through a 30 cm Vigreux column column bp  $94^{\circ}$ , 0.2 torr. Each fraction was analyzed by gc (10 ft, 7% carbowax,  $150^{\circ}$ ).

Fraction	Wt.	Diallyl compound
1	7.0 g	5%
2	5.5	1
3	71.0	0.5
4	8.8	—

The third fraction was carefully redistilled and the fraction bp  $102-103^{\circ}$  (0.5 torr), lit. (6) bp  $99-101^{\circ}$  (0.5 torr), was free from the diallyl compound 40 44.5 g (49% based on sodium hydride). The nmr spectrum (Figure 9) displayed signals at  $\delta$  1.25 (triplet, 6H, ester methyls),  $\delta$  4.12 (overlapping doublet and quartet, 6H, allylic and ester methylenes),  $\sim\delta$  5.12 (multiplet, 2H, vinylidene),  $\sim\delta$  5.86 (multiplet, 1H, methine) and  $\delta$  7.45 (broad singlet, exchangeable with  $D_2O-NaOD$ , 1H, NH).

The synthesis of diethyl N-methylbicarbamate (39) was achieved in the same manner described for the preparation of diethyl N-allyl-bicarbamate (38) except that methyl iodide was used instead of allyl bromide. The yield was 74% based on sodium hydride, bp  $94^{\circ}$  (0.5 torr), lit. (106) mp  $131^{\circ}$ . The nmr spectrum (Figure 10) displayed signals at  $\delta$  1.26 (triplet, 6H, ester  $CH_3$ ),  $\delta$  3.16 (singlet, 3H, N- $CH_3$ ),  $\delta$  4.18 (quartet, 4H, ester methylenes) and  $\delta$  7.66 (broad singlet, exchangeable with  $D_2O-NaOD$ , 1H, N-H).





The mass spectrum (MS-9, inlet temperature 185°) gave a parent peak at mass 190.0950 (calculated for  $C_7H_{14}N_2O_4$ , 190.0954).

Preparation of diethyl N-allyl-N'-methylbicarbamate (37).

Sodium hydride (9.9 g of a 53.8% slurry, 0.216 mole) was added to a mixture of 38 (44.5 g, 0.206 mole) in 300 ml of dimethoxyethane. The solution was maintained at room temperature under a blanket of nitrogen and stirring was continued for three hours after the addition of methyl iodide (60 g, 0.422 mole) was complete. After stirring overnight the mixture was treated with ice-water and the product was extracted with benzene. The benzene solution was dried over potassium carbonate and the solvent was removed on a rotary evaporator. The residue separated into two layers, and the upper layer (the mineral oil from the sodium hydride) was discarded. The lower layer was fractionally distilled through a 30 cm Vigreux column and each fraction was analyzed by gc (10 ft, 7% Carbowax column at 150°). After a small forerun there was obtained a 35 g (74%) sample, bp 72-73° (0.05 torr) free from impurities. The nmr spectrum (Figure 11) displayed signals at  $\delta$ 1.25 (triplet, 6H, ester methyls),  $\delta$ 3.08 (singlet, 3H, N-CH<sub>3</sub>),  $\delta$ 4.2 (overlapping doublet and quartet, 6H, allylic and ester methylenes),  $\delta$ 5.2 (multiplet, 2H, vinylidene) and  $\delta$ 5.9 (multiplet, 1H, methine).  
 Anal. Calcd. for  $C_{10}H_{18}O_4N_2$ : C, 52.16; H, 7.88; N, 12.17  
 Found: C, 52.16; H, 7.96; N, 12.29

Starting from 39 the compound 37 was prepared in the analogous manner described above except that allyl bromide was

used instead of methyl iodide. The yield was 87%.

Preparation of 1-allyl-2-methylhydrazine (42) and methylazo-3-propene (36).

A) Methanol method

A solution of 37 (11.5 g, 0.05 mole) and potassium hydroxide (11.2 g, 0.20 mole) in a methanol (60 ml) water (10 ml) mixture was refluxed under a nitrogen atmosphere for one hour. The solvent was then distilled off and concentrated hydrochloric acid was added to the distillate to give 0.9 g of 1-allyl-2-methylhydrazine hydrochloride upon further evaporation.

The original reaction residue was further distilled in vacuo and 3.5 g of the hydrazine hydrochloride was obtained by adding concentrated hydrochloric acid and evaporating the solvent. The residue of the last distillation was then taken up in water (50 ml) and methanol (20 ml) and refluxed for five hours under nitrogen. A repeated distillation, conc. hydrochloric acid treatment gave an additional 2.0 g of the hydrazine hydrochloride.

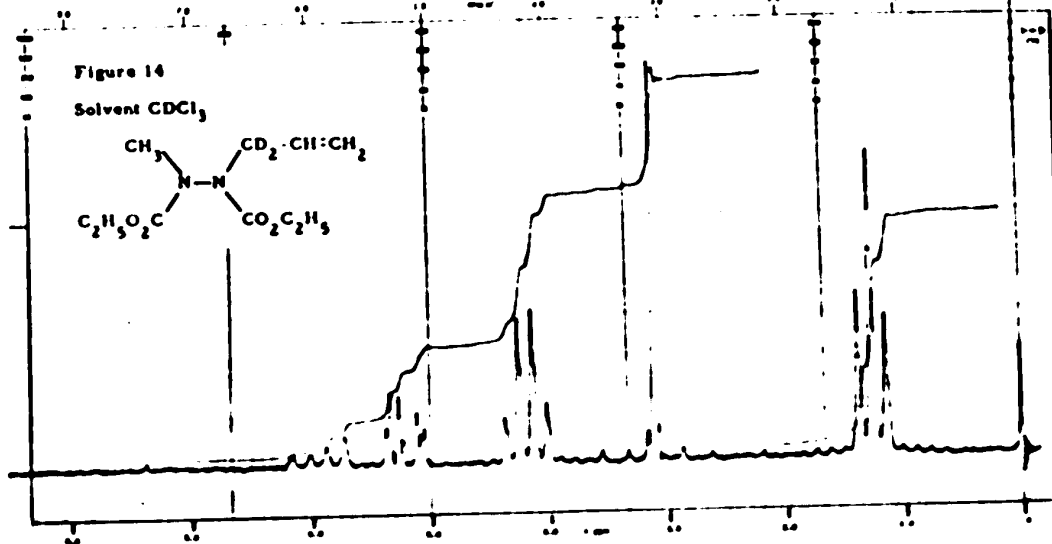
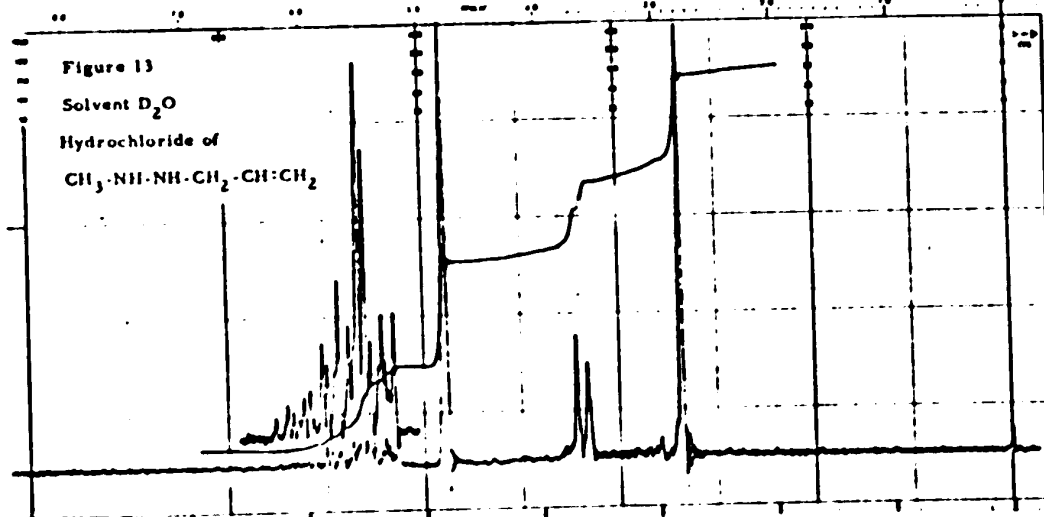
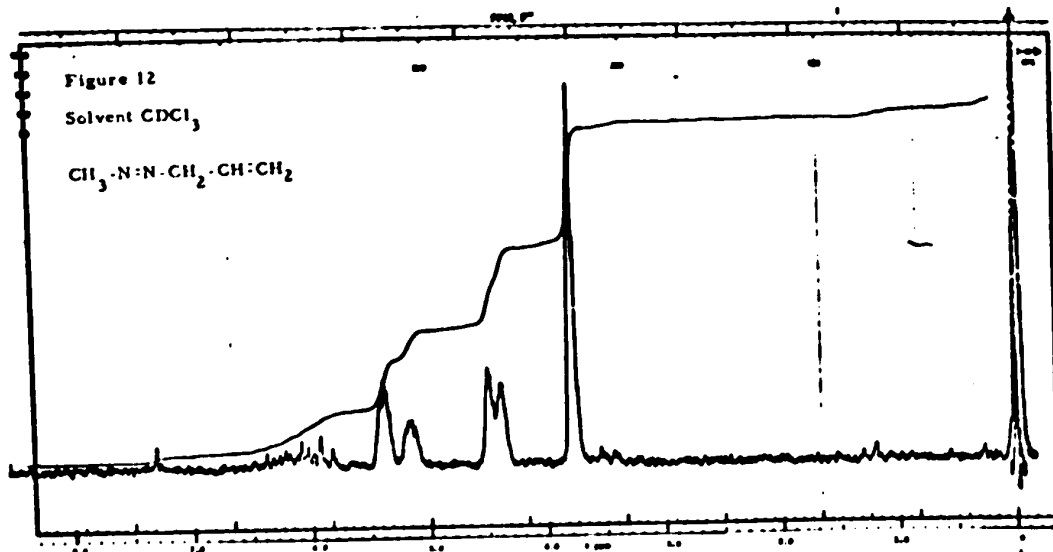
Potassium hydroxide (6 g, 0.12 mole) was added to a solution of the combined hydrazine hydrochloride portions in 15 ml water. The inorganic salt was filtered off and the aqueous filtrate was extracted with ether using a continuous extractor. The ether layer was then concentrated to 10 ml for use in the preparation of 36.

Preparation of methylazo-3-propene(36). A solution of 1-allyl-2-methylhydrazine (42) (1.0 g, 0.016 mole) in ether (10 ml) was added dropwise to a well stirred slurry of red mercuric oxide

(50 g, 0.23 mole) and anhydrous sodium sulfate (10 g) in dry ether (35 ml). After five hours the solution was filtered, concentrated to 3.5 ml by distillation through a Vigreux column, and the azo compound was separated by preparative gc using a 10%, 10 ft, Ucon 550X on Chromasorb column at 35°. The yield was 0.8 g (80%). The nmr spectrum (Figure 12) displayed signals at  $\delta$  3.78 (singlet, 3H, N-methyl),  $\delta$  4.46 (doublet, 2H, allylic methylene),  $\sim\delta$  5.3 (multiplet, 2H, vinylidene) and  $\sim\delta$  6.1 (multiplet, 1H, methine). The uv spectrum has a  $\lambda_{\max}$  at 345 nm ( $\epsilon = 20$  in gas). The mass spectrum (MS-9, inlet temperature 25°) gave a parent peak at mass 84.0687 (calculated for  $C_4H_8N_2$ , 84.0688). The following peaks were also observed; 15,  $CH_3^+$ ; 27,  $C_2H_3^+$ ; 28,  $N_2^+$  and  $C_2H_4^+$ ; 39,  $C_3H_3^+$ ; 41,  $C_3H_5^+$ ; 43,  $CH_3N_2^+$ ; 84,  $C_4H_8N_2^+$  parent; 99 (weak),  $C_5H_{11}N_2^+$ .

#### B) Ethylene glycol method

A slow stream of nitrogen was bubbled through 100 ml of warm ethylene glycol for 20 minutes in a mechanically stirred three necked flask. The gas inlet tube was replaced with a condenser and a thermometer, and potassium hydroxide (9.52 g, 0.168 mole) was added in four portions. The ethylene glycol solution was heated to 125° and 37 (8.5 g, 0.37 mole) was added as rapidly as possible to the stirred solution. After the addition, the temperature of the reaction was maintained at 125-130° for one hour. After being cooled, the mixture was cautiously added to 50 g each of ice and water and 30 ml of 12N hydrochloric acid. The ethylene glycol



and water were distilled off at 1-2 torr. The distillation residue was dissolved in water and extracted with ether. The ether extract contained a small amount of brown oil. The aqueous solution was basified with potassium hydroxide (5.0 g), then extracted overnight with ether using a continuous extractor. The ether was distilled off through a Vigreux column. An aliquot of the residue was shaken with diluted hydrochloric acid and then the excess hydrochloric acid and water were distilled off at  $90^{\circ}$  (2.0 torr). The nmr spectrum of the hydrazine hydrochloride (Figure 13) displayed signals at  $\delta$  2.81 (singlet, 3H, N-CH<sub>3</sub>),  $\delta$  3.67 (doublet, 2H, allyl),  $\delta$  4.84 (singlet, 4H, -NH<sub>2</sub><sup>+</sup>-) and  $\sim$  $\delta$  5.6 (multiplet, 3H, vinyl).

A solution of the crude hydrazine 42 in ether (50 ml) was treated with a well stirred slurry of red mercuric oxide (50 g, 0.23 mole) and anhydrous sodium sulfate (10 g). After five hours the solution was filtered, concentrated to 3 ml by distillation through a Vigreux column and the azo compound was separated by preparative gc. The yield was 0.9 g (20% yield based on 37).

Allyl-1,1-d<sub>2</sub> benzenesulfonate was prepared by the addition of allyl-1,1-d<sub>2</sub> alcohol to a mixture of benzene sulfonylchloride and 2,4,6-collidine at  $-4^{\circ}$  using the procedure described by Bergstrom et al.(107). The nmr analysis showed that the compound is completely deuterated in the desired position. Allyl-1,1-d<sub>2</sub>-alcohol was prepared from the reduction of acryl chloride with lithium aluminum deuteride using the method of Schultz et al. (108).

Diethyl N-(allyl- $1,1-d_2$ )-N'-methylbicarbamate (44).

Sodium hydride (1.05 g of a 57.2% slurry, 0.025 mole) was added to a well stirred mixture of 39 (4.75 g, 0.025 mole) in 40 ml of dimethoxyethane. The solution was stirred at room temperature under a nitrogen atmosphere for three hours, Allyl- $1,1-d_2$  benzene-sulfonate (5 g, 0.025 mole) in 10 ml of dimethoxyethane was then added and the solution stirred for an additional four hours. After standing overnight the reaction mixture was treated with ice-water and the product was extracted with benzene. The benzene solution was dried over potassium carbonate and the solution was removed on a rotary evaporator. The residue separated into two layers and the upper layer (the mineral oil from sodium hydride) was discarded. The lower layer was fractionally distilled through a 30 cm Vigreux column and each fraction was analyzed by gc.

After a small forerun a 3.0 g (52%) sample bp  $80^\circ$  (1 torr) free from impurities was obtained. The late fractions (1.0 g) were contaminated with 30% of the unreacted starting material. The nmr spectrum (Figure 14) displayed signals at  $\delta$  1.27 (triplet, 6H, ester methyls),  $\delta$  3.11 (singlet, 3H, N-CH<sub>3</sub>),  $\delta$  4.2 (quartet, 4H, ester methylene),  $\sim\delta$  5.2 (multiplet, 2H, vinylidene) and  $\sim\delta$  5.9 (multiplet, 1H, methine), and no allylic hydrogens at  $\sim\delta$  6.0.

Methylazo-3-propene- $3,3-d_2$ (43) was prepared by the hydrolytic decarboxylation (ethylene glycol method) of 44 (2.9 g, 0.125 mole), then subsequent oxidation using the same procedure used for the preparation of the afore-mentioned neutral compound 36.

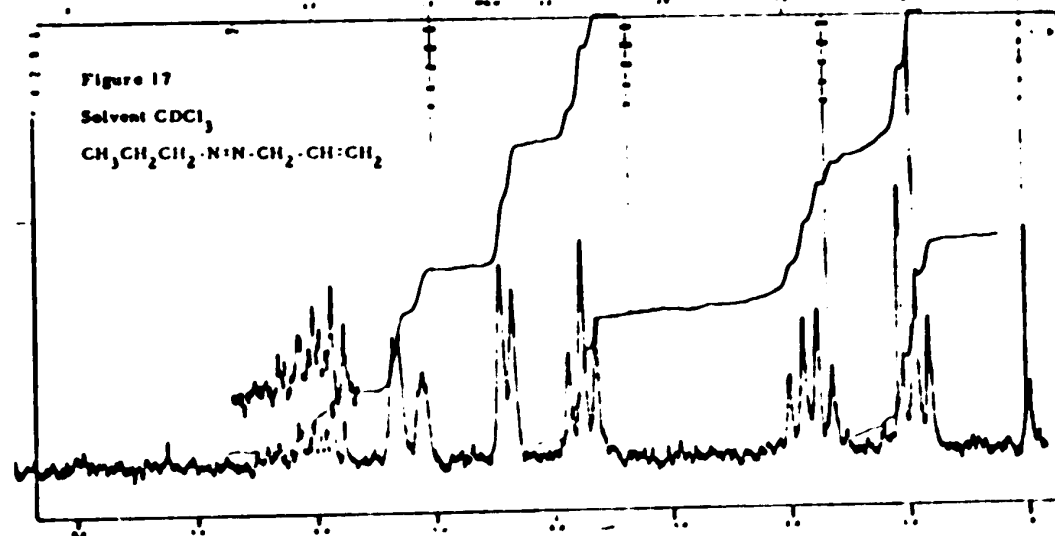
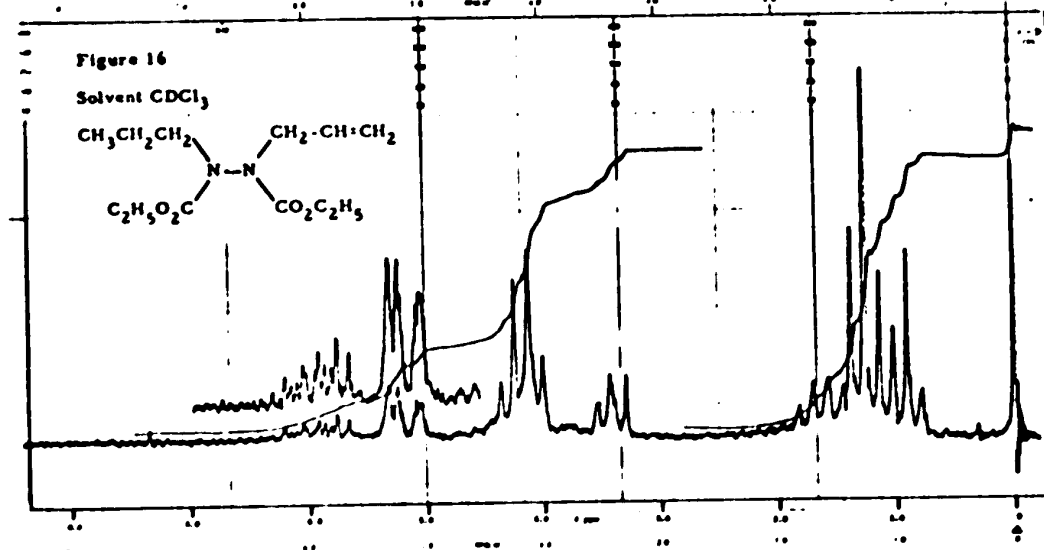
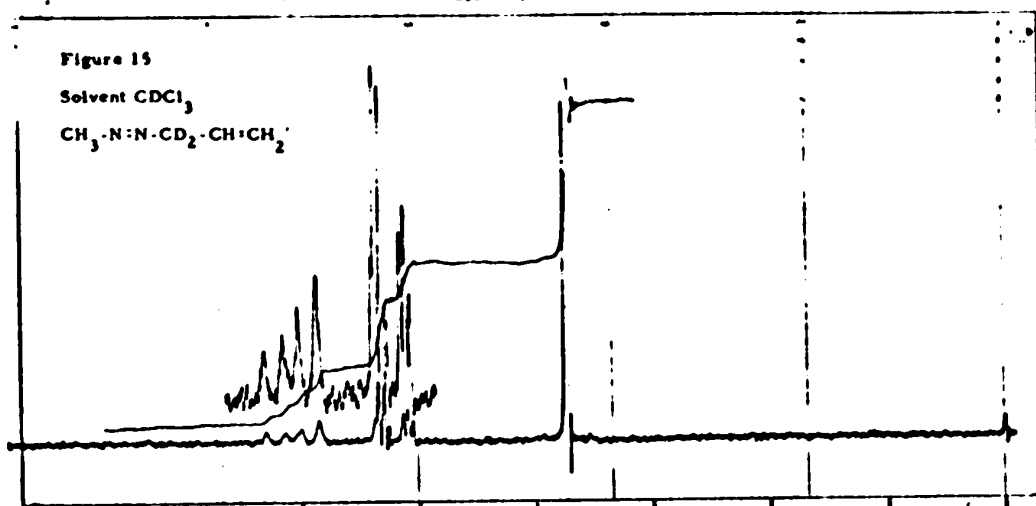
The yield was 0.2 g (19%). The nmr spectrum (Figure 15) displayed signals at  $\delta$  3.77 (singlet, 3H, N-methyl),  $\sim\delta$ 5.2 (multiplet, 2H, vinylidene),  $\sim\delta$ 6.1 (multiplet, 1H, methine) and no allylic hydrogens at  $\delta$  4.46. The mass spectral analysis showed a molecular ion which has a mass of 86.0824 (calculated for  $C_4H_6N_2D_2$ , 86.0813).

(b) 1-Propylazo-3'-propene (46).

Preparation of diethyl N-allyl-N'-(1-propyl)-bicarbamate

(45). Sodium hydride (2.53 g of a 57.2% slurry, 0.0602 mole) was added to a well stirred solution of 38 (13.0 g, 0.0602 mole) in 100 ml of dimethoxyethane. The solution was maintained at room temperature under a protective atmosphere of nitrogen and stirring was continued for an additional three hours. n-Propyl bromide (10 g, 0.0813 mole) and potassium iodide (1 g, 0.006 mole) were then added and the solution stirred for ten hours. An aliquot was taken out from the reaction mixture and after being treated with water, analyzed by gc (10 ft SF-96, 150<sup>o</sup>). 40% of the starting material was found unreacted. n-Propyl iodide (5.1 g, 0.030 mole) was added to the reaction mixture. The reaction was found to complete after the solution was stirred for an additional 20 hours. The mixture was treated with ice-water and the product was extracted with ether. The ether solution was dried over potassium carbonate, the solvent was removed on a rotary evaporator and the product was purified by distillation through a 30 cm Vigreux column, which gave 7.0 g (45% yield) bp 94-95<sup>o</sup> (1.0 torr). The nmr spectrum (Figure 16)





displayed signals at  $\sim\delta 1.25$  (overlapping triplets and sextet, 1H,  $\text{CH}_3\text{CH}_2\text{CH}_2\text{N-}$  and  $\text{CH}_3\text{CH}_2\text{O-}$ ),  $\delta 3.43$  (distorted triplet, 2H,  $\text{CH}_3\text{CH}_2\text{CH}_2\text{N-}$ ),  $\sim\delta 4.19$  (overlapping doublet and quartet, 6H, allyl and  $\text{CH}_3\text{CH}_2\text{-O-}$ ),  $\sim\delta 5.15$  (multiplet, 2H, vinylidene),  $\sim\delta 5.9$  (multiplet, 1H, methine). The mass spectrum (MS-9, inlet temperature,  $100^\circ$ ) gave a parent peak at mass 258.1576 (calculated for  $\text{C}_{12}\text{H}_{22}\text{N}_2\text{O}_4$ , 258.1580).

#### Preparation of 1-propylazo-3'-propene (46).

A slow stream of nitrogen was bubbled through 70 ml of ethylene glycol for 20 minutes in a mechanically stirred flask with mild heating. 6.7 g (0.118 mole) of potassium hydroxide was heated to  $125^\circ$  and  $\underline{45}$  (6.7 g, 0.026 mole) added as rapidly as possible to the stirred solution. After the addition the solution was stirred at  $125-130^\circ$  for one hour under a nitrogen atmosphere. The solution was colored slightly yellow. After being cooled, the mixture was cautiously added to 35 g each of ice and water and 21 ml of 12N hydrochloric acid. When acidification was complete, the mixture was warmed to about  $40^\circ$ . The water and ethylene glycol were distilled off at 1-2 torr. The solid residue obtained was dissolved in 70 ml of water and then extracted with ether. The evaporation of the ether gave 1 g of the starting material. The aqueous solution was basified by solid potassium hydroxide. 1-Allyl-2-(1-propyl) hydrazine was extracted with ether using a continuous extractor. The ether solution was dried over anhydrous sodium sulfate and used immediately for oxidation to  $\underline{46}$ .

The ether solution of 1-allyl-2-(1-propyl) hydrazine was stirred with a slurry of red mercuric oxide (10 g, 0.104 mole) and anhydrous sodium sulfate (20 g) for four hours. The ether was condensed to 3 ml through a 30 cm Vigreux column. A gas chromatographic analysis showed that the condensed solution contained ca. 20% of 1-propylazo-3'-propene (46) which was separated by gc using a 20%, 6 ft,  $\beta$ ,  $\beta'$ -oxydipropionitrile on Chromosorb P.

The nmr spectrum (Figure 17) displayed signals at  $\delta$  0.97 (triplet, 3H,  $\underline{\text{CH}_3}$ -CH<sub>2</sub>-CH<sub>2</sub>-N-),  $\delta$  1.82 (sextet, 2H, CH<sub>3</sub>- $\underline{\text{CH}_2}$ -CH<sub>2</sub>-N-),  $\delta$  3.76 (triplet, 2H, CH<sub>3</sub>-CH<sub>2</sub>- $\underline{\text{CH}_2}$ -N-),  $\delta$  4.40 (doublet, 2H, allyl methylene),  $\sim\delta$  5.2 (multiplet, 2H, vinylidene) and  $\sim\delta$  6.2 (multiplet, 1H, methine). The uv spectrum has a  $\lambda_{\text{max}}$  at 355 nm ( $\epsilon = 20$  in gas). The mass spectrum gave a parent peak at 112.1008 (calculated for C<sub>6</sub>H<sub>12</sub>N<sub>2</sub>, 112.1001). The following peaks were also observed: 27, C<sub>2</sub>H<sub>3</sub>; 28, N<sub>2</sub>, C<sub>2</sub>H<sub>4</sub>; 39, C<sub>3</sub>H<sub>3</sub>; 41, C<sub>3</sub>H<sub>5</sub>; 43, C<sub>3</sub>H<sub>7</sub>; 69, C<sub>3</sub>H<sub>5</sub>N<sub>2</sub>; 83, C<sub>6</sub>H<sub>11</sub>; 112, C<sub>6</sub>H<sub>12</sub>N<sub>2</sub> parent.

(c) tert-Butylazo-3-propene (47).

Benzophenone hydrazone was prepared from the reaction of benzophenone with hydrazine hydrate with acetic acid as a catalyst using the method of Curtius and Rauterberg (109).

Diphenyl diazomethane was prepared from the oxidation of benzophenone hydrazine with yellow oxide of mercury using the method of Organic Syntheses (110).

Benzophenone tert-butylhydrazone was prepared from the reaction of tert-butyl magnesium chloride with diphenyl diazomethane using the procedure described by Smith et al.(111).

tert-Butylhydrazine (48) was prepared from the hydrolysis of benzophenone tert-butylhydrazone with concentrated hydrochloric acid modifying the method of Smith et al.(111).

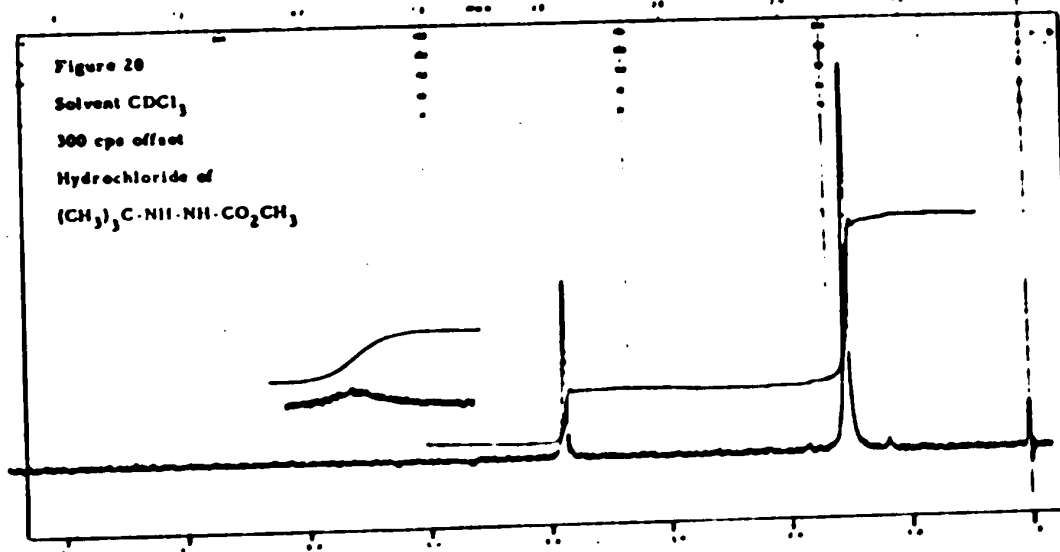
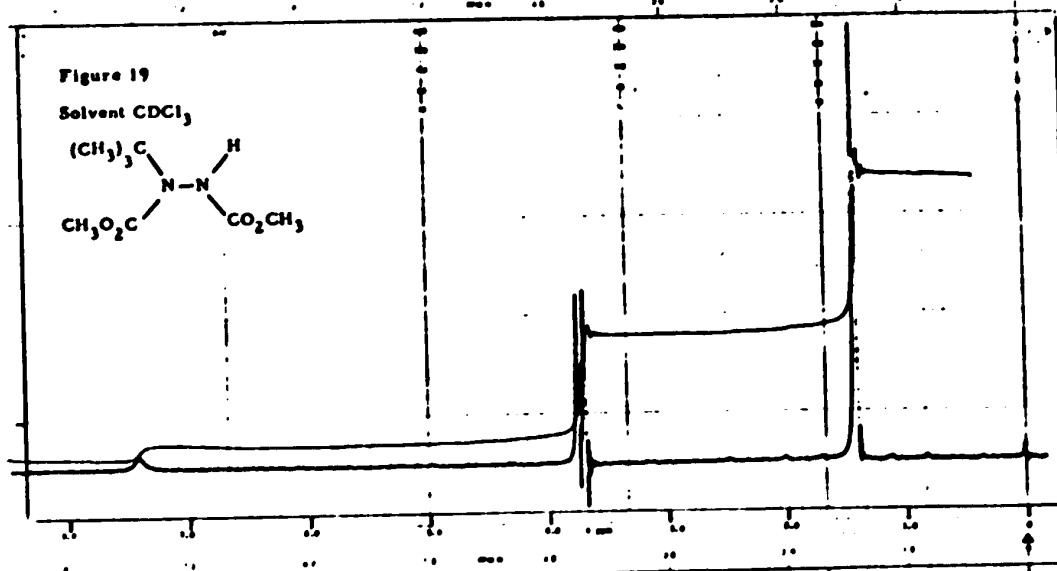
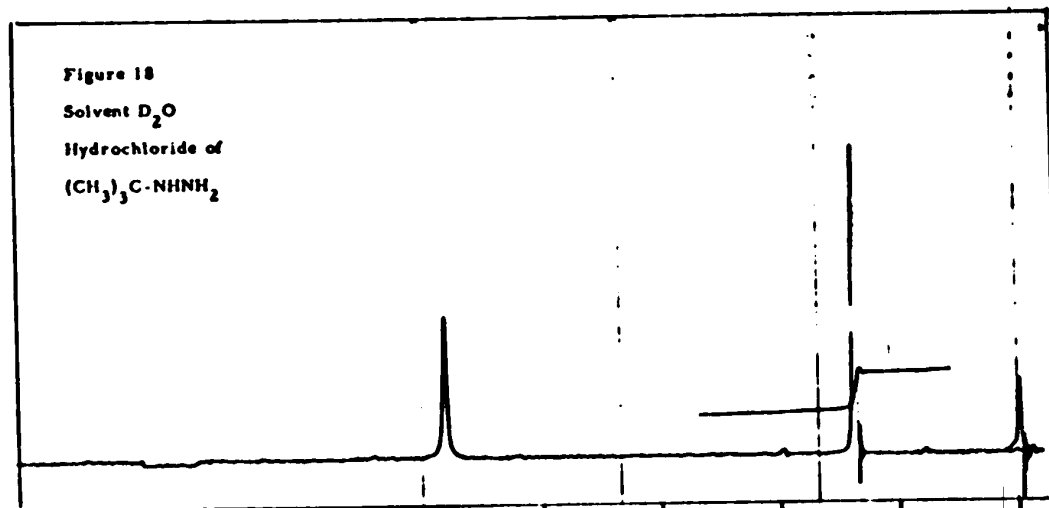
A mixture of 24.5 g (0.097 mole) of benzophenone tert-butylhydrazone, 35 ml of concentrated hydrochloric acid and 52 ml of 98% ethanol was allowed to stand at room temperature for 30 hours. The ethanol was evaporated and to the residue were added ether and water. The ether layer was separated and washed with water two times. The evaporation of the combined aqueous layer gave 3.5 g of tert-butylhydrazine hydrochloride mp 193-195<sup>o</sup> (lit. (111) 189<sup>o</sup>). The nmr spectrum in D<sub>2</sub>O (Figure 18) displayed signals at  $\delta$  1.39 (singlet, tert-butyl) and  $\delta$  4.83 (singlet, N-H).

The ether layer on evaporation left a mixture of benzophenone and benzophenone tert-butylhydrazone.

The further hydrolysis of the unreacted benzophenone tert-butylhydrazone in the same condition gave 3.5 g of tert-butylhydrazine hydrochloride. The hydrolysis was not complete. The further hydrolysis at 60<sup>o</sup> gave 3.5 g of tert-butylhydrazine hydrochloride.

Preparation of dimethyl N-tert-butylbicarbamate (50).

tert-Butylhydrazine hydrochloride (8.8 g, 0.0707 mole) was dissolved in 50 ml of water. Solid sodium hydroxide (6 g, 0.15 mole) was



then added to the solution. tert-Butylhydrazine was extracted by ether using a continuous extractor for ten hours.

The ether solution (50 ml) of tert-butylhydrazine was placed in a 300 ml Morton flask. When the stirred mixture had cooled to 5° methyl chloroformate (13.2 g, 0.14 mole) was added without allowing the temperature to rise above 5°. When almost half of the chloroformate had been added, a cold solution of sodium hydroxide (5.6 g, 0.14 mole) in 10 ml of water was added gradually along with the rest of the chloroformate at such a rate that the final portions of the two solution were added simultaneously. After standing for fifteen minutes the ether layer was separated and the aqueous solution was extracted with ether. The combined ether layers were rapidly dried by shaking for a short time with about 1 g of sodium carbonate in two portions. On evaporation of the ether the crude solid product (8 g) was obtained. After a small amount (ca. 0.3 g) of benzene insoluble impurity was removed 50 was crystallized from benzene-hexane, mp 82-83°. The yield was 6.5 g (45%).

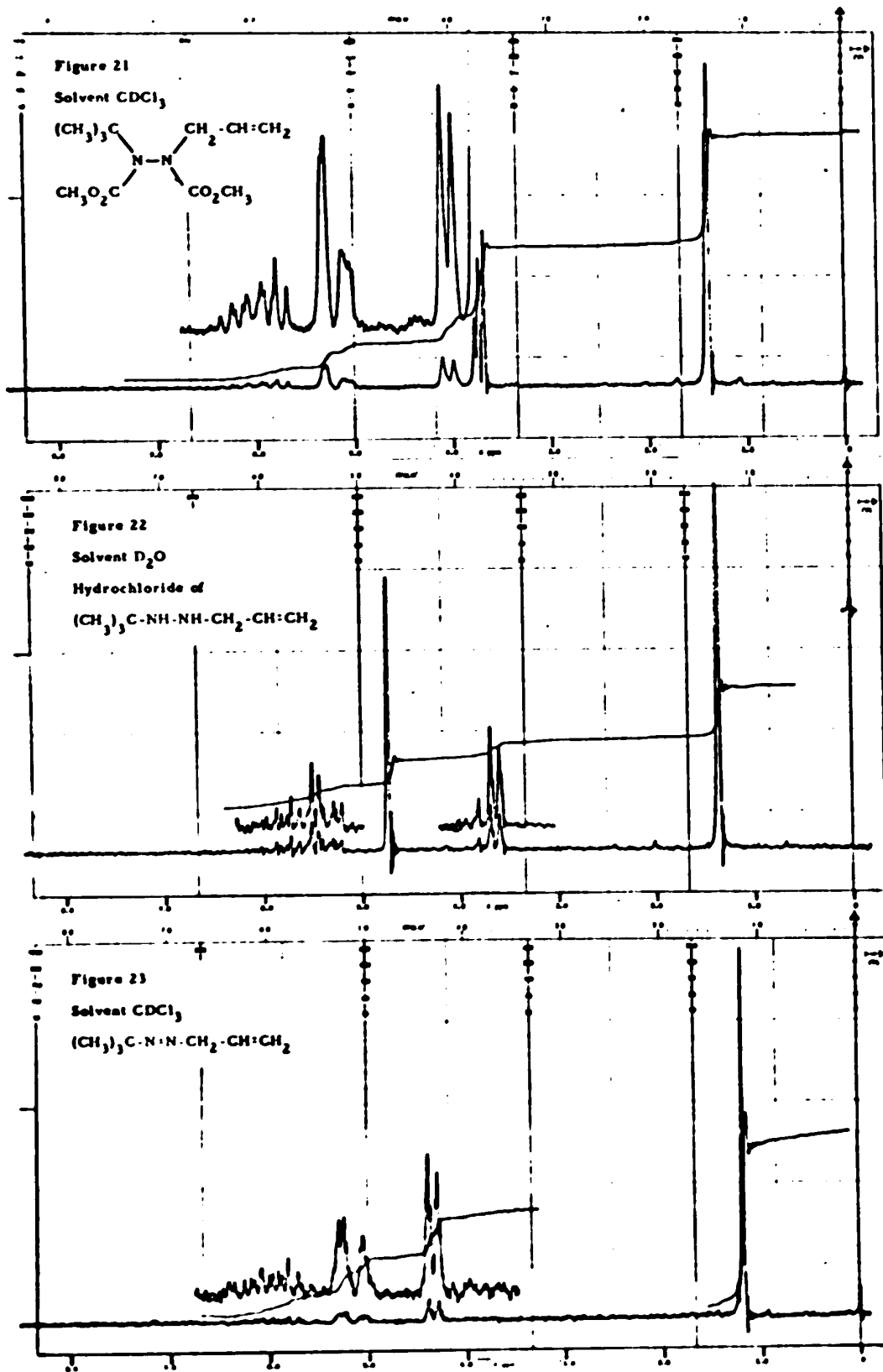
The nmr spectrum (Figure 19) displayed signals at  $\delta$ 1.41 (singlet, 9H, tert-butyl),  $\delta$ 3.69 (singlet, 3H, ester CH<sub>3</sub>),  $\delta$ 3.76 (singlet, 3H ester CH<sub>3</sub>) and  $\delta$ 7.40 (broad singlet, exchangeable with D<sub>2</sub>O-NaOD, 1H, NH). The mass spectrum (MS-9, inlet temperature, 100°) gave a parent peak at mass 204.1106 (calculated for C<sub>8</sub>H<sub>16</sub>N<sub>2</sub>O<sub>4</sub>, 204.1110).

The benzene-insoluble impurity (mp 180°) was soluble in

chloroform and water. The structure was assigned to 1-tert-butyl-2-carbomethoxyhydrazine hydrochloride by nmr spectrum. The nmr spectrum (Figure 20) displayed signals at  $\delta$  1.51 (singlet, 9H, tert-butyl),  $\delta$  3.88 (singlet, 3H, ester CH<sub>3</sub>) and  $\delta$  10.6 (broad singlet, exchangeable with D<sub>2</sub>O, 3H, N-H).

Preparation of dimethyl-N-allyl-N'-tert-butylbicarbonate (49). Sodium hydride (1.23 g of a 57.2% slurry, 0.03 mole) was added to a mixture of 50 (6.0 g, 0.0294 mole) and 50 ml of dry dimethoxyethane. The solution was maintained at room temperature under a blanket of nitrogen and stirring was continued for three hours. Allyl bromide (4 g, 0.033 mole) was then added and the solution stirred for an additional four hours. After standing overnight the reaction mixture was treated with ice and water and the product was extracted with benzene. The benzene solution was dried over anhydrous sodium sulfate and the solvent was removed on a rotary evaporator.

The crude product was distilled through a Vigreux column. The fraction which boiled at 90° (1.8 torr) was collected. The yield was 6.0 g (84%). The nmr spectrum (Figure 21) displayed signals at  $\delta$  1.39 (singlet, 9H, tert-butyl),  $\delta$  3.68, 3.74 and 3.78 (singlets, 6H, ester methyls),  $\delta$  4.04 (doublet, 2H, allylic methylene),  $\delta$  5.2 (multiplet, 2H, vinylidene) and  $\delta$  6.0 (multiplet, 1H, methine). The two singlets at  $\delta$  3.78 and  $\delta$  3.74 were found to coalesce at the temperature of 40 to 45° (see Figure 24). The mass spectrum (MS-9, inlet temperature 70°) gave a parent peak at mass 244.1418





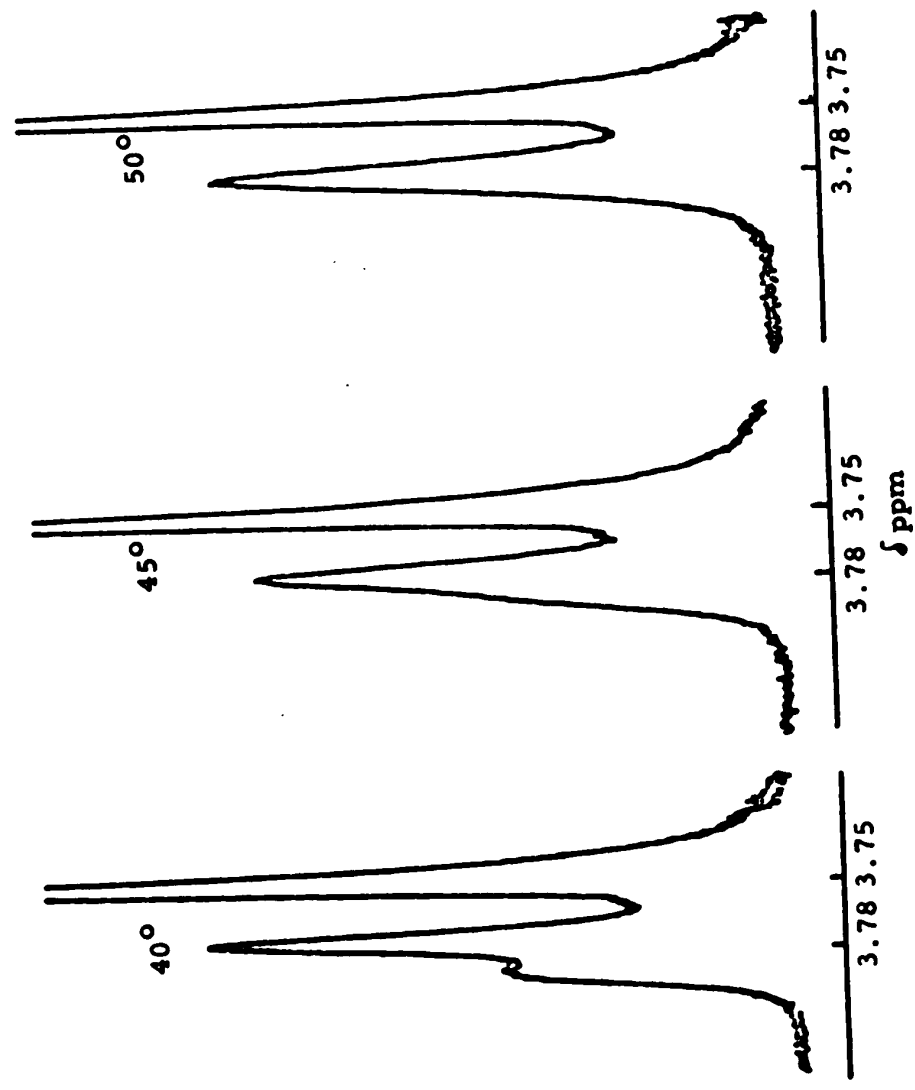


Figure 24. Temperature dependence of the peak corresponding to the ester methyl in dimethyl N-allyl-N'-tert-butylbucarbamate (49) in dimethyl sulfoxide.

(calculated for  $C_{11}H_{20}N_2O_4$ , 244.1423).

Preparation of 1-allyl-2-*tert*-butylhydrazine (51).

A slow stream of nitrogen was bubbled through 60 ml of ethylene glycol for 20 minutes in a mechanically stirred flask with mild heating. Potassium hydroxide (6.07 g, 0.107 mole) and the bicarbamate 49 (1.7 g, 0.0236 mole) were added. The mechanical stirrer was replaced with a Liebig condenser. The hydrazine 51 was distilled under a stream of nitrogen at the bath temperature of 150-160° along with the methanol formed. Concentrated hydrochloric acid was added to the distillate to give, upon further evaporation, 1.7 g of 1-allyl-2-*tert*-butylhydrazine hydrochloride mp 165-175°. The nmr spectrum in  $D_2O$  (Figure 22) displayed signals at  $\delta$  1.37 (singlet, 9H, *tert*-butyl),  $\delta$  3.64 (doublet, 2H, allylic methylene),  $\delta$  4.74 (singlet, 4H, N-H),  $\sim\delta$  5.5 (multiplet, 2H, vinylidene), and  $\sim\delta$  5.8 (multiplet, 1H, methine). The yield was 36%.

Preparation of *tert*-butylazo-3-propene (47).

Potassium hydroxide (3 g, 0.06 mole) was added to a solution of the hydrochloride of the hydrazine 51 (1.7 g, 0.00845 mole) in 20 ml of water. The hydrazine 51 was extracted with ether and the ether solution dried over anhydrous sodium carbonate. The dried solution of the hydrazine 51 (0.00845 mole) in ether (50 ml) was stirred at room temperature with a slurry of red mercuric oxide (10 g, 0.046 mole) and anhydrous sodium sulfate (20 g). After six

hours the solution was filtered, concentrated to two ml by distillation through a Vigreux column, and the azo compound 47 was separated by gc using a 20%, 2 ft, dimethylsulfolane on Chromosorb P at room temperature. The yield was 0.8 g (75%). The nmr spectrum (Figure 23) displayed signals at  $\delta$ 1.19 (singlet, 9H, tert-butyl),  $\delta$ 4.34 (doublet, 2H, allylic methylene),  $\sim\delta$ 5.2 (multiplet, 2H, vinylidene), and  $\sim\delta$ 6.2 (multiplet, 1H, methine). The uv spectrum has a  $\lambda_{\text{max}}$  at 355 nm ( $\epsilon = 25$  in gas). The mass spectrum gave a parent peak at mass 126.1159 (calculated for  $\text{C}_7\text{H}_{14}\text{N}_2$ , 126.1157). The following peaks were also observed: 28,  $\text{N}_2^+$ ,  $\text{C}_2\text{H}_4^+$ ; 29,  $\text{C}_2\text{H}_5^+$ ; 41,  $\text{C}_3\text{H}_5^+$ ; 57,  $\text{C}_4\text{H}_9^+$ ; 111,  $\text{C}_6\text{H}_{11}\text{N}_2^+$ ; 126,  $\text{C}_7\text{H}_{14}\text{N}_2^+$  parent.

2-Methyl-2-nitrosopropane was prepared from the oxidation of tert-butylhydroxylamine with bromine using the method of Emmons (112).

The synthesis of 3,3'-azo-1-propene (52) was achieved by mercuric oxide oxidation of the corresponding hydrazine which was in turn obtained from the hydrolysis of diethyl N,N'-diallyl-bicarbamate (40) according to the procedure of Al-Sader and Crawford (6).

2,2'-Azobutane was prepared from the oxidation of tert-butyl amine with iodine pentfluoride according to the procedure of Stevens (113).

(D) Control Experiments(a) Mass spectrometric analysis of nitrogen and isotopic nitric oxide  
 $^{15}\text{NO}$ .

The mass spectrometric analysis of  $^{15}\text{NO}$  used for the inhibition experiments were found reproducible (entries 1-5 in Table XIX). The mass spectrometric analysis of a pure nitrogen (entry 6) and of the nitrogen produced from methylazo-3-propene (36) and tert-butylazo-3-propene (47) (entries 8 and 9) was found consistent with the natural abundance of nitrogen ( $^{14}\text{N}^{15}\text{N}/^{14}\text{N}^{14}\text{N} = 7.4 \times 10^{-3}$  and  $^{15}\text{N}^{15}\text{N}/^{14}\text{N}^{14}\text{N} = \text{nil}$ ) (114). The entry 7 indicates no scrambling between  $^{15}\text{NO}$  and  $\text{N}_2$  under the thermolysis conditions.

(b) Reaction of 1-butene with nitric oxide

The reaction of 1-butene with NO was carried out in order to test the inertness of the olefinic bond in the azo compounds at the inhibited thermolysis condition. Table XX shows that the olefinic bond is expected to be stable toward NO less than  $130^\circ$  which is the highest temperature of the inhibited thermolysis of the azo compounds studied.

(c) Nmr analysis of the unreacted methylazo-3-propene-3,3-d<sub>2</sub> (43)

Mixtures of 43 and  $^{15}\text{NO}$  (29.1 - 31.4  $\mu\text{moles}$  of 43,  $^{15}\text{NO}/(43) = 0.161$ ) were thermolyzed at  $126.00^\circ$  for 30-130 min. The unreacted 43 was collected and analyzed by 100 Mc nmr. Figure 25 shows that the signal at  $\delta 4.46$  for allylic protons is completely absent indicating no scrambling during thermolysis, less than 1%.

Table XIX. Mass spectrometric analyses of some control experiments.

	Molecule	P <sub>28</sub>	P <sub>29</sub>	P <sub>30</sub>	P <sub>31</sub>
1	<sup>15</sup> NO	0.04	0.02	0.45	100
2	<sup>15</sup> NO	0.13	0.01	0.45	100
3	<sup>15</sup> NO	0.05	0.01	0.43	100
4	<sup>15</sup> NO	0.36	0.03	0.44	100
5	<sup>15</sup> NO	0.02	0.01	0.43	100
6	N <sub>2</sub>	100	0.71	nil	nil
7	N <sub>2</sub> from <sup>15</sup> NO + N <sub>2</sub> <sup>a</sup>	100	0.72	0.19	nil
8	N <sub>2</sub> from <u>36</u> <sup>b</sup>	100	0.74	0.41	nil
9	N <sub>2</sub> from <u>43</u> <sup>c</sup>	100	0.71	nil	nil

<sup>a</sup> A mixture of N<sub>2</sub> and <sup>15</sup>NO was heated at 129.5° for 1 hour.

<sup>b</sup> 36 was heated at 129.5° for 1 hour.

<sup>c</sup> 43 was heated at 122.3° for 15 minutes.

Table XX. Reaction of 1-butene (50  $\mu$ moles, 50 torr) with NO (150  $\mu$ moles, 150 torr).

Temperature $^{\circ}\text{C}$	Time hours	$\text{N}_2$ formed $\mu$ mole
130 - 133	10	0
140 - 145	2	0
140 - 145	10	6.4

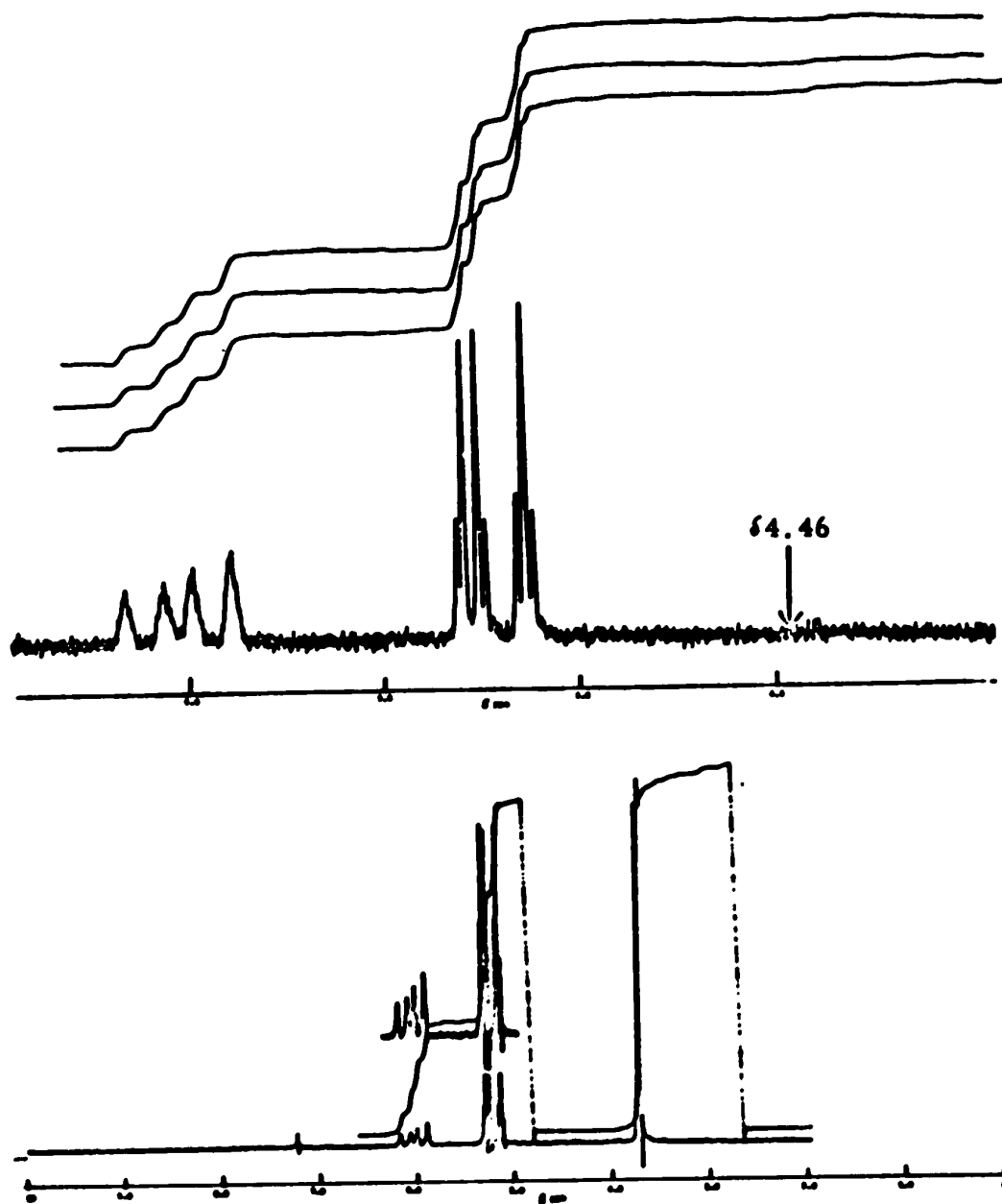
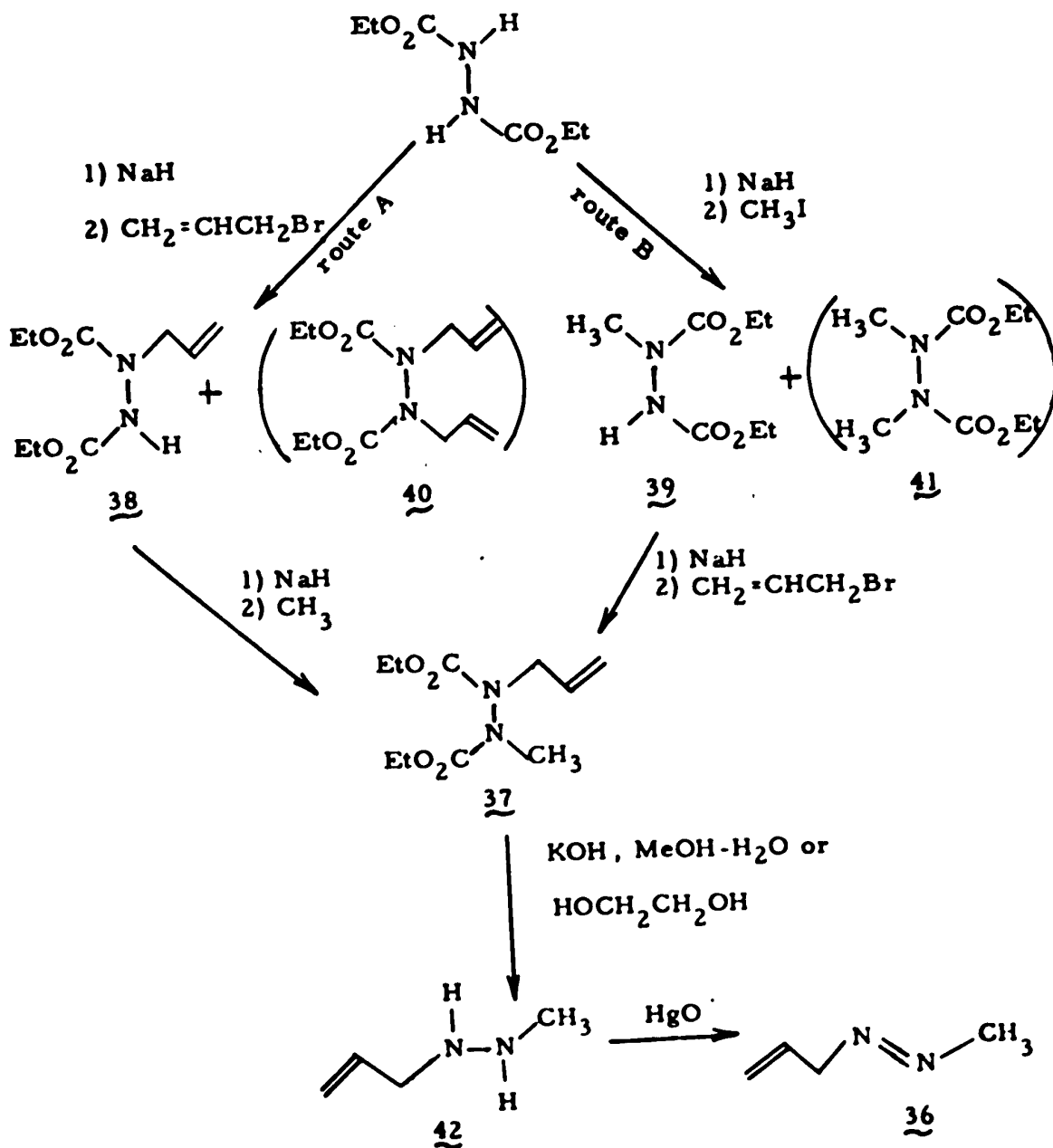


Figure 25. 100 Mc nmr spectrum of methylazo-3-propene-3,3-d<sub>2</sub> (43) recovered after the inhibited thermolysis with <sup>15</sup>NO.

## RESULTS AND DISCUSSION

(A) Syntheses

The synthesis of methylazo-3-propene (36) was achieved in the following manner:

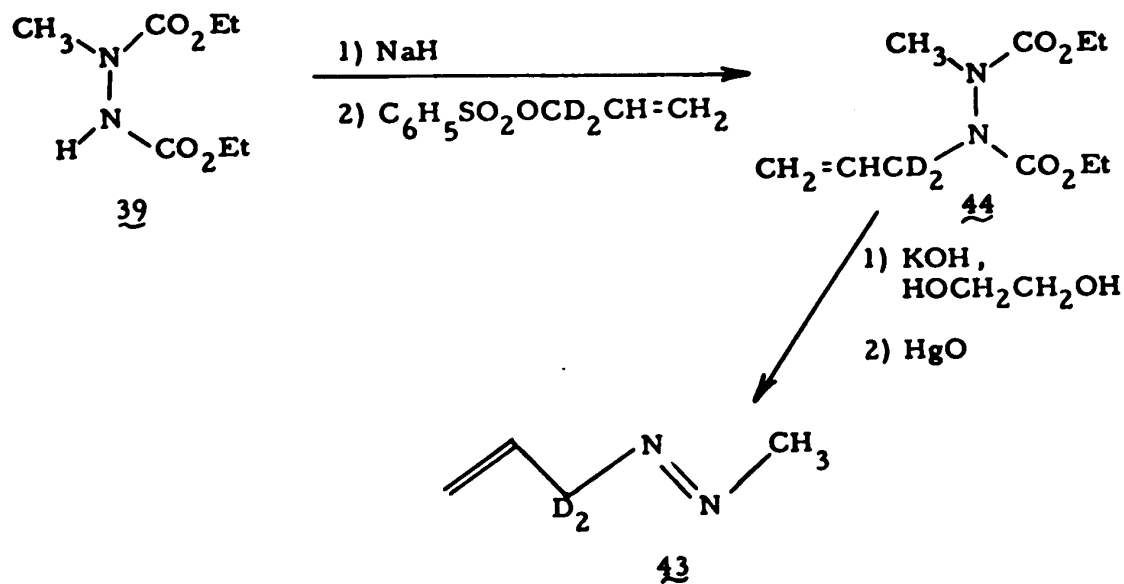




The synthesis of diethyl N-allyl-N'-methylbicarbamate (37) was accomplished by introducing methyl and allyl groups step-wise (both by route A and B).

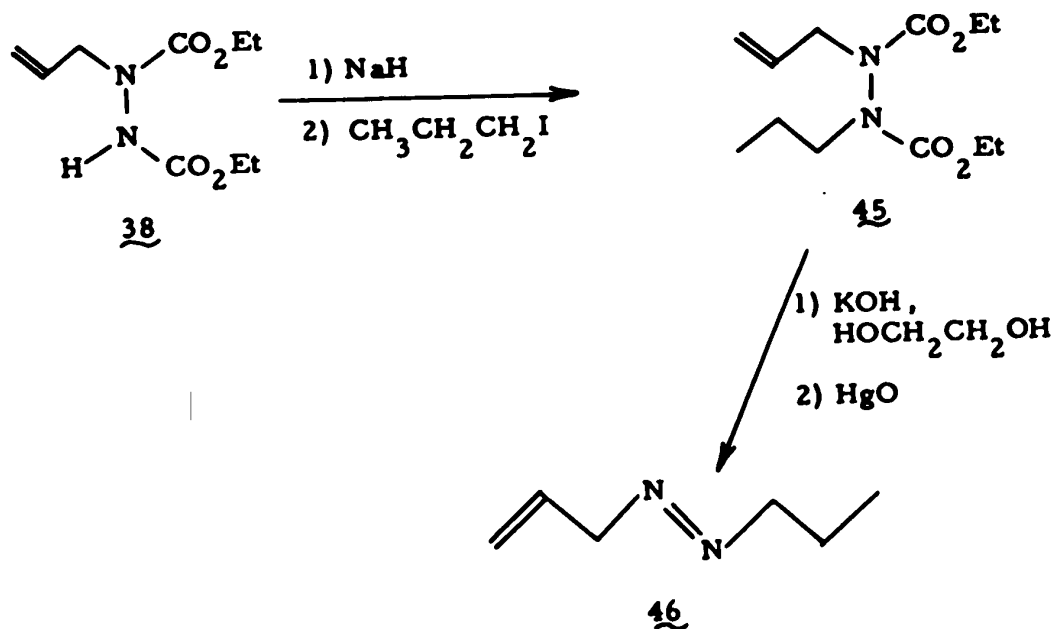
Special precaution was taken to minimize the formation of the dialkylated compounds 40 and 41 during the synthesis of the monoalkylated compounds 38 and 39. A two fold excess of diethyl bicarbamate was used and the crude monoalkyl compounds 38 and 39 were subjected to a very careful fractional distillation to separate the pure monoalkylated compounds 38 and 39 from traces of the dialkylated compounds 40 and 41. The nmr spectrum of 37 (Figure 11) displayed signals for the ester methyl (triplet at  $\delta$ 1.25), N-methyl (singlet at  $\delta$ 3.08), allyl and methylene (overlapping doublet and quartet at  $\sim\delta$ 4.2), vinylidene (multiplet at  $\sim\delta$ 5.2) and methine (multiplet at  $\sim\delta$ 5.9) protons with integration values of 6:3:6:2:1. The hydrolytic decarboxylation of 37 was achieved in an aqueous methanol or ethylene glycol solution, and the hydrazine 42 was oxidized to the azo compound 36 by mercuric oxide. The structure of 36 was established in the following manner. The nmr spectrum (Figure 12) shows signals at  $\delta$ 3.78 (singlet, 3H, N-methyl),  $\delta$ 4.46 (doublet, 2H, allylic methylene)  $\sim\delta$ 5.3 (multiplet, 2H, vinylidene) and  $\sim\delta$ 6.1 (multiplet, 1H, methine). The mass spectrum (MS-9, inlet temperature 25<sup>o</sup>) gave a parent peak at mass 84.0687 (calculated for C<sub>4</sub>H<sub>8</sub>N<sub>2</sub>, 84.0688). The synthesis of methylazo-3-propene-3,3-d<sub>2</sub> (43) was accomplished in the same manner described for the preparation of 36 except that allyl-1,1-d<sub>2</sub> benzenesulfonate

was used instead of allyl bromide.



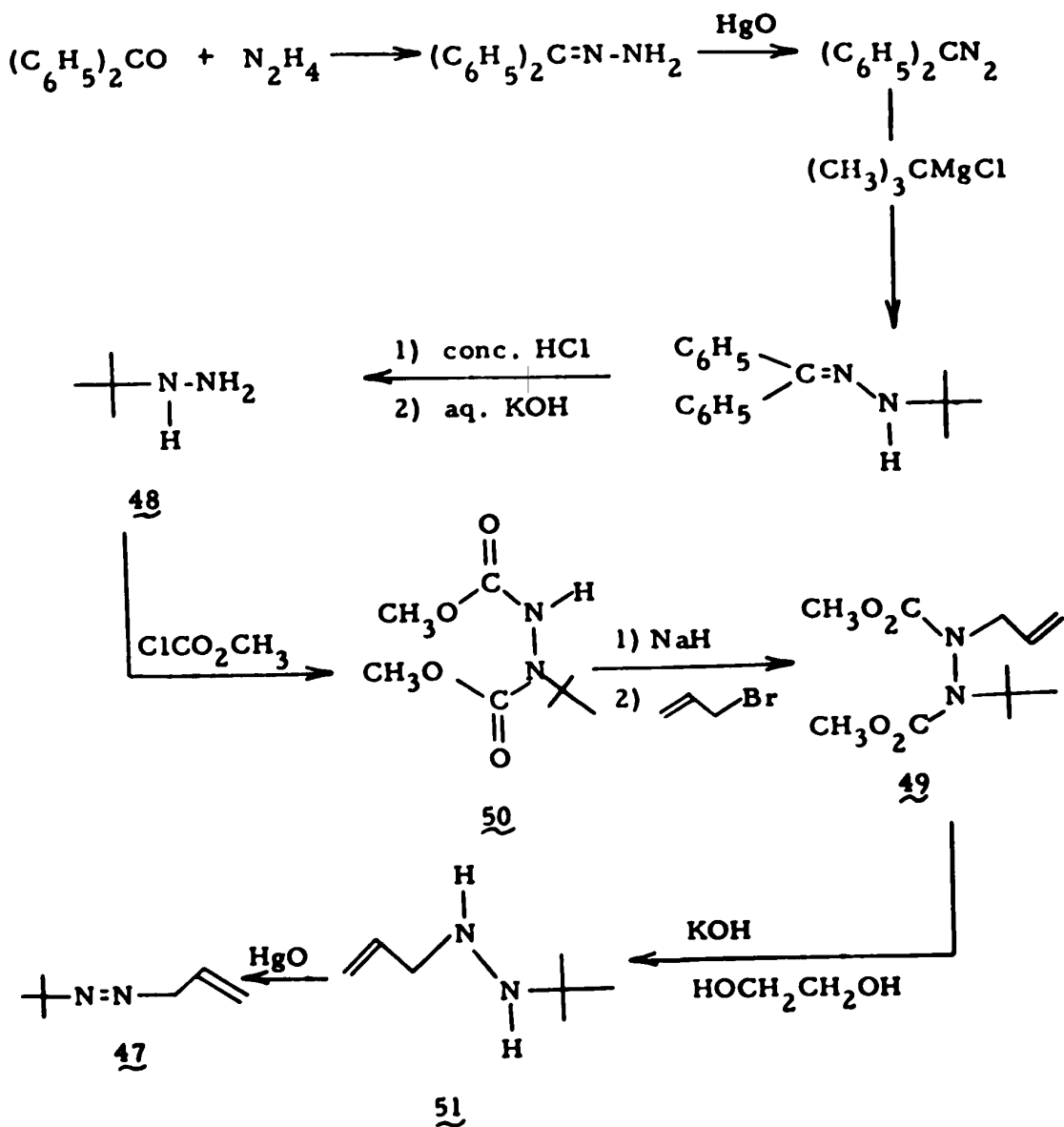
The nmr spectrum (Figure 14) for 44 displayed signals at  $\delta$  1.27 (triplet, 6H, ester methyl),  $\delta$  3.11 (singlet, 3H, N-methyl),  $\delta$  4.2 (quartet, 4H, methylene),  $\sim\delta$  5.2 (multiplet, 2H, vinylidene) and  $\sim\delta$  5.9 (multiplet, 1H, methine). The nmr spectrum of compound 43 is shown in Figure 15. The allylic proton signal at  $\delta$  4.46 found in 36 is completely absent. Mass spectral analysis (MS-9, inlet temperature 25 $^{\circ}$ ) showed a molecular ion which has a mass of 86.0816 (calculated for C<sub>4</sub>H<sub>6</sub>N<sub>2</sub>D<sub>2</sub>, 86.0813).

The synthesis of 1-propylazo-3'-propene (46) was achieved by the mercuric oxide oxidation of the corresponding hydrazine which was in turn obtained from the hydrolysis of 45 with an ethylene glycol solution of potassium hydroxide. The compound 45 was obtained by the reaction of n-propyl iodide with the bicarbamate 38.



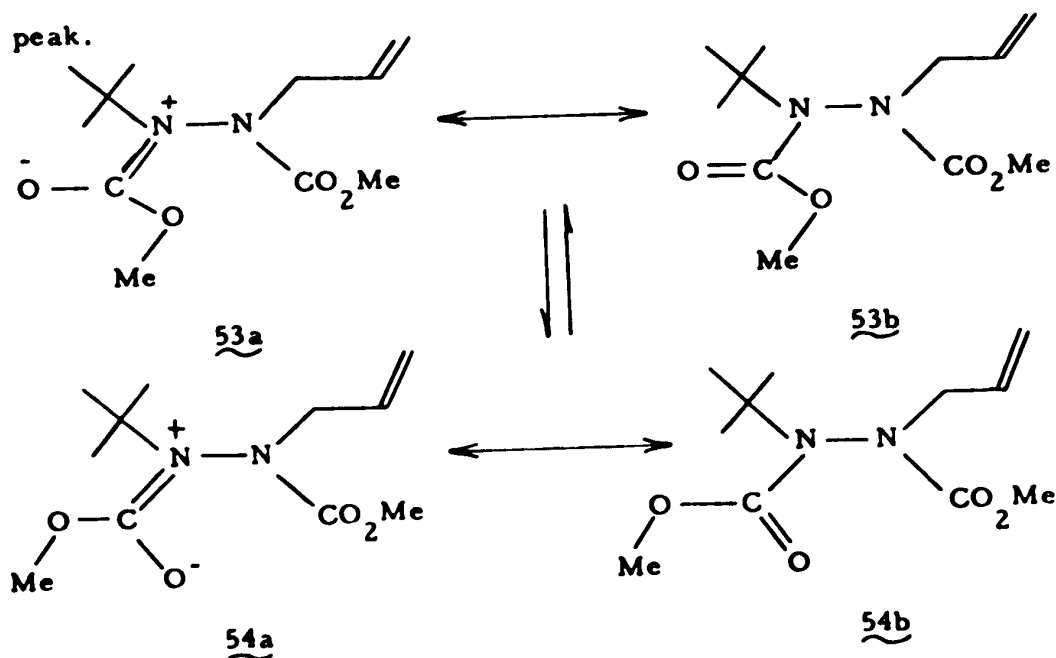
The structure of 46 was confirmed by nmr and mass spectral analysis. The nmr spectrum (Figure 17) displayed a triplet at  $\delta$ 0.97 ( $\text{CH}_3\text{CH}_2\text{CH}_2\text{-N-}$ ), sextet at  $\delta$ 1.82 ( $\text{CH}_3\text{CH}_2\text{CH}_2\text{-N-}$ ), a triplet at  $\delta$ 3.76 ( $\text{CH}_3\text{CH}_2\text{CH}_2\text{-N-}$ ), a doublet at  $\delta$ 4.40 (allyl protons), a multiplet at  $\sim\delta$ 5.2 (vinylidene) and a multiplet at  $\sim\delta$ 6.0 (methine) in the ratio of 3:2:2:2:2:1. The mass spectrum gave a parent peak at a mass of 112.1008 (calculated for  $\text{C}_6\text{H}_{12}\text{N}_2$ , 112.1001).

The synthesis of tert-butylazo-3-propene (47) was accomplished in the following manner:



tert-Butylhydrazine (48) was prepared according to the method of Smith et al.(111). The hydrazine 48 was converted to the dicarbomethoxy derivative 50 which was allylated to give the bicarbamate 49. The nmr spectrum of 50 (Figure 19) displayed signals at  $\delta$  1.41 (singlet, 9H, tert-butyl),  $\delta$  3.69 (singlet, 3H, ester methyl),  $\delta$  3.76 (singlet, 3H, ester methyl) and  $\delta$  7.40 (broad singlet, exchangeable

with  $D_2O$ -NaOD, 1H, N-H). Upon introducing the allyl group into 50, the singlet peak at  $\delta$  3.76 was split into two singlets at  $\delta$  3.74 and  $\delta$  3.78 as is shown in the nmr spectrum of 49 (Figure 21). The nmr spectrum shows signals corresponding to tert-butyl (singlet at  $\delta$  1.39), ester methyl (three singlets at  $\delta$  3.68,  $\delta$  3.74 and  $\delta$  3.78), allyl (doublet at  $\delta$  4.04), vinylidene (multiplet at  $\sim\delta$ 5.0) and methine (multiplet at  $\sim\delta$ 5.6) protons with integration values of 9:6:2:2:1. Figure 24 shows that the two singlets at  $\delta$  3.74 and 3.78 coalesce at the temperature of 40-45°. This behavior can be ascribed to the restricted rotation about the amide bond (117) which gives two geometrical isomers 53 and 54 at room temperature. With rapid isomerization at 40-45° the signals merge into a single peak.



The structure of 47 was established from its nmr and mass spectra. The nmr spectrum shows signals at  $\delta$  1.19 (singlet, 9H, tert-butyl),



Table XXI. Product composition from the thermolysis of methylaceto-3-propene (36) (57 torr) at 131.6°.

Time (min)	Completion %	Product composition relative to nitrogen formed						allyl radicals recovered	
		methane	1-butene	1,5-hexadiene	acetylene	ethane	n-pentane		methyl radicals recovered
105	12.2	30.8%	35.7%	19.4%	4.5%	0.9%	0.7%	78.1%	75.6%
330	30.3	36.0	33.3	18.7	4.6	0.7	0.7	80.7	71.8
465	38.5	35.3	31.0	18.0	4.4	0.7	0.8	77.3	68.2
600	48.3	34.3	27.1	16.5	3.8	0.7	0.7	71.2	61.2

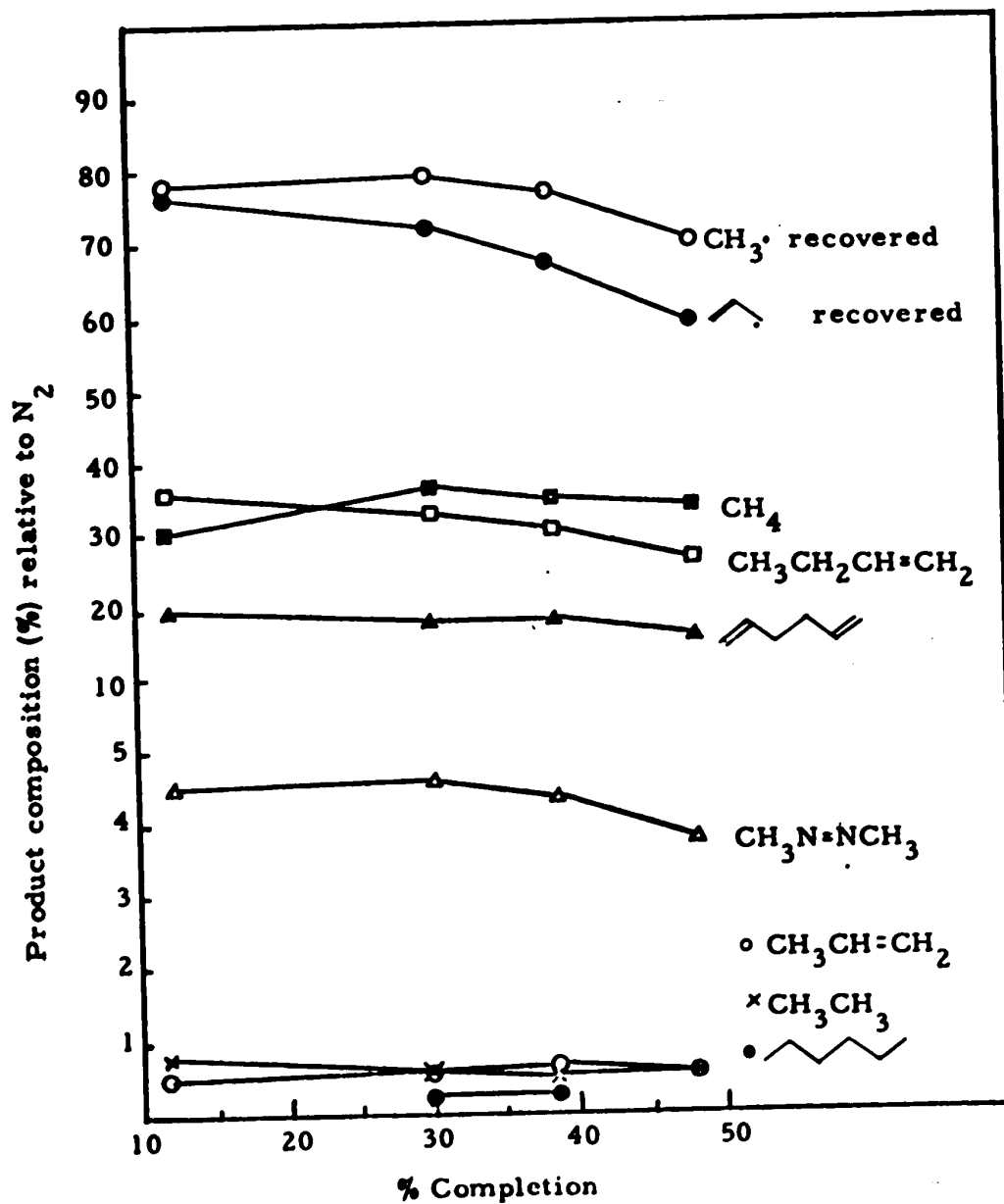


Figure 26. Product composition from the thermolysis of methyl-azo-3-propene (36), 57 torr at  $131.6^\circ$ .



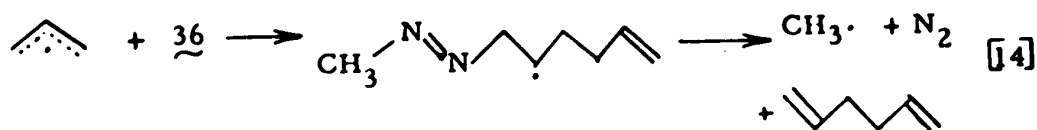
Table XXII. Mass spectral data of the thermolysis products of methylazo-3-propene (36).

Product	Ten strongest peaks observed	Ten strongest peaks listed in the literature (115)
Ethane	28, 30, 27, 29, 26	28, 27, 30, 26, 29
Propene	41, 42, 39, 40, 27, 38, 37, 26, 15, 14	41, 39, 42, 27, 40, 38, 37, 26, 15, 14
1-Butene	41, 56, 39, 28, 27, 55, 29, 26, 40, 53	41, 56, 39, 28, 55, 27, 29, 53, 40, 26
n-Pentane	43, 42, 41, 27, 29, 28, 39, 72, 57, 56	43, 42, 41, 27, 29, 39, 57, 72, 28, 15
Azomethane	15, 43, 58, 28, 27, 42, 57, 41, 14, 30	15, 43, 28, 42, 58, 27, 14, 13, 30, 41
Hexadiene	67, 41, 54, 39, 27, 81, 53, 55, 42, 40	41, 67, 39, 54, 27, 53, 81, 40, 28, 38

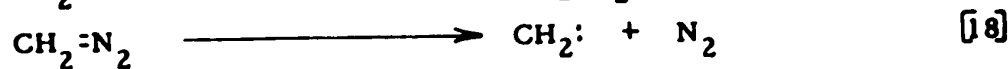
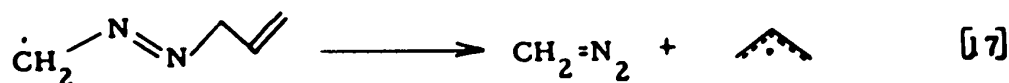




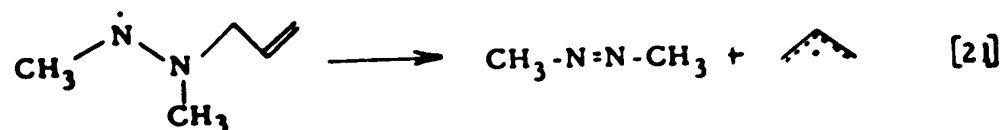
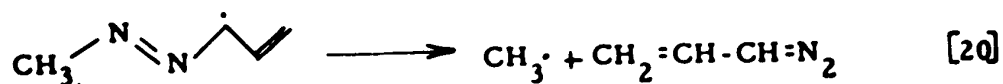
of 3,3'-azo-1-propene-3,3-d<sub>2</sub> (6).

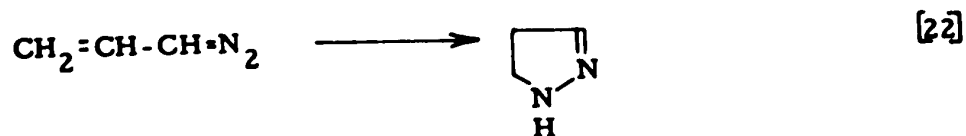


Since the rate of thermolysis of 36 was followed by the rate of formation of nitrogen, reaction 10-13 will affect the rate only if the ultimate fate of the radicals 56 - 59 is the formation of nitrogen. The ratio of the non-inhibited rate constant to the inhibited rate constant is ca. 1.6 (see the kinetic section) suggesting that about 38% of nitrogen produced comes from the radicals 56 - 59. The most probable reactions which produce nitrogen and which are part of radical chains and increase the rate of thermolysis of 36 are reaction 15-19.



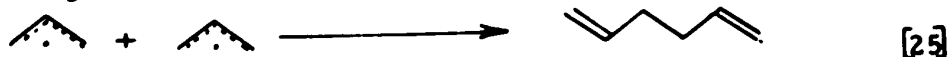
Reactions 20 and 21 do not produce nitrogen, since vinyldiazomethane isomerizes to 2-pyrazoline (118) via reaction 22 and azomethane is stable under the thermolysis conditions (11).



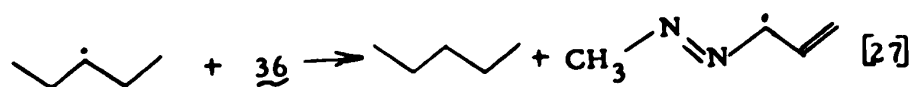
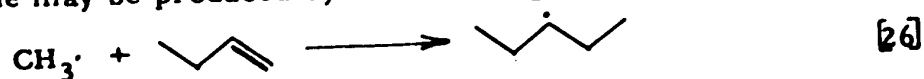


No 2-pyrazoline and only 5% of azomethane were produced, hence reactions 20 and 21 which lead to nitrogen-containing products are relatively unimportant.

Reactions 23 - 25 deal with the combination of methyl and allyl radicals which produced ethane, 1-butene and 1,5-hexadiene.



n-Pentane may be produced by the following reactions.



A mixture of 9 torr of 36 and 46 torr of xenon was decomposed at  $131.6^\circ$  to examine the effects of the initial pressure of 36 on the product composition. The results at varying percentage completion are given in Table XXIII and plotted in Figure 27. The product composition was found to be almost the same as that at the higher initial pressure.

Product studies of the gas phase thermolysis of tert-butylazo-3-propene (47) were carried out at  $122.3^\circ$  for 15 to 75 minutes and 1320 minutes was used for the infinity samples. The initial pressure of 47 was 46 torr (11.87  $\mu$ moles of 47 in a 4.5 ml

**Table XXIII. Product composition from the thermolysis of methylazo-3-propene (36) in the presence of xenon at 131.6°.**

Time (min)	Conversion	Product composition (relative to nitrogen formed)				
		methane	1-butene	1,5-hexadiene	azomethane	ethane propene
100	9.47%	30.6%	32.1%	22.4%		
200	16.54	28.1	37.2	22.1		
300	21.5	28.0	30.0	21.0		
465	34.5	27.6	33.7	21.4	3.6%	1.6% 1.2%
600	38.4	29.4	33.6	20.9	3.6	1.1 1.1

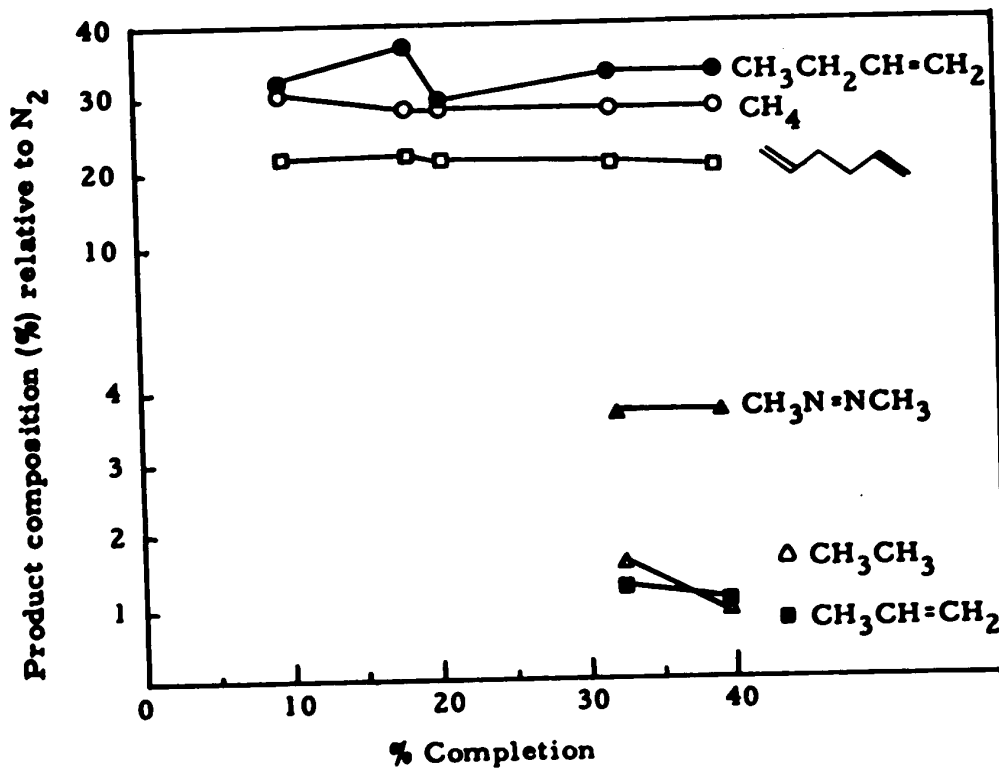
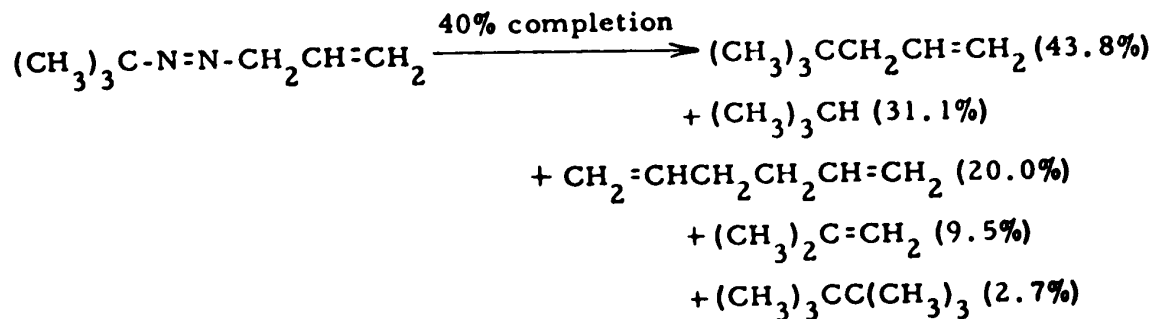


Figure 27. Product composition from the thermolysis of methyl-azo-3-propene (36), torr in the presence of xenon, 46 torr at 131.6°.

break-seal). The thermolysis products were identified by their gas chromatographic retention times and their mass spectrometric cracking patterns.



The results at varying percentage completion are given in Table XXIV and plotted in Figure 28. The results of the mass spectrometric analysis are shown in Table XXV.

The mole percent of allyl and tert-butyl radicals recovered are calculated according to the equations:

$$\frac{\% \text{ allyl radicals recovered}}{\% \text{ allyl radicals recovered}} = \% \text{ 4,4-methyl-1-pentene} + 2(\% \text{ 1,5-hexadiene})$$

$$\frac{\% \text{ tert-butyl radicals recovered}}{\% \text{ tert-butyl radicals recovered}} = \% \text{ isobutane} + \% \text{ isobutene} + \% \text{ 4,4-dimethyl-1-pentene} + 2(\% \text{ 2,2,3,3-tetramethylbutane})$$

The following reactions 28 - 35 are probably the most important ones which account for the products of the thermolysis of tert-butyl-3-propene (47).

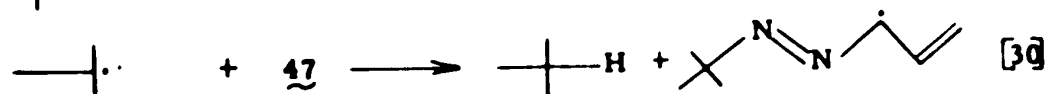




Table XXIV. Product composition from the thermalolysis of *tert*-butylazo-3-propene (47) at 122.3°.

Reaction time minutes	Conversion	Product composition (relative to nitrogen formed)				allyl radicals recovered	<i>tert</i> -butyl radicals recovered	
		isobutane	isobutene	1,5-hexadiene	4,4-dimethyl- 1-pentene			2,2,3,3-tetra- methylbutane
15	21.6%	49.2%	11.6%	20.9%	44.6%	2.7%	86.4%	110.9%
30	40.0	33.1	9.5	20.0	43.8	2.7	83.8	91.8
45	52.7	30.0	7.6	18.6	40.8	2.7	78.0	84.0
60	63.5	30.3	8.2	19.3	40.1	2.6	78.7	82.8
75	71.0	30.1	8.3	20.1	47.1	3.1	87.3	85.5
1320	100.0	28.8	8.5	15.3	34.2	2.8	64.6	77.1

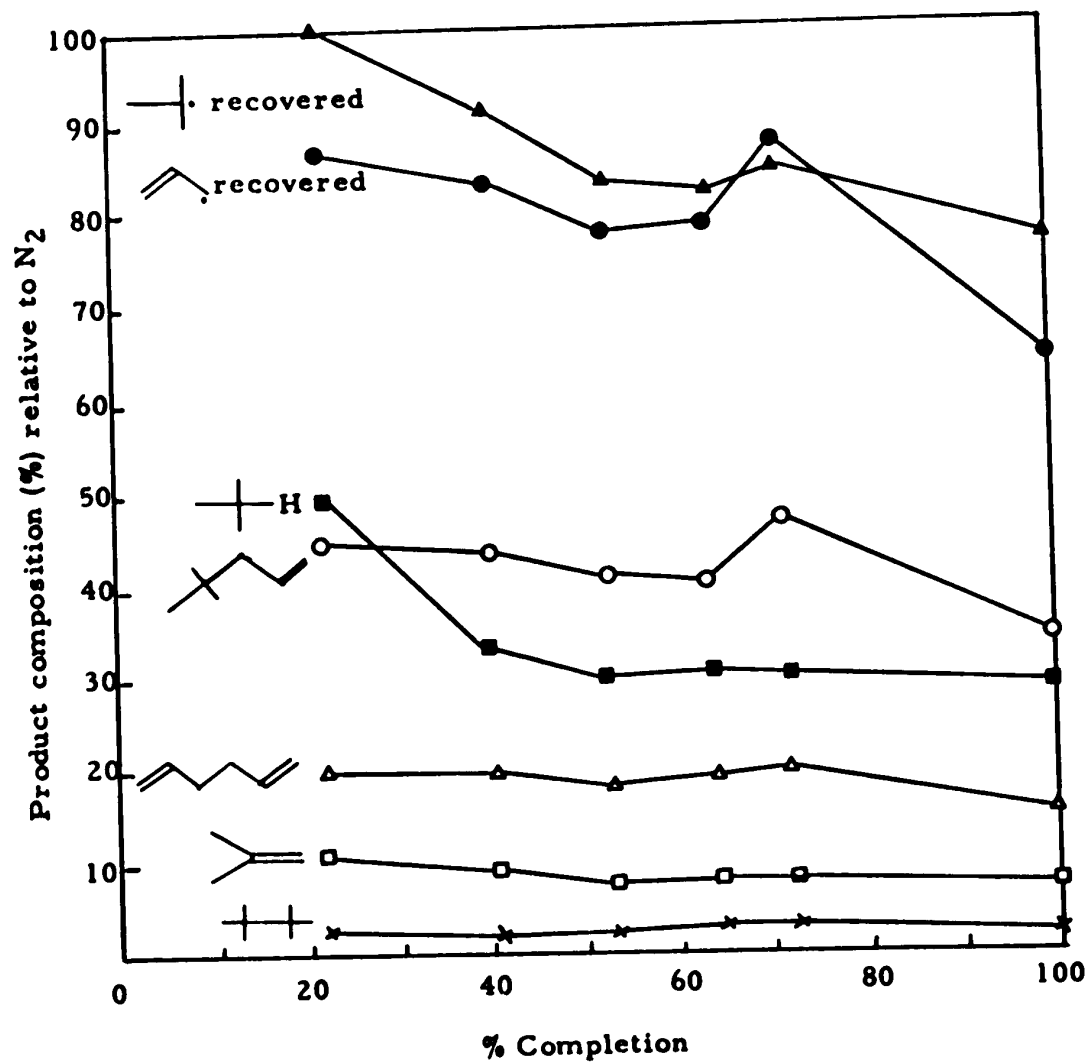
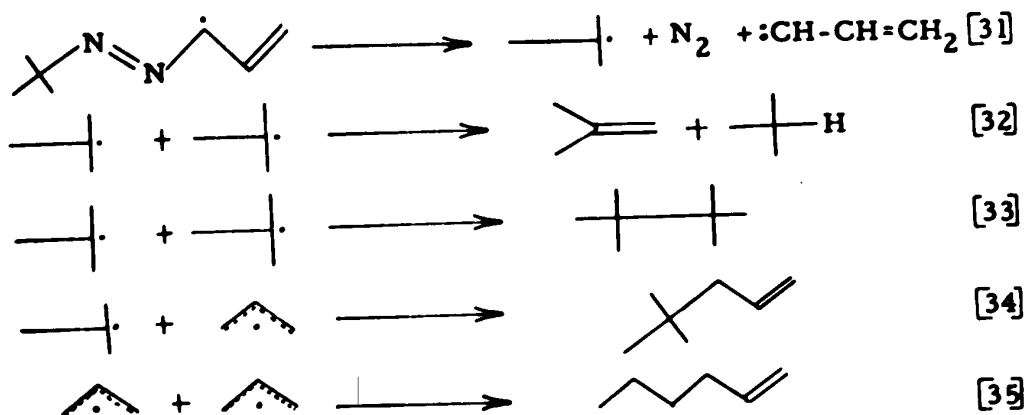


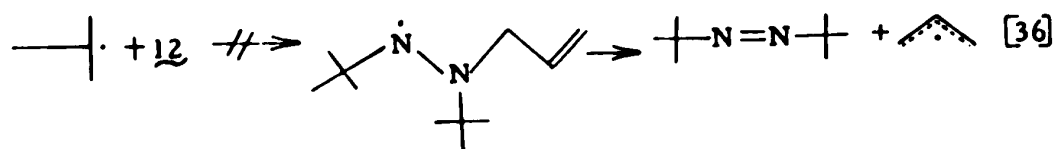
Figure 28. Product composition from the thermolysis of tert-butylazo-3-propene (47), 95 torr at 122.3°.

Table XXV. Mass spectral data of the thermolysis products of tert-butylazo-3-propene (47).

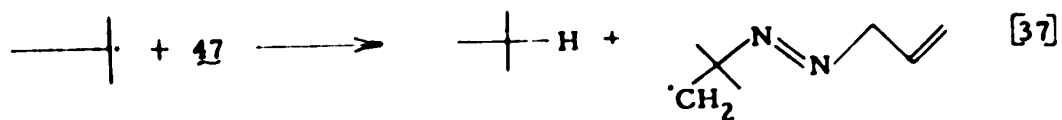
Product	Ten strongest peaks observed	Ten strongest peaks literature (115)
Isobutane	43, 42, 41, 27, 39, 29, 58, 57, 44, 38	43, 41, 42, 27, 39, 15, 29, 44, 57, 38
Isobutene	41, 56, 39, 55, 28, 27, 29, 40, 53, 50	41, 39, 36, 28, 27, 55, 29, 40, 38, 26
1,5-Hexadiene	67, 41, 54, 39, 27, 81, 53, 55, 42, 40	41, 67, 39, 54, 27, 53, 81, 40, 28, 38
4,4-Dimethyl-1-pentene	57, 41, 55, 29, 83, 39, 56, 27, 58, 70	57, 41, 56, 43, 29, 39, 27, 99, 15, 58
2,2,3,3-Tetramethylbutane	57, 56, 41, 43, 99, 29, 58, 55, 37, 27	57, 41, 29, 55, 39, 27, 83, 56, 15, 58



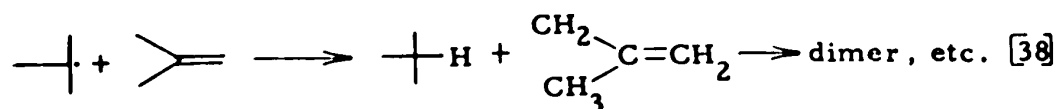
No 2,2'-azoisobutane was detected in the thermolysis suggesting that the bulky tert-butyl radicals are not as facile at adding to the azo nitrogens as are the methyl radicals.



Since the rate of thermolysis of azo-bis-tert-butane was unaffected by the presence of isobutane (17) and the rate of the photolysis of di-tert-butyl ketone was unaffected by the presence of nitric oxide (119), the following hydrogen abstraction reaction by tert-butyl radicals seems to be of little importance.



The fact that the amount of isobutane is eight times that of isobutene may arise from the abstraction of allylic hydrogens by tert-butyl radicals (reaction 30) or by process wherein isobutane is formed at the expense of isobutene e.g. reaction 38 (17).



If reaction 38 is not important, then ratio of the rate constant for the disproportionation reaction (reaction 27) and the combination reaction (reaction 28),  $k_{27} / k_{28}$ , can be calculated according to the following equation,

$$\frac{k_{27}}{k_{28}} = \frac{\text{yield of isobutene}}{\text{yield of 2,2,3,3-tetramethylbutane}} \times \frac{1}{2}$$

The values obtained are 5 at low conversion and 3 at high conversion, which compare favorably with the value of 4.6 obtained from the photolysis of di-tert-butyl ketone (119) and in the mercury photo-sensitized hydrogenation of isobutene (120).

### (C) Kinetics of the Non-inhibited Reactions

The rate of the non-inhibited thermolysis of methylazo-3-propene (36) was obtained by following the increase of pressure with time during the thermolysis or by measuring the amounts of nitrogen produced.

The pressure change was measured by use of the null-point reactor described in the thesis of A. Mishra (116). A sample of 50  $\mu\text{l}$  was injected into the stainless steel reactor by means of a Hamilton syringe having a 6 in. needle. The amount of sample corresponded to an initial pressure of 90 torr. The thermolysis was carried out to greater than nine half-lives at which stage the pressure inside the reactor had doubled to 180 torr. The rate

constant was evaluated from the slope of plots of  $\log (P_{\infty} - P_t)$  versus time. The linearity of the plots displays good first order behavior (Figure 29) in spite of the radical chain induced decomposition discussed in the previous section. The kinetic studies were carried out at four different temperatures.

The effect of temperature on the rate constant is given by the Arrhenius equation 1,

$$k = Ae^{-E_a/RT} \quad (1)$$

where  $E_a$  is the activation energy and  $A$  is the frequency factor.

Equation 1 can also be expressed in the logarithmic form 2.

$$\log k = \log A - \frac{E_a}{2.303 R} \left( \frac{1}{T} \right) \quad (2)$$

Thus, plotting  $\log k$  versus  $1/T$  gives  $-E_a/2.303R$  as the slope, from which the activation energy can be obtained. The intercept is  $\log A$ . Both parameters were determined by the least squares method.

For a gas phase reaction

$$\Delta H^\ddagger = E_a - nRT \quad (3)$$

where  $\Delta H^\ddagger$  is the enthalpy of activation and  $n$  is the order of the reaction. For a first order reaction, equation 3 becomes

$$\Delta H^\ddagger = E_a - RT \quad (4)$$

From the transition state theory

$$k = \frac{k'T}{h} \times e^{-\Delta H^\ddagger/RT} \times e^{\Delta S^\ddagger/R} \quad (5)$$

where  $k'$  and  $h$  are Boltzmann and Plank's constants respectively,

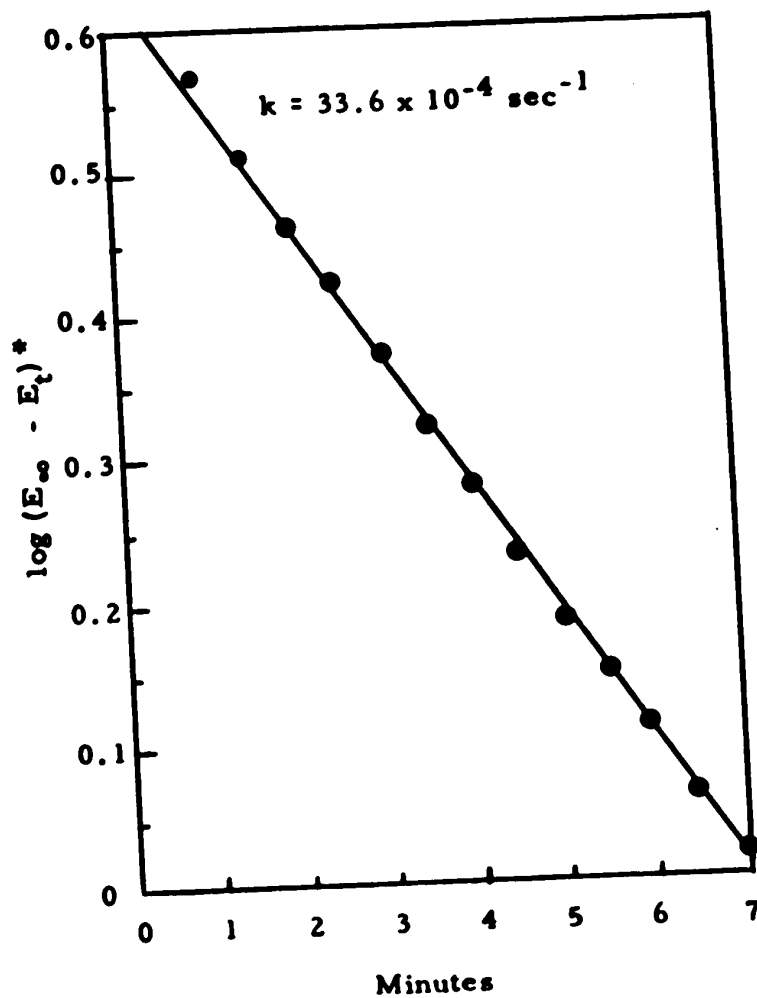


Figure 29. Plot of  $\log(E_{\infty} - E_t)$  versus time for the thermolysis of methylazo-3-propene (36) at  $182.8^{\circ}$ .

\*  $E$  = emp in millivolts as obtained from the strip chart recorder. The emp is proportional to the pressure on the transducer and is linearly related to the internal pressure in the reactor.

and  $\Delta H^\ddagger$  and  $\Delta S^\ddagger$  are the enthalpy and entropy of activation respectively. Combining equations 1, 4 and 5 gives an expression for  $\Delta S^\ddagger$ ,

$$\Delta S^\ddagger = R \ln \frac{Ah}{k'Te} \quad (6)$$

$$\Delta S^\ddagger = 2.303 \log \frac{h}{k'Te} + \log A \quad (7)$$

Equation 7 was used to calculate the entropy of activation at  $120.0^\circ$ . The rate constants and the activation parameters are given in Table XXVI.

The rate constant for the non-inhibited thermolysis of methylazo-3-propene (36) was also evaluated from the amounts of nitrogen produced. After heating a sample of 36 in a break-seal, at ca. 57 torr and  $131.6^\circ$ , the nitrogen produced was collected and measured in the gas buret. The results at varying reaction times are given in Table XXVII. Rate constants were evaluated from the following equation and are listed in the final column of the table. Only a preliminary evaluation of the rate constant was made

$$k = \frac{-2.303}{60 \times t \text{ (min)}} \log (1 - N_2 / [\text{36}]^0)$$

as a detailed study was not necessary. The average rate constant obtained by measuring the rate of the nitrogen production is  $1.81 \times 10^{-5} \text{ sec}^{-1}$  and may be compared with that obtained by extrapolation from the pressure increase data,  $2.57 \times 10^{-5} \text{ sec}^{-1}$  at  $131.6^\circ$ . The rate measurement for the thermolysis of 36 was also carried out in the presence of xenon at  $131.6^\circ$  (Table XXVIII). The rate constant



Table XXVI. Rate constants and activation parameters for the thermolysis of methylazo-3-propene (36).

Run No.	Temperature °C	10 <sup>4</sup> k (sec <sup>-1</sup> )	Activation parameters
1	163.3	5.88	$E_a = 35.4 \pm 0.7 \text{ kcal mole}^{-1}$ $\log A = 14.51 \pm 0.32$ $\Delta S^\ddagger = 5.3 \pm 1.5 \text{ eu (at } 120^\circ)$
2	169.8	11.10	
3	175.0	18.10	
4	182.8	33.6	

Table XXVII. Rate measurement of the thermolysis of methylazo-3-propene (36) at 131.6°

[36] <sup>o</sup> μmoles	Time min	N <sub>2</sub> μmoles	N <sub>2</sub> / [36] <sup>o</sup>	-log (1 - N <sub>2</sub> / [36] <sup>o</sup> )	Rate constant 10 <sup>5</sup> k (sec <sup>-1</sup> )
36.2	105	4.41	0.122	0.0565	(2.206)
35.6	330	10.80	0.303	0.1568	1.827
36.2	465	13.92	0.385	0.2111	1.780
36.7	600	17.72	0.483	0.2865	1.833
Av.					1.813 (σ, 0.029)

Table XXVIII. Rate measurement of the thermolysis of methylazo-3-propene (36) in the presence of xenon at 131.6°. Xe / [36]° = 4.8.

[36]° μmoles	Time min	N <sub>2</sub> μmoles	N <sub>2</sub> / [36]°	- log (1 - N <sub>2</sub> / [36]°)	Rate constant 10 <sup>5</sup> k (sec <sup>-1</sup> )
7.30	100	0.692	0.0947	0.0432	1.661
7.13	200	1.180	0.1654	0.0785	1.511
7.16	300	1.540	0.215	0.1051	1.350
7.16	465	2.47	0.345	0.1838	1.518
7.30	600	2.80	0.384	0.2104	1.350
Av. 1.478 (σ, 0.095)					

obtained,  $1.48 \times 10^{-5} \text{ sec}^{-1}$ , is slightly lower than that at the higher initial pressure of 36.

The rate constant for the non-inhibited thermolysis of tert-butylazo-3-propene (47) was obtained from the data produced by measuring the rate of nitrogen production. The rate constant at an initial pressure of 46 torr (11.87  $\mu$ moles of 47 in a 4.5 ml break-seal) at  $122.3^\circ$  is  $2.78 \times 10^{-4} \text{ sec}^{-1}$  (Table XXIX).

(D) Inhibition by Nitric Oxide

Evidence was presented in the previous section that shows that there is a chain in the thermolysis of methylazo-3-propene (36) and tert-butylazo-3-propene (47). Since nitric oxide (NO) was found to be a better inhibitor in the azomethane thermolysis than olefins (11), nitric oxide was chosen as the inhibitor in the thermolysis of the azo compounds prepared in Section A.

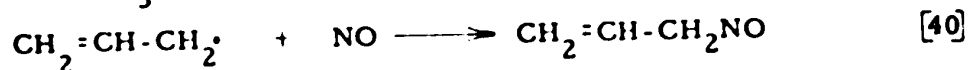
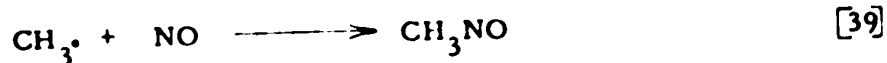
Although an authoritative text states that reactions between nitric oxide and the normal ethylenic bond do not occur (121) Brown has reported that the reaction of nitric oxide with isobutene occurs readily in the presence of traces of nitrogen dioxide ( $\text{NO}_2$ ) such as are usually present in samples of nitric oxide (63). As a control experiment the reaction of 1-butene with nitric oxide was carried out in order to test the inertness of olefinic bond in the azo compound (Table XX, p. 94). The olefinic bond in the azo compound is thus assumed to be stable toward nitric oxide at temperatures lower than  $130^\circ$ .

Table XXIX. Rate measurement of the thermolysis of tert-butylazo-3-propene (47) at 122.3°.

[47] <sup>o</sup> μmoles	Time min	N <sub>2</sub> μmoles	N <sub>2</sub> /[47] <sup>o</sup>	- log (1 - N <sub>2</sub> /[47] <sup>o</sup> )	Rate constant 10 <sup>4</sup> k (sec <sup>-1</sup> )
11.87	15	2.58	21.8	0.1068	2.74
11.87	30	4.75	40.0	0.2219	2.84
11.87	45	6.26	52.7	0.3251	2.77
11.87	60	7.35	63.5	0.4377	2.81
11.87	75	8.41	71.0	0.5376	2.75
11.87	1320	12.90	108.0	--	--
					Av. 2.78 (σ, 0.04)

In a set of experiments designed to test the efficiency of nitric oxide as a radical trap a number of mixtures of methylazobutene (36) and nitric oxide were prepared in such a manner that the pressure of 36 was constant at 60 torr, but the ratio of nitric oxide to 36 was varied from 0.0 to 1.04. The mixtures were then heated to 125.9° for exactly 100 minutes. At a nitric oxide to azo ratio of 0.06 or greater less than 0.5% (based on nitrogen produced) of hydrocarbon products could be detected, see Figure 30. The amount of nitrogen formed was at a minimum over the range 0.06 to 0.22. The recovered 36 was measured by gc. Table XXX indicates a satisfactory material balance.

The observed inhibition with nitric oxide is consistent with the interpretation given in the previous section. A reduction in rate implies the removal of radicals 56, 57 and 58, or of their precursor, the methyl radicals. Since the bulk of hydrocarbons must be due to subsequent reactions of the methyl radicals, the drastic reduction by nitric oxide of the yield of hydrocarbons indicates the removal of the methyl radicals rather than removal of the radicals 56, 57 and 58. Absence of the hydrocarbons suggests that the methyl and allyl radicals are removed by the process,



although it is generally appreciated that nitrosoalkanes react further in a variety of processes (see historical section p. 26).

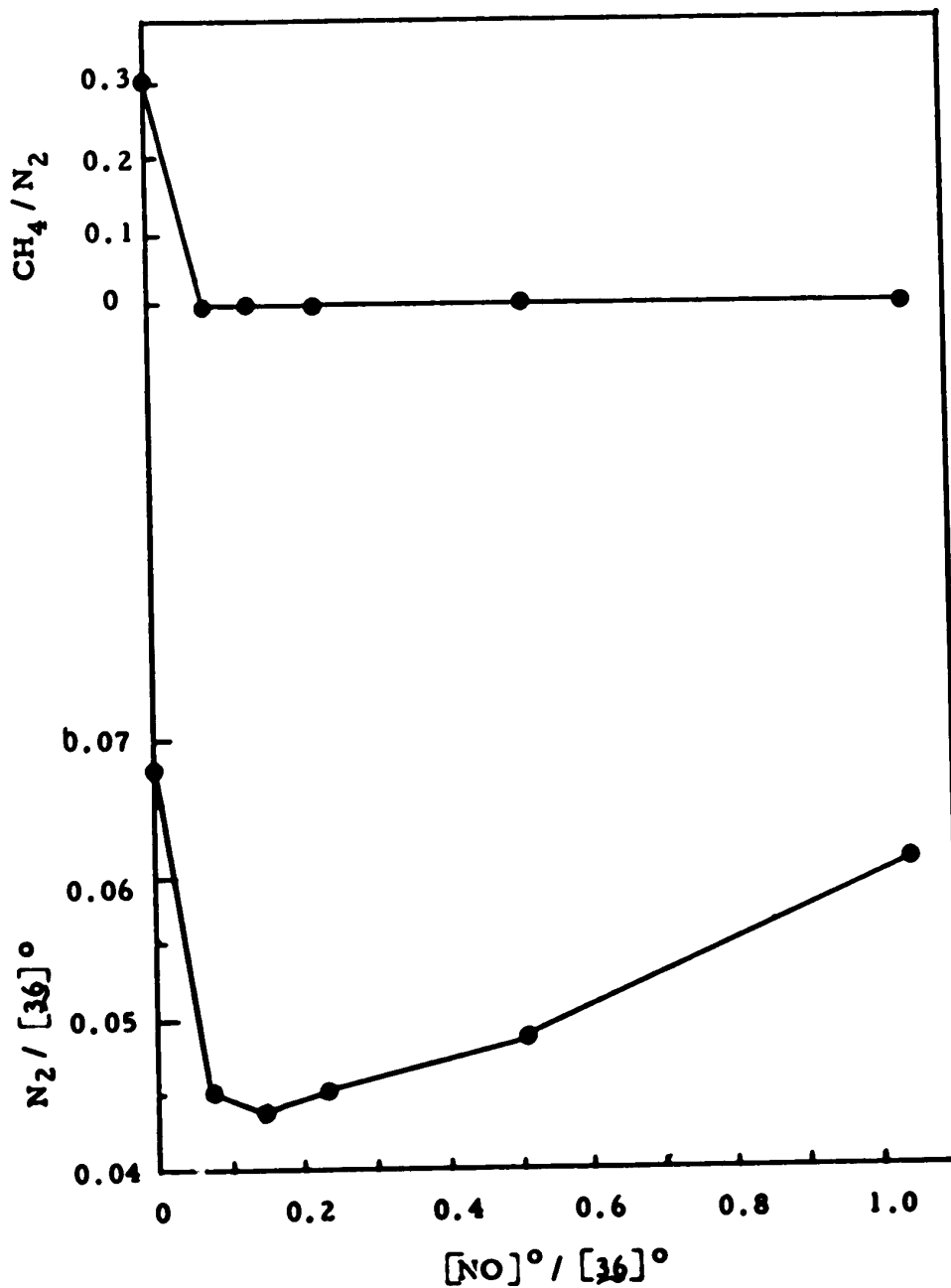


Figure 30. Inhibited thermolysis of methylazo-3-propene (36) with nitric oxide at  $125.9^\circ$  for 100 minutes.

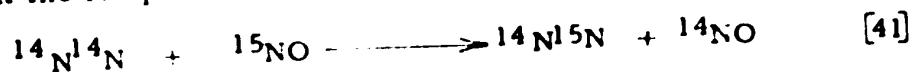
Table XXX. Recovery of unreacted methylazo-3-propene (**36**).

Initial conc. of <b>36</b>	[NO] / [ <b>36</b> ] <sup>o</sup>	Conversion %	Calculated amount of <b>36</b> recovered	Gc peak area	<b>36</b> recovered
22.9 $\mu$ moles	0	0	22.9 $\mu$ moles	40.6	22.9 <sup>a</sup> $\mu$ moles
22.4	0.103	0.0495	21.3	38.6	21.7
22.9	0.210	0.0483	21.8	38.1	21.5

<sup>a</sup> Reference value.



Since both  $\underline{36}$  and nitric oxide contain nitrogen, and the rate of the inhibited thermolysis with nitric oxide is measured by the rate of formation of nitrogen, the accelerating effect of nitric oxide i.e. the rate increase at high nitric oxide pressure, indicated in Table XXX, could be due to the production of nitrogen either from  $\underline{36}$  or from the nitric oxide. Experiments with the isotopic nitric oxide ( $^{15}\text{NO}$ , isotopic purity 99.6%) permit a distinction between the two possible sources of nitrogen. An initial pressure of 58 torr of  $\underline{36}$  (ca. 30  $\mu$ moles in a 16 ml break-seal) was kept constant and the ratio of isotopic nitric oxide to  $\underline{36}$  was varied from 0.047 to 0.915. The nitrogen produced was first measured volumetrically and then an aliquot analyzed by mass spectrometry. Table XXXI shows the results obtained by placing each tube in a bath at  $126.35^\circ$  for exactly 90 minutes. The single-point rate constant based on total nitrogen produced is indicated as  $k_1^{\text{tot}}$ . Using mass 28, corresponding to  $^{14}\text{N}^{14}\text{N}$  as the parent peak (1.00) the relative values for peaks at mass 29 ( $^{15}\text{N}^{14}\text{N}$ ) and 30 ( $^{15}\text{N}^{15}\text{N}$ ) are listed in Table XXXI. There is in fact formation of molecules  $^{15}\text{N}^{14}\text{N}$  and  $^{15}\text{N}^{15}\text{N}$ , indicating that part of the nitrogen is formed from  $^{15}\text{NO}$ . A control experiment excludes the following isotopic exchange reaction at the temperature of the experiment (Table XIX, p. 93).



The values of  $k_1^{\text{corr}}$  in the penultimate column of Table XXXI were calculated on the assumption that no  $^{14}\text{N}^{14}\text{N}$  was lost by an exchange reaction. The natural abundance of  $^{15}\text{N}^{14}\text{N}$  in ordinary nitrogen

Table XXXI. Mass spectrometric analysis from the runs of methylazo-3-propene ( $^{36}$ ) with  $^{15}\text{NO}$  at 126.35° for 90 minutes.

$^{15}\text{NO}$ [ $^{36}$ ] <sup>o</sup> / [ $^{36}$ ] <sup>o</sup>	$\frac{\text{N}_2^{\text{tot}}}{[\text{36}]^{\text{o}}}$ x 100	$10^6 k_1^{\text{tot}}$ (sec <sup>-1</sup> )	$\frac{\text{P}_{29}}{\text{P}_{28}}$	$\frac{\text{P}_{30}}{\text{P}_{28}}$	$f_{\text{N}_2}^{36}$	$10^6 k_1^{\text{corr}}$ (sec <sup>-1</sup> )	$\frac{^{15}\text{NO consumed}}{f_{\text{N}_2}^{36} \text{ tot}}$
0.0407	4.06	7.69	0.0075	0.0031	0.996	7.67	1.00
0.0427	4.22	8.00 <sup>a</sup>					
0.0982	4.33	8.21 <sup>a</sup>				7.77	1.92
0.1038	4.23	8.01	0.0107	0.0361	0.968	7.80	1.89
0.171	4.32	8.19	0.0097	0.0486	0.954	8.09	1.78
0.172	4.58	8.68	0.0162	0.0705	0.932	8.01	2.27
0.351	4.63	8.78	0.0159	0.0969	0.911	8.98	1.94
0.371	5.13	9.77	0.0127	0.0797	0.924		
0.502	4.98	9.46 <sup>b</sup>					
0.511	5.05	9.61	0.0631	0.0698	0.914	8.76	2.38

Continued

Table XXXI. - Continued

$[^{15}\text{NO}]$	$\frac{\text{N}_2^{\text{tot}}}{[^{36}]^{\circ}}$	$10^6 k_1^{\text{tot}}$ ( $\text{sec}^{-1}$ )	$\frac{\text{P}_{29}}{\text{P}_{28}}$	$\frac{\text{P}_{30}}{\text{P}_{28}}$	$f_{\text{N}_2}^{36}$	$10^6 k_1^{\text{corr}}$	$\frac{^{15}\text{NO}}{\text{consumed}}$ $\frac{^{36}\text{N}_2^{\text{tot}}}{f_{\text{N}_2}}$
0.779	5.07	9.65	0.0132	0.200	0.832	8.00	3.02
0.792	5.36	10.21	0.0124	0.215	0.823	8.38	2.47
0.915	5.13	9.77	0.0111	0.236	0.810	7.88	2.67
						Av. 8.13	( $\sigma$ , 0.44)

a Hydrocarbon analysis indicated no  $\text{CH}_4$  formed.

b Break-seal for  $\text{N}_2$  analysis inadvertently broken.

is 0.738 mole% (114), thus the contribution from this source is 0.00738  $P_{28}$  and the fraction of nitrogen\*, of natural isotopic composition, from  $\underline{36}$ ,  $f_{N_2}^{\underline{36}}$ , is then :

$$f_{N_2}^{\underline{36}} = \frac{1.0037 + 0.5 P_{29}/P_{30}}{1.000 + P_{29}/P_{28} + P_{30}/P_{28}}$$

The first order rate constants  $k_1^{\text{tot}}$  and  $k_1^{\text{corr}}$  were calculated according to the following equation:

$$k_1^{\text{tot}} = \frac{-2.303}{90 \times 60} \log \left( 1 - \frac{N_2^{\text{tot}}}{[\underline{36}]^0} \right)$$

and

$$k_1^{\text{corr}} = \frac{-2.303}{90 \times 60} \log \left( 1 - \frac{f_{N_2}^{\underline{36}} [N_2^{\text{tot}}]}{[\underline{36}]^0} \right)$$

The values of the rate constant  $k_1^{\text{corr}}$  given in the penultimate column of Table XXXI are reproducible. A plot of  $k_1^{\text{tot}}$  versus nitric oxide pressure, Figure 31, shows a rough correlation ( $r = 0.901$ ). Extrapolation to zero nitric oxide pressure gives a rate constant of  $7.99 \times 10^{-6} \text{ sec}^{-1}$  which compares favourably with the average value of  $k_1^{\text{corr}}$  of  $8.13 \times 10^{-6} \text{ sec}^{-1}$ . We may conclude that if the nitric oxide does induce the thermolysis of  $\underline{36}$  it is not significantly detected, and that the products of thermolysis  $\underline{36}$  in the presence of nitric oxide provoke a small conversion of nitric oxide to nitrogen.

---

\* The fraction of peak 28 (or 29) derived from the 0.4% mole%  $^{14}\text{NO}$  is  $0.004 P_{30}/P_{28}$  and is not significant.

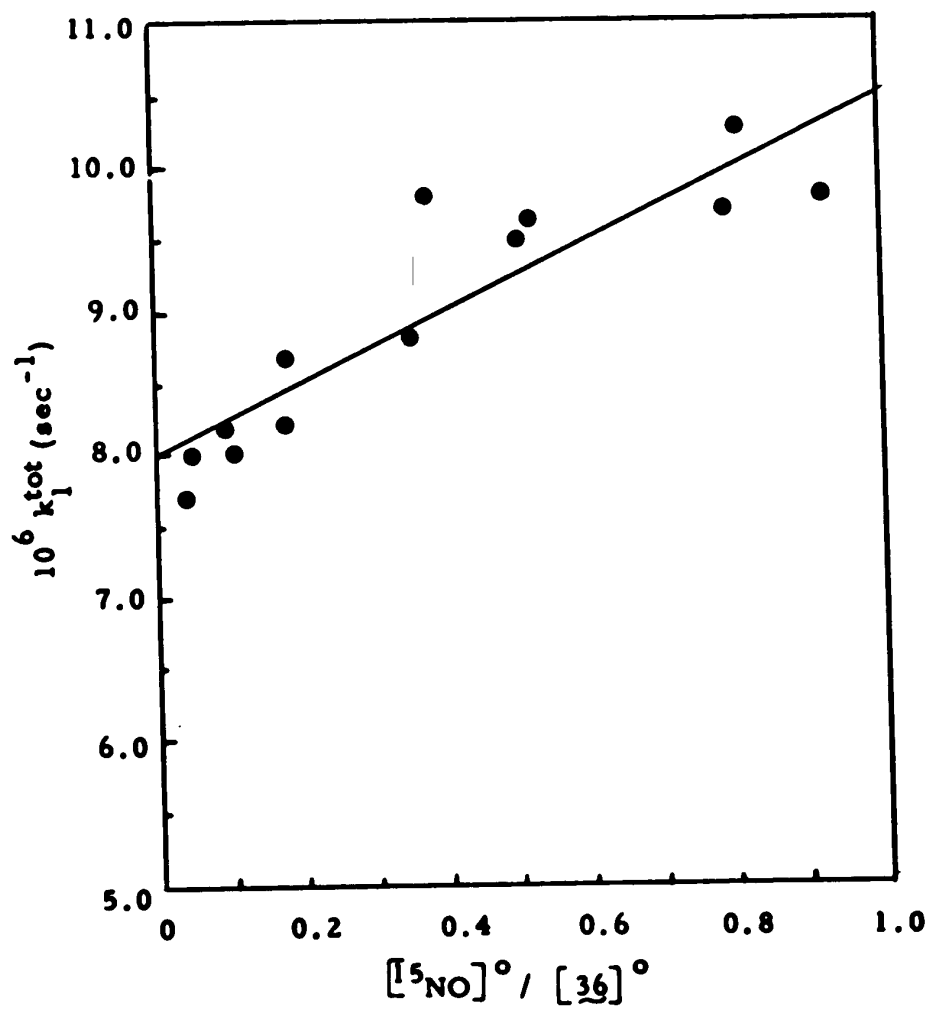
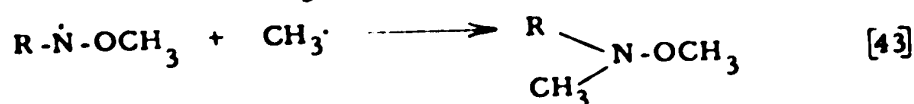
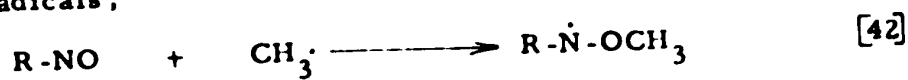


Figure 31. Plot of  $10^6 k_1^{\text{tot}}$  versus  $[^{15}\text{NO}]^0 / [^{36}]^0$  showing best line from least square data.

Since two radicals (methyl and allyl radical) are formed per nitrogen molecule produced, a complete removal of the radicals by nitric oxide according to reaction 39 and 40 should lead to the consumption of two molecules of NO per nitrogen produced. The amount of  $^{15}\text{NO}$  frozen in the solid nitrogen trap was measured and the quantity of  $^{15}\text{NO}$  consumed was calculated by subtracting the recovered amount from the quantity originally placed in the tube. The results expressed as the number of moles of  $^{15}\text{NO}$  consumed per mole of nitrogen produced from  $\underline{36}$  ( $f_{\text{N}_2}^{36} \text{N}_2^{\text{tot}}$ ) are listed in the final column of Table XXXI. The ratios are in the range of 1.8 - 3.0, except at the low pressure of  $^{15}\text{NO}$ , and rise gradually with increasing  $^{15}\text{NO}$  pressure. These results are similar to those obtained by Forst and Rice (11) in the thermolysis of azomethane at  $303^\circ$ . The ratios less than two in the lower  $^{15}\text{NO}$  pressures require an inhibitor other than  $^{15}\text{NO}$ . Nitrosoalkanes are known to act as inhibitors, although less efficient than nitric oxide (69), since the nitroso compounds formed according to reactions 34 and 35 are capable of trapping radicals,



The values larger than two at the high  $^{15}\text{NO}$  pressures coincide with the formation of nitrogen from  $^{15}\text{NO}$  as previously discussed.

The formation of nitrogen from nitric oxide has been postulated by several workers as due to a reaction with nitrosoalkanes (11, 63-65).

Although previous investigators (9b, 11, 16) agree that packing has little influence on the thermolysis of azoalkanes, an inhibited thermolysis was carried out in a break-seal packed with glass beads to check upon the surface effects. The surface to volume ratio was varied over the range of 3.5 to 16.6 cm<sup>-1</sup> and the thermolysis was carried out at 126.00° for 60 minutes. Table XXXII shows no dependence of  $k_1^{\text{tot}}$  and  $k_1^{\text{corr}}$  upon the surface to volume ratio.

Table XXXIII lists single point rate constants for various mixtures of nitric oxide, 36 and xenon over a range of initial pressures. The nitric oxide and 36 pressures were kept constant at 58 torr (NO/36 = 0.211) and the total pressure was varied over the range of 58 to 135 torr by adding xenon. Each sample was then thermolyzed at 129.29° for 60 minutes. No dependence upon the initial pressure was noted, indicating 58 torr is above the pressure-sensitive region of the unimolecular decomposition of 36.

The detailed rate studies of the thermolysis of 36 were carried out at the optimum NO : 36 ratio of 0.15 to 0.20. Under these conditions the value of  $N_2^{\text{tot}}$  can be used directly to calculate the rates with very little loss of precision and all of the chain induced component of the reaction will be inhibited. Mixtures of

Table XXII. Surface effects on the inhibited thermolysis of methylazo-3-propene (36) at 126.00° for 90 minutes.  $^{15}\text{NO} / [36]^\circ = 0.170$ .

S/V cm <sup>-1</sup>	$\text{N}_2^{\text{tot}} / [36]^\circ \times 100$	$10^6 k_1^{\text{tot}} (\text{sec}^{-1})$	$\text{P}_{29} / \text{P}_{28}$	$\text{P}_{30} / \text{P}_{28}$	$f_{\text{N}_2}^{36}$	$10^6 k_1^{\text{tot}} (\text{sec}^{-1})$
3.5 (unpacked)	4.06	7.69	0.0089	0.0145	0.985	7.57
8.5 (packed)	4.03	7.62	0.0098	0.0033	0.994	7.58
8.5 (packed)	4.21	7.96	0.0114	0.0038	0.993	7.92
16.6 (packed)	3.98	7.53	0.0087	0.0013	0.997	7.51



**Table XXXIII. Rate constants for the inhibited thermolysis of methylazo-3-propene (36) at various total pressures at 129.29°.**

<b>Total pressure</b> <b>torr</b>	<b>Rate constant</b> <b><math>10^6 k_1</math> (sec<sup>-1</sup>)</b>
58	12.27
67	12.42
74	12.36
87	12.54
116	12.42
135	11.73
	Av. 12.3 ( $\sigma$ , 0.3)

36 (30 - 40  $\mu$ moles, ca. 40 torr) and nitric oxide (6 - 8  $\mu$ moles, 6 - 8 torr) were allowed to react to 6% conversion. Rate constants were evaluated from the slopes of the plots of  $-\log(1 - N_2/[36]^0)$  versus time (Table XXXIV). The linearity of the plots displays good first-order behavior (Figure 32). Kinetic studies were carried out at five different temperatures. Equations 2 and 7 were used to calculate the activation parameters,  $E_a$ ,  $\log A$  and  $\Delta S^\ddagger$ . The rate constants and the activation parameters are given in Table XXXV.

Kinetic studies of the inhibited thermolysis of 1-propyl-azo-3'-propene (46) with nitric oxide were carried out in the same manner as those of methylazo-3-propene (36) (Table XXXVI). The rate constants and the activation parameters are given in Table XXXVII. Some of the runs were carried out using the isotopic nitric oxide  $^{15}\text{NO}$ . The results of the mass spectrometric analysis of the nitrogen formed are shown in Table XXXVIII.

The gas phase thermolysis and nitric oxide inhibited thermolysis of 3,3'-azo-1-propene (52) were examined at  $100.73^\circ$ . As is shown in Table XXXIX, rates are the same whether nitric oxide was added or not.

tert-Butylazo-3-propene (47) was allowed to react in the presence of isotopic nitric oxide,  $^{15}\text{NO}$ . The products consisted of nitrogen and isobutene. The fraction of nitrogen produced from the azo compound was calculated in the same manner as for 36. The plots of  $-\log(1 - f_{N_2}^{47} [N_2^{\text{tot}}]/[47]^0)$  versus time, see

Table XXXIV. Inhibited thermolyses of methylazo-3-propene (36).

Temp °C	NO / [36]°	Time min	[36]° μmole	N <sub>2</sub> μmole	N <sub>2</sub> / [36]° x 100	- log (1 - N <sub>2</sub> / [36]°)	10 <sup>6</sup> k <sub>1</sub> (sec <sup>-1</sup> )
109.90	0.184	110	35.4	0.30	0.85	0.00371	1.29
109.90	0.184	220	35.4	0.63	1.77	0.00776	1.35
109.90	0.184	330	33.9	0.83	2.44	0.00073	1.25
109.90	0.184	440	33.9	1.11	3.28	0.01448	1.26
109.90	0.184	660	34.1	1.15	4.55	0.02018	1.17
115.54	0.184	100	38.1	0.48	1.25	0.00546	2.10
115.54	0.184	160	38.1	0.84	2.21	0.00971	2.33
115.54	0.184	240	39.1	1.27	3.25	0.01435	2.30
115.54	0.184	320	39.4	1.69	4.29	0.01904	2.29
115.54	0.184	400	37.9	2.08	5.49	0.02452	2.35
							Av. 1.27 (σ, 0.08)
							Av. 2.27 (σ, 0.10)

Table XXXIV - Continued

Temp °C	NO [36]°	Time min	[36]° μmole	N <sub>2</sub> μmole	N <sub>2</sub> / x 100	[36]° - log(1 - N <sub>2</sub> /[36]°)	10 <sup>6</sup> k <sub>1</sub> (sec <sup>-1</sup> )
125.90	0.197	20	40.2	0.24	0.85	0.00371	7.14
125.90	0.197	40	40.4	0.73	1.81	0.00793	7.62
125.90	0.197	60	39.6	1.17	2.96	0.01305	8.37
125.90	0.197	80	39.6	1.46	3.69	0.01633	7.83
125.90	0.197	100	39.5	1.85	4.68	0.02082	7.99
125.90	0.197	120	39.6	2.52	6.37	0.02858	7.83
							Av. 7.80 (σ, 0.41)
129.52	0.179	10	30.0	0.24	0.80	0.00349	13.3
129.52	0.179	20	30.5	0.44	1.44	0.00630	12.1
129.52	0.179	30	29.5	0.64	2.17	0.00953	12.2
129.52	0.179	40	31.4	0.90	2.87	0.01265	12.1
129.52	0.179	50	30.6	1.04	3.40	0.01502	11.5
129.52	0.179	60	30.8	1.27	4.12	0.01827	11.7
							Av. 12.2 (σ, 0.6)

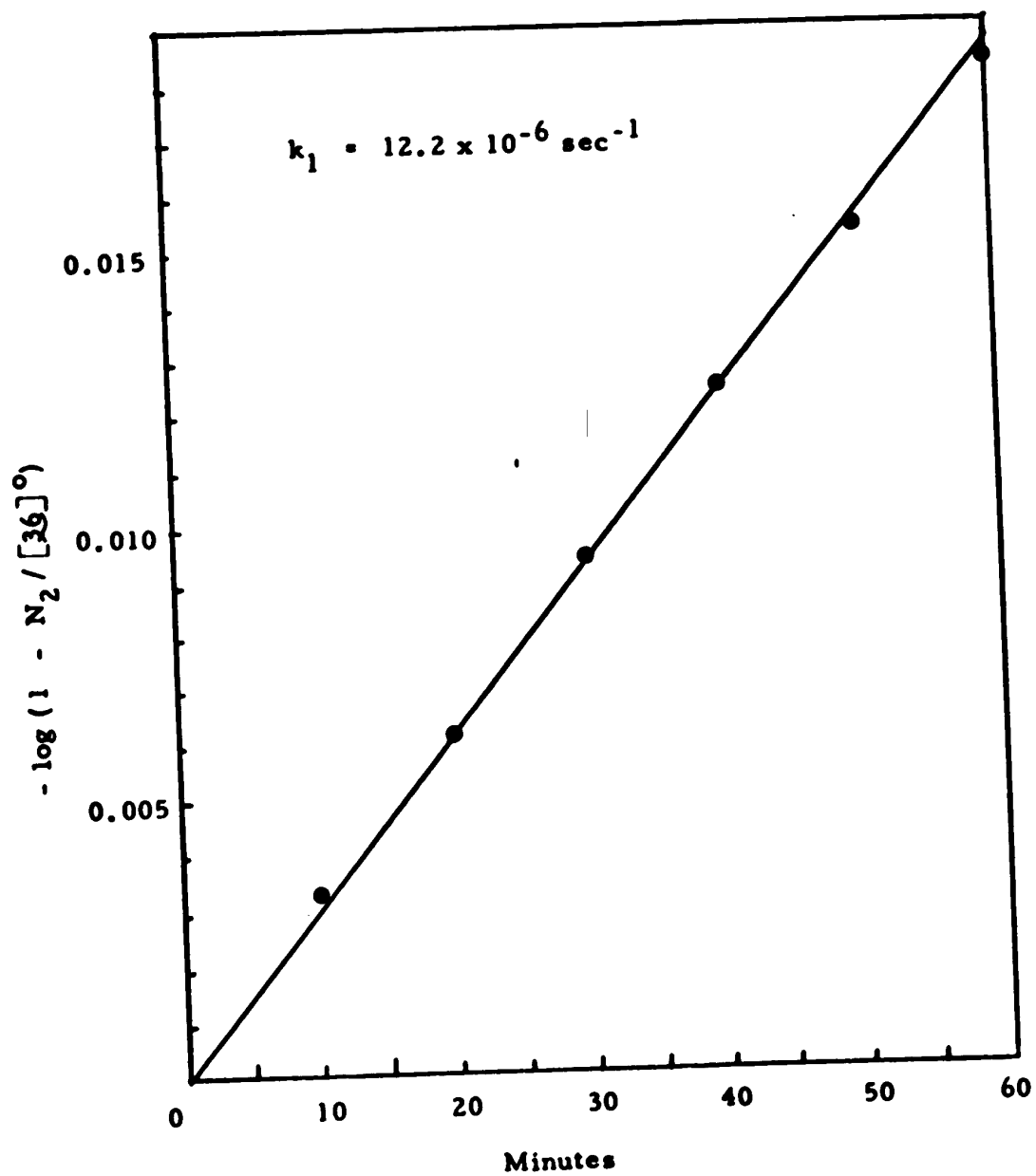


Figure 32. Plot of  $-\log(1 - N_2 / [36]_0)$  versus time for the inhibited thermolysis of methylazo-3-propene (36) at  $129.52^\circ$ .

Table XXXV. Rate constants and activation parameters for the thermolysis of methylazo-3-propene (36) in the presence of nitric oxide. Pressure range 50 - 60 torr.

Run No.	Temperature °C	$10^6 k$ ( $\text{sec}^{-1}$ )	Activation parameters
1	109.90	1.27	$E_a = 35.5 \pm 0.7 \text{ kcal mole}^{-1}$ $\log A = 14.36 \pm 0.38$ $\Delta S^\ddagger = 4.6 \pm 1.8 \text{ e.u. (at } 120^\circ)$
2	115.53	2.27	
3	125.92	7.80	
4	129.52	12.2	

Table XXXVI. Inhibited thermolysis of 1-propylazo-3'-propene (46).

Temp °C	NO [46]°	Time min	N <sub>2</sub> μmole	N <sub>2</sub> [46]°	N <sub>2</sub> / x 100	-log (1 - N <sub>2</sub> / [46]°)	10 <sup>6</sup> k <sub>1</sub> (sec <sup>-1</sup> )
101.32	0.143	240	32.6	0.50	1.53	0.00670	1.07
101.32	0.143	240	32.9	0.49	1.50	0.00656	1.05
101.32	0.143	360	32.3	0.78	2.41	0.01059	1.13
101.32	0.143	600	32.3	1.31	4.06	0.01800	1.15
							Av. 1.10 (σ, 0.05)
114.10	0.151	30	32.6	0.33	1.01	0.00441	5.64
114.10	0.151	60	32.6	0.65	1.99	0.00873	5.58
114.10	0.151	90	32.6	0.99	3.04	0.01350	5.76
114.10	0.151	150	32.4	1.54	4.75	0.02114	5.41
							Av. 5.60 (σ, 0.15)

Continued

Table XXXVI. - Continued

Temp °C	NO /[46]°	Time min	[46]° μmole	N <sub>2</sub> μmole	N <sub>2</sub> / x 100	-log (1 - N <sub>2</sub> / [46]°)	10 <sup>6</sup> k <sub>1</sub> (sec <sup>-1</sup> )
126.02	0.112	10	33.8	0.44	1.30	0.00568	21.8
126.02	0.112	20	33.8	0.84	2.48	0.01091	21.0
126.02	0.195	30	31.9	1.15	3.61	0.01597	20.4
126.02	0.195	30	32.2	1.20	3.73	0.01651	21.1
126.02	0.112	40	21.5	1.07	4.98	0.02218	21.3
Av. 21.1 (σ, 0.5)							



Table XXXVII. Rate constants and activation parameters for the thermolysis of 1-propyl-azo-3'-propene (46) in the presence of nitric oxide. Pressure range 50 - 60 torr.

Run No.	Temperature °C	$10^6 k$ (sec <sup>-1</sup> )	Activation parameters
1	101.32	1.101	$E_a = 35.6 \pm 0.5 \text{ kcal mole}^{-1}$
2	114.10	5.60	$\log A = 14.80 \pm 0.28$
3	126.02	21.12	$\Delta S^\ddagger = 6.6 \pm 1.3 \text{ eu (at } 120^\circ)$

Table XXXVIII. Mass spectrometric analysis of nitrogen produced during the thermolysis of 1-propylazo-3'-propene (46) with  $^{15}\text{NO}$ .

Temp $^{\circ}\text{C}$	$[^{15}\text{NO}]^{\circ}$ / $[^{46}]^{\circ}$	time min	$\text{N}_2^{\text{tot}}$ / $[^{46}]^{\circ}$	$\text{P}_{29}$ / $\text{P}_{28}$	$\text{P}_{30}$ / $\text{P}_{28}$	$f_{\text{N}_2}^{46}$	$10^6 k_1$ ( $\text{sec}^{-1}$ ) corr
101.32	0.143	360	0.0241	0.0153	0.0351	0.963	1.08
114.10	0.151	150	0.0477	0.0163	0.0247	0.972	5.26
126.02	0.195	30	0.0374	0.0156	0.0136	0.984	20.8
126.02	0.195	30	0.0361	0.0091	0.0080	0.992	20.3

Table XXXIX. Rate constants for the thermolysis of 3,3'-azo-1-propene (52) at 100.73°.

$[\text{NO}]^{\circ} / [\underline{52}]^{\circ}$	Rate constant $10^6 k_1 \text{ (sec}^{-1}\text{)}$
0.165	4.06
0	4.00
0	3.35 (extrapolated) <sup>a</sup>

<sup>a</sup> B. Al-Sader and R. J. Crawford, *Can. J. Chem.*, 48, 2745 (1970).

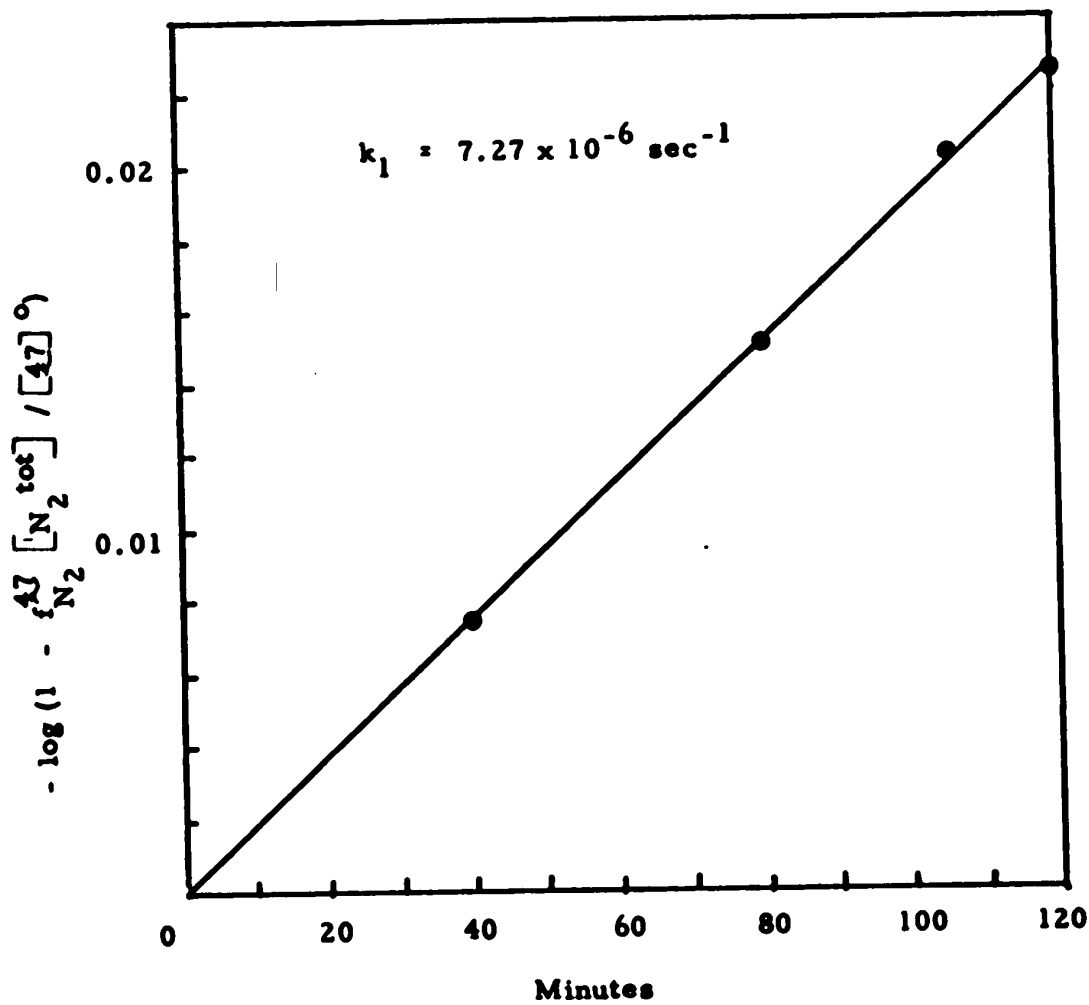
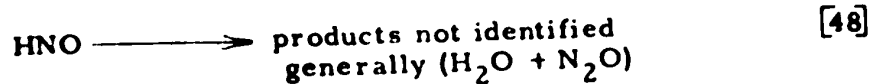
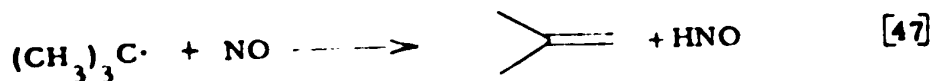
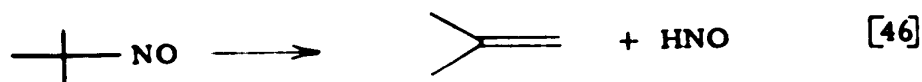
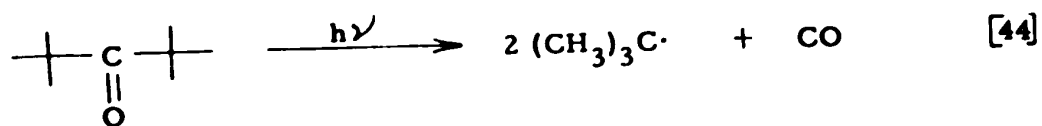


Figure 33. Plot of  $-\log(1 - f_{N_2}^{47} [N_2^{tot}] / [47]^0)$  versus time for the inhibited thermolysis of tert-butylazo-3-propene (47) at  $90.90^\circ$ .

Figure 33, gave good straight lines. The results of the product analysis are shown in Table XL and the rate constants and activation parameters in Table XLI.

Because of the isobutene and large amounts of  $^{15}\text{N}^{15}\text{N}$  found as products from the isotopic  $^{15}\text{NO}$  reaction with  $\underline{47}$  a sample of the known 2-methyl-2-nitrosopropane was allowed to react with  $^{15}\text{NO}$  and the nitrogen produced was submitted to mass spectrometric analysis. The results in Table XLII indicate that the peak of mass 29 is largest suggesting that one of the nitrogens in the  $\text{N}_2$  produced is from 2-methyl-2-nitrosopropane and the second from the nitric oxide. The formation of isobutene was observed in the photolysis of di-tert-butyl ketone in the presence of nitric oxide and proposed to be consistent with the following sequence of reactions (119).



Levy and Copeland (17) reported that the thermolysis of 2,2'-azoisobutane in the presence of nitric oxide gave not only isobutene but also 2-methyl-2-nitrosopropane and proposed the following mechanism, although they did not detect nitrous oxide  $\text{N}_2\text{O}$ .

Table XI. Inhibited thermolyses of *tert*-butylazo-3-propene (47).

Temp °C	[15NO] <sup>o</sup>	[47] <sup>o</sup>	Time min	[47] <sup>o</sup> μmole/mole	N <sub>2</sub> <sup>tot</sup>	P <sub>29</sub> / P <sub>28</sub>	P <sub>30</sub> / P <sub>28</sub>	isobutene [47] [N <sub>2</sub> <sup>tot</sup> ]	15NO consumed [47] [N <sub>2</sub> <sup>tot</sup> ]	-log (1 - [47] / [47] <sub>o</sub> )	10 <sup>6</sup> k <sub>1</sub> <sup>corr</sup> (sec <sup>-1</sup> )
80.00	0.210	27.8	100	0.74	0.6122	0.160	0.061	0.320	0.01006	2.14	
80.00	0.210	27.8	300	1.22	0.0183	0.179	0.046	0.328	0.01651	2.11	
											Av. 2.13 (σ, 0.03)
90.90	0.236	28.3	40	0.65	0.0150	0.0988	0.908	0.381	0.00771	7.40	
90.90	0.236	28.3	80	1.11	0.0149	0.149	0.868	0.253	0.01502	7.03	
90.90	0.236	28.3	105	1.64	0.0099	0.193	0.838	0.362	0.02027	7.42	
90.90	0.236	28.3	120	1.75	0.0189	0.218	0.820	0.362	0.02260	7.23	
											Av. 7.27 (σ, 0.18)
91.90	0.210	27.6	60	0.90	0.0145	0.194	0.865	0.320	0.01180	7.56	
91.90	0.210	27.8	130	1.17	0.0125	0.138	0.878	0.328	0.02498	7.39	
											Av. 7.47 (σ, 0.12)
106.81	0.195	26.6	15	1.06	0.0099	0.0388	0.945	0.342	0.01768 <sup>a</sup>	45.2 <sup>a</sup>	
106.81	0.195	26.7	30	1.67					0.02803 <sup>a</sup>	35.8 <sup>a</sup>	
106.81	0.195	26.6	45	2.55	0.0059	0.0059	0.990		0.04378 <sup>a</sup>	37.4 <sup>a</sup>	
106.81	0.195	26.6	60	3.32					0.05789 <sup>a</sup>	37.0 <sup>a</sup>	
											Av. 38.9 (σ, 4.3)

<sup>a</sup> Rate constants are calculated with  $\frac{[47]}{[47]_0} = 1.00$ .

Table XLI. Rate constants and activation parameters for the thermolysis of tert-butylaso-3-propene (47) in the presence of nitric oxide. Pressure range 50 - 60 torr.

Run No.	Temperature		Activation parameters
	°C	$10^6$ k (sec <sup>-1</sup> )	
1	80.88	2.13	$E_a = 29.8 \pm 0.3$ kcal mole <sup>-1</sup>
2	90.90	7.27	$\log A = 12.73 \pm 0.16$
3	91.50	7.47	$\Delta S^\ddagger = -2.8 \pm 0.7$ eu (at 120°)
4	106.81	38.9	

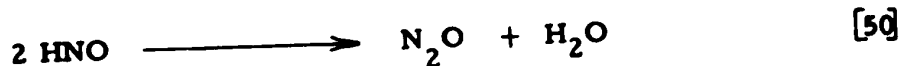
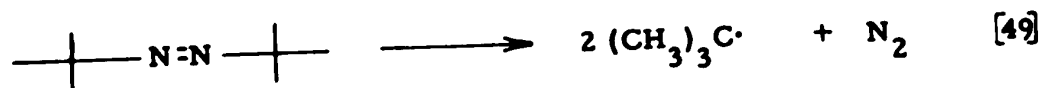
Table XLII. Reaction of 2-methyl-2-nitrosopropane (7.22  $\mu$ moles) with  $^{15}\text{NO}$  (29.2  $\mu$ moles).

Temp $^{\circ}\text{C}$	Time	$\text{N}_2$ $\mu$ mole	$\text{N}_2\text{O}$ isobutane		$^{15}\text{NO}$ consumed		$^{15}\text{NO}$ consumed		$\text{P}_{28}$	$\text{P}_{29}$	$\text{P}_{30}$
			$\text{N}_2$	$\text{N}_2$	$\text{N}_2$	$\text{N}_2$	$\text{N}_2$	$\text{N}_2$			
room temp	16 hrs	6.63	0.077	0.437	2.28	1.93 <sup>a</sup>	12.53	100	18.73		
91.05	40 min	6.98	0.053	0.432	2.21	1.90 <sup>a</sup>	6.35	100	11.85		
room temp	b	4.52	0.067	0.705	2.72		10.42	100	2.94		
room temp	b	1.253	0.045	0.942	3.82		28.3	100	2.73		

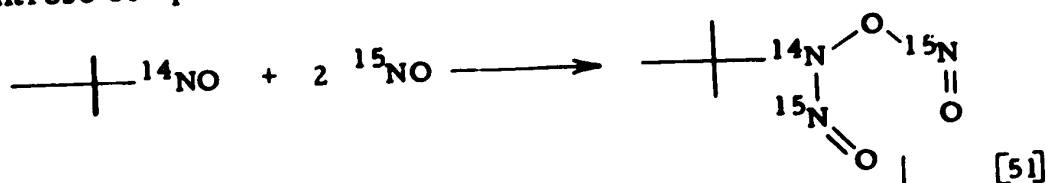
<sup>a</sup> No 2-methyl-2-nitrosopropane detected.

<sup>b</sup> The mixture was kept at  $-194^{\circ}$  after mixing which took ca. one hour.

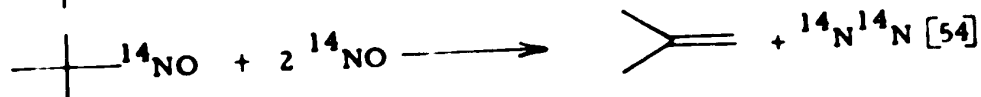
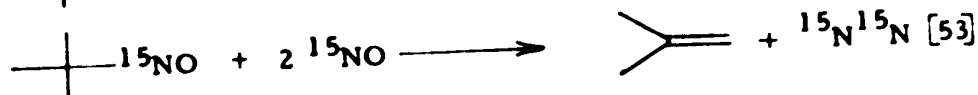




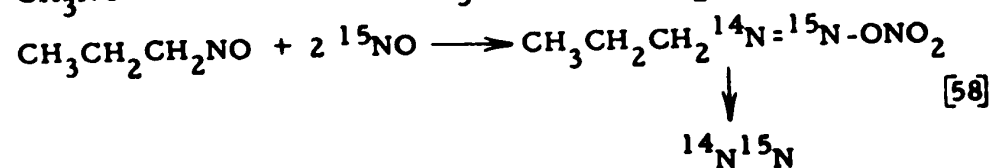
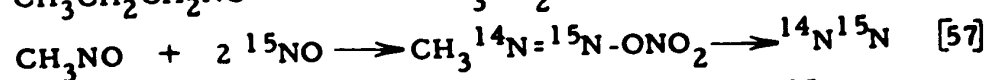
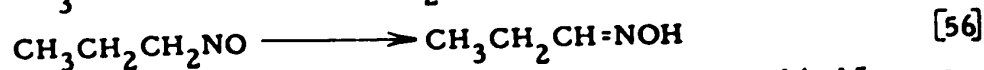
The predominant formation of  $^{14}\text{N}^{15}\text{N}$  in reaction of nitroso-tert-butane with  $^{15}\text{NO}$  is not compatible with the afore-mentioned mechanism which should produce  $\text{N}_2\text{O}$ , but not  $^{14}\text{N}^{15}\text{N}$ . The formation of  $^{14}\text{N}^{15}\text{N}$  requires a step where the nitrogen in nitroso-tert-butane and the nitrogen in nitric oxide form a bond. The following mechanism is consistent with the observed fate of the nitroso compound in the presence of  $^{15}\text{NO}$ .



The formation of  $^{14}\text{N}^{14}\text{N}$  and  $^{15}\text{N}^{15}\text{N}$  in minor amounts is possibly due to the exchange reaction between the nitroso compound and nitric oxide (53).



The production of  $^{14}\text{N}^{15}\text{N}$  and the consumption of  $^{15}\text{NO}$  are larger in the thermolysis of tert-butylazo-3-propene (47) than methylazo-3-propene (36) and 1-propylazo-3'-propene (46). The nitrosomethane and 1-nitrosopropane formed in the thermolysis of 36 and 46 are possibly removed by the isomerization to the corresponding oximes (reactions 55 and 56), which is in competition with reactions 57 and 58, while removal of the nitroso compound by



isomerization of the oxime is not possible for nitroso-tert-butane which predominantly produces  $^{14}\text{N}^{15}\text{N}$  and isobutene by reaction 51.

The kinetic parameters and the rate constants obtained for methylazo-3-propene (36), 1-propylazo-3'-propene (46), 3,3'-azo-1-propene (52) and tert-butylazo-3-propene (47) are listed in Table XLIII. It is interesting to compare the ratios of the non-inhibited rate constant to the inhibited rate constant for 36, 47 and 52. Forst and Rice (11) defined "chain length" as a non-inhibited rate constant divided by an inhibited rate constant. The chain length for 36, 47 and 52 at 122.3° are 1.6, 1.7 and 1.0 respectively. These values correspond to the capability of the methyl, tert-butyl and allyl radicals to propagate chains. The value obtained for 36 and 47 are

Table XLIII. Kinetic parameters for azoalkane thermolysis.

$R_1$	$R_2$	$R_1$ - $R_2$ - $R_3$	Inhibitor	$E_a$ kcal mole <sup>-1</sup>	$\log A$	$\Delta S^\ddagger$ eu at 120°	rate constant at 122.3° (sec <sup>-1</sup> )	rate constant at 120° (sec <sup>-1</sup> )	$k_B / k_{B_2}$	$\log k_B / k_{B_2}$	relative rate
methyl	allyl	26	NO	35.5	14.36	4.6	$4.90 \times 10^{-6}$	$4.07 \times 10^{-6}$	0.138	-0.86	
methyl	allyl	28	none	35.4	14.51	5.3	$7.94 \times 10^{-6}$				
1-propyl	allyl	46	NO	35.6	14.00	6.6	$1.20 \times 10^{-5}$	$1.00 \times 10^{-5}$	0.339	-0.47	
tert-butyl	allyl	47	NO	29.8	12.73	-2.8	$1.74 \times 10^{-4}$	$1.45 \times 10^{-4}$	4.92	+0.69	
tert-butyl	allyl	47	none				$2.78 \times 10^{-4}$				
allyl	allyl	23	NO				$3.55 \times 10^{-5}$				
allyl	allyl	23	none	36.1	15.94	10.0	$3.55 \times 10^{-5}$	$2.95 \times 10^{-5}$	1.00	0	

© B. H. Al-Seder and R. J. Crawford, Can. J. Chem., 49, 2745 (1970).

consistent with the chain propagating processes discussed in the previous section and may be compared with the values of 1.77 - 3.35 and 1.2 obtained by Rice and coworkers in the thermolysis of azomethane and azomethane- $d_6$  (11, 12). The chain length of 1.0 for 52 is consistent with the observation that only a very small amount of propene was produced in the thermolysis of 36 and 52.

The logarithms of the relative rate constants based on 52,  $\log k_n / k_{52}$  are calculated and listed in the final column of Table XLIII to make a choice between Scheme A (concerted cleavage of both carbon-nitrogen bonds) and Scheme B (two step process) according to the criteria proposed in the chapter titled research objectives. Figure 34 shows that for all the unsymmetrical azo compounds studied, 36, 46 and 47,  $\log k_n / k_{52}$  falls in the dotted region where the mechanism is best represented by Scheme B.

The  $k_n / k_{52}$  increases as the group  $R_1$  is bulkier and may be regarded as steric in origin. As indicated in the historical section, steric effects are generally encountered in the thermolysis of azo compounds.

The question may well be asked "What of 52, is the symmetrical compound not proceeding via the same mechanism?" Comparison of 46 and 52 at  $122.3^\circ$  demonstrates that the latter is only 2.96 times faster. Because 52 has twice as many allyl groups we must apply a simple statistical correction and the difference is

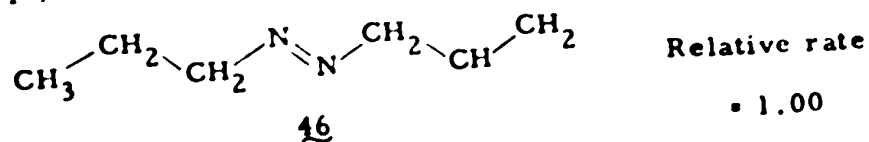
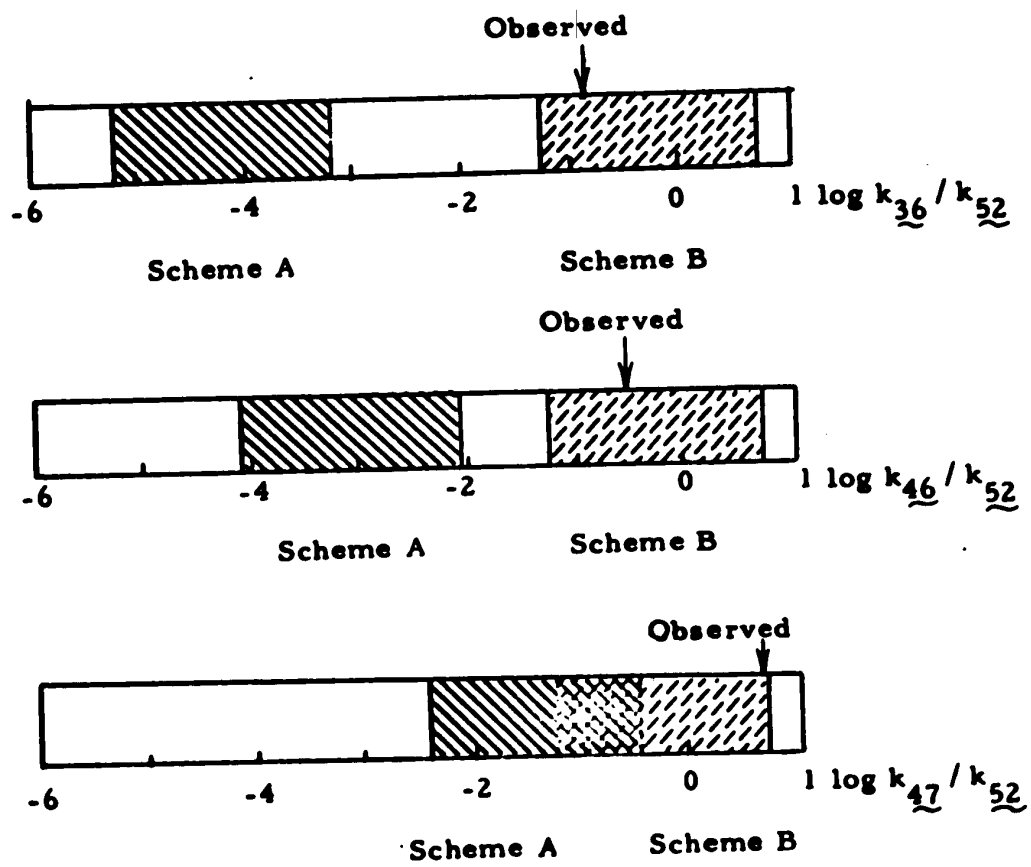
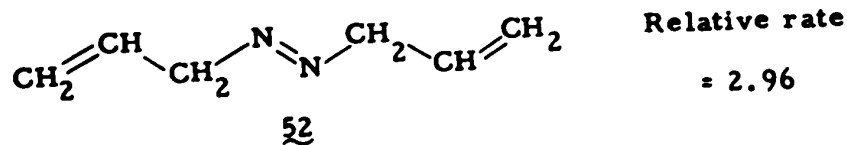


Figure 34. Choice between Scheme A and Scheme B





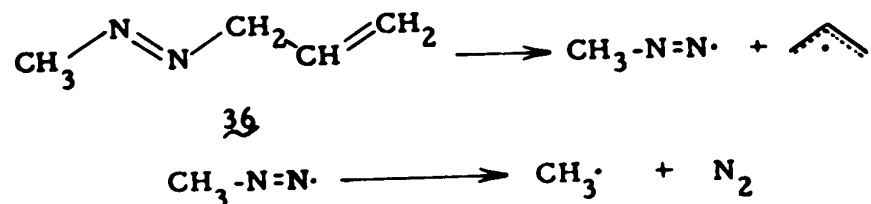
now a factor of 1.48. It is reasonable to assume that the steric factors associated with the n-propyl and allyl groups are similar, but not identical, and in view of the subtlety of rate and steric factors (see Table VIII, p. 20) we may conclude that both compounds are proceeding via the same sequential mechanism. Because of the rather good Polanyi plot observed by Al-Sader (6) it also implies that all gas-phase azo compounds thermolyze via the two-step sequential mechanism.

(E) Allylic Resonance Energy

It is of particular interest to compare the activation energy obtained for 36, 46 and 52 (35.5 - 36.1 kcal mole<sup>-1</sup>) with that of azoethane (48.5 kcal mole<sup>-1</sup>). The decrease in activation energy, 12.4 - 13.0 kcal mole<sup>-1</sup>, may be attributed to a contribution from the allylic resonance energy to the rate-determining transition state. This is comparable to the value generally accepted (~12 kcal mole<sup>-1</sup>). Since the full significance of the allylic resonance energy is manifested, the transition state is thus like the initial cleavage products.

(F) Secondary Deuterium Kinetic Isotope Effects

A further test of Scheme B, as outlined for 36 is readily apparent from the work of Al-Sader and Crawford (6).



They observed that if Scheme A is operative the value of  $\delta\Delta G^\ddagger$  is 60 cal mole<sup>-1</sup>, but if Scheme B is operating then  $\delta\Delta G^\ddagger$  is 120 cal mole<sup>-1</sup>. The latter result is far more acceptable when compared with established values of  $\delta\Delta G^\ddagger$ . It was pointed out that the allyl radical may not be fully formed in the rate determining transition state (6). Examination of methylazo-3-propene-3,3-d<sub>2</sub> (43) would give a more valid assessment of  $\delta\Delta G^\ddagger$  for the allyl-d<sub>2</sub> radical.

The nitric oxide inhibited thermolysis of 36 and methylazo-3-propene-3,3-d<sub>2</sub> (43) was examined at 126.00° using <sup>15</sup>NO. The amount of nitrogen formed was measured volumetrically and then analyzed by mass spectrometry. The fraction of nitrogen coming from 36 and 43 was then calculated and plotted in the usual manner (Table XLIV). Figure 35 shows plots for both the corrected and uncorrected data and the rate constants are listed in Table XLIV.

The unreacted 43 was recovered and analyzed by 100 Mc nmr. Figure 25 (p. 95) shows that the allylic proton signal at  $\delta$ 4.46 is completely absent indicating no scrambling during the thermolysis.

The  $\delta\Delta G^\ddagger$  values obtained, 95 and 98 cal mole<sup>-1</sup>, are comparable to the values generally encountered in the thermolysis of azo compounds where the transition of the fragmentation occurs late

Table XLIV. Inhibited thermolysis with  $^{15}\text{NO}$  of methylazo-3-propene ( $\underline{36}$ ) and methylazo-3-propene- $3,3\text{-d}_2$  ( $\underline{43}$ ) at  $126.00^\circ$ .

Time min	$\text{N}_2^{\text{tot}}$ / $[\underline{36} \text{ or } \underline{43}]^\circ$	$10^6 k_1^{\text{tot}}$ ( $\text{sec}^{-1}$ )	$\text{P}_{29}$ / $\text{P}_{28}$	$\text{P}_{30}$ / $\text{P}_{28}$	$f_{\text{N}_2}^{\underline{36} \text{ or } \underline{43}}$	$10^6 k_1^{\text{corr}}$ ( $\text{sec}^{-1}$ )
			$\text{CH}_3\text{-N=N-CH}_2\text{-CH=CH}_2$ ( $\underline{36}$ )			
			$\frac{[^{15}\text{NO}]^\circ}{[\underline{36}]^\circ} = 0.171$			
30	1.48	8.35	0.0233	0.1292	0.880	7.27
50	2.29	7.72	0.0259	0.0625	0.936	7.21
70	3.38	7.95	0.0378	0.0824	0.913	7.48
90	4.30	8.14	0.0097	0.0497	0.953	7.75
100	5.07	7.89	0.0128	0.0156	0.983	7.73

Continued





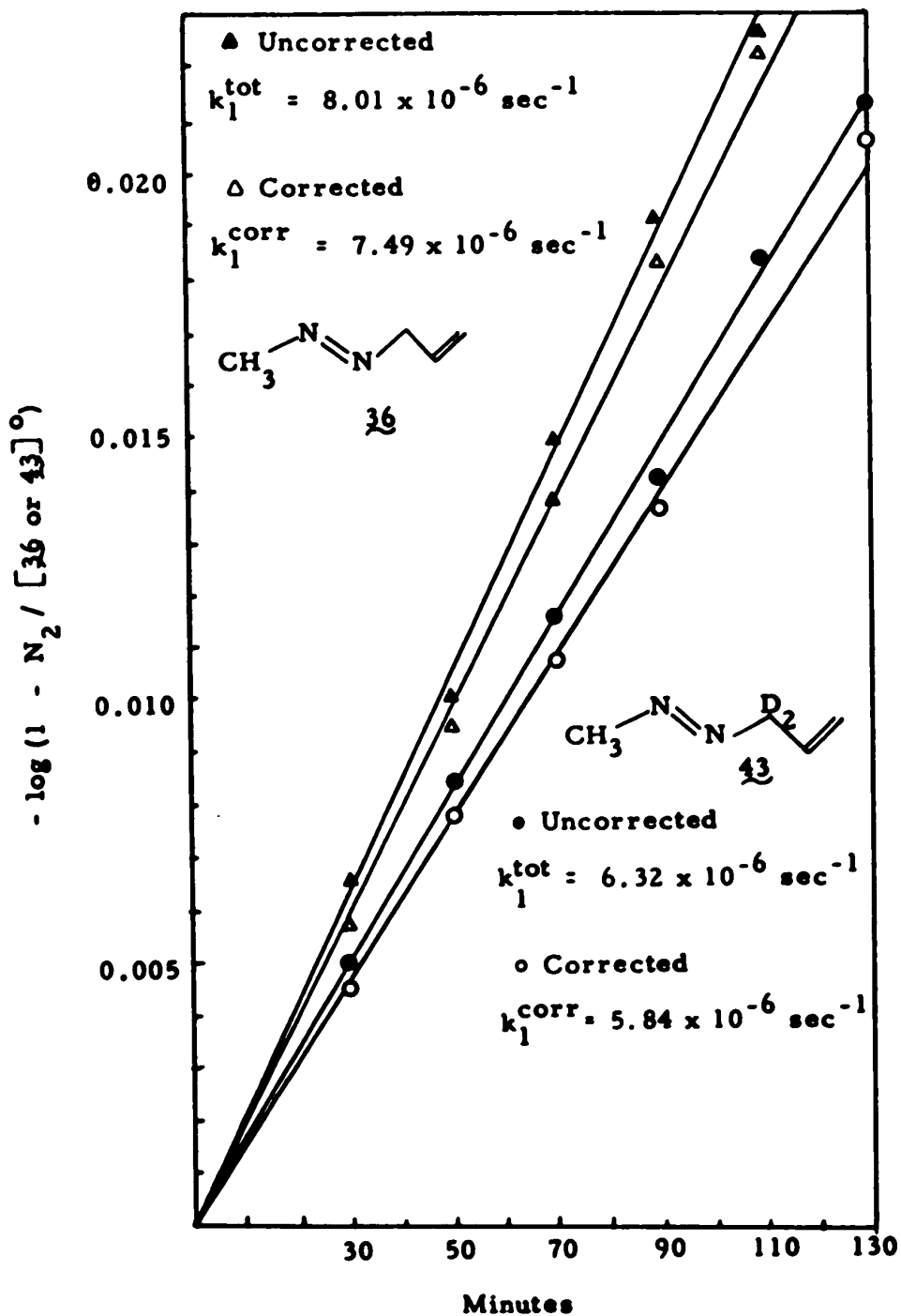


Figure 35. Nitric oxide inhibited thermolysis of **36** and **43**.

Table XLV. Secondary deuterium kinetic isotope effects for  $\alpha$ -deuterated methylazo-3-propene at 126.00°.

Compound	$10^6 k_1^{\text{tot}}$ (sec <sup>-1</sup> )	$10^6 k_1^{\text{corr}}$ (sec <sup>-1</sup> )	rate constant
$\text{CH}_3\text{---N=N---CH}_2\text{---CH=CH}_2$	8.01 ( $\sigma$ , 0.24) <sup>a</sup>	7.49 ( $\sigma$ , 0.25) <sup>a</sup>	4.0
$\text{CH}_3\text{---N=N---CD}_2\text{---CH=CH}_2$	6.32 ( $\sigma$ , 0.14) <sup>a</sup>	5.84 ( $\sigma$ , 0.20) <sup>a</sup>	
	$(k_{\text{H}} / k_{\text{D}})_{\text{uncorr}} = 1.27 \pm 0.05^{\text{b}}$	$(k_{\text{H}} / k_{\text{D}})_{\text{corr}} = 1.28 \pm 0.06^{\text{b}}$	
	$\delta\Delta G^\ddagger = 95 \pm 16 \text{ cal}^{\text{b}}$	$\delta\Delta G^\ddagger = 98 \pm 19 \text{ cal}^{\text{b}}$	

<sup>a</sup> Standard deviation

<sup>b</sup> Probable error

on the reaction coordinate (see Table XI in the historical section). A relatively large  $\delta\Delta G^\ddagger$  value obtained for methylazo-3-propene (36) implies that the transition state is more like the product than the reactant and that Scheme B is applicable to 52 as well as 43.

## CONCLUSIONS

(1) The ratios of the rate constant of the inhibited thermolysis of methylazo-3-propene (36), 1-propylazo-3'-propene (46) and tert-butylazo-3-propene (47) to that of 3,3'-azo-1-propene (52), 0.138, 0.339 and 4.92, are consistent with Scheme B, where only one carbon-nitrogen bond cleaves in the rate determining step.

(2) The decrease in activation energy, 12.4 - 13.0 kcal mole<sup>-1</sup>, on going from azoethane to 36, 46 and 52 is consistent with the cleavage of one carbon-nitrogen bond in the rate determining step, where the full significance of the allylic resonance energy is manifested.

(3) The secondary deuterium kinetic isotope effect for  $\alpha$ -deuterated methylazo-3-propene,  $\delta\Delta G^\ddagger = 97$  cal mole<sup>-1</sup>, is consistent with the one bond cleavage mechanism where the transition of the fragmentation occurs late on the reaction coordinate.

(4) The regular decrease in activation energy with decrease in bond dissociation energy suggests that all gas phase azoalkene thermolyses of symmetrical azo compounds proceed via Scheme B.

## REFERENCES

1. H. Zollinger, "Azo and Diazo Chemistry, Aliphatic and Aromatic Compounds" Interscience Publishers, Ltd., London, 1961, Chapter 12.
2. C. Rüchardt, *Angewandte Chemie, Internat. Edit.*, 9, 830 (1970).
3. S. W. Benson and H. E. O'Neal, "Kinetic Data on Gas-Phase Unimolecular reactions", National Standard Data Reference Series NBS21, U. S. Government Printing Office, Washington, D.C. 1970, p. 31-34.
4. N. A. Porter, M. E. Landis, and L. J. Marnott, *J. Amer. Chem. Soc.*, 93, 795 (1971).
5. Y. Paquin and W. Forst, 54th Meeting of the Chemical Institute of Canada, Halifax, N.S., 1971 Abstract, Phys. IX 3.
6. B. H. Al-Sader and R. J. Crawford, *Can. J. Chem.*, 48, 2745 (1970).
7. J. A. Kerr, *Chem. Rev.*, 66, 465 (1966); see Section IV.
8. H. C. Ramsperger, *J. Amer. Chem. Soc.*, 51, 2134 (1929).
9. (a) L. S. Kassel, "Kinetics of Homogeneous Gas Reactions", Chemical Catalog Co. Inc., New York, 1932.  
(b) O. K. Rice and D. V. Sickman, *J. Chem. Phys.*, 4, 242 (1936).  
(c) H. A. Tayler and F. P. John, *J. Chem. Phys.*, 7, 470 (1939).

10. (a) C. Steel and A. F. Trotman-Dickenson, *J. Chem. Soc.*, **75** (1959).
11. W. Forst and O. K. Rice, *Can. J. Chem.*, **41**, 562 (1963).
12. D. Chong and O. K. Rice, *Internat. J. Chem. Kinetics*, **1**, 171, (1969).
13. W. D. Clark, Ph.D. Dissertation, Univ. of Oregon, Eugene, Oregon, 1959.
14. H. S. Sandhu, *J. Phys. Chem.*, **72**, 1857 (1968).
15. G. Geiseler and J. Hoffmann, *Zeit. Phys. Chem.*, **57**, 318 (1968).
16. H. C. Ramsperger, *J. Amer. Chem. Soc.*, **50**, 914 (1928).
17. J. B. Levy and B. K. W. Copeland, *J. Amer. Chem. Soc.*, **82**, 5314 (1960).
18. G. Williams and A. S. L. Lawrence, *Proc. Roy. Soc.*, **A156**, 455 (1936).
19. S. Seltzer and F. T. Dunne, *J. Amer. Chem. Soc.*, **87**, 2628 (1965).
20. C. G. Overberger and A. V. DiGiulio, *J. Amer. Chem. Soc.*, **81**, 2154 (1959).
21. S. G. Cohen and C. H. Wang, *J. Amer. Chem. Soc.*, **77**, 3628, (1955).
22. G. L. Davies, D. H. Hey and G. H. Williams, *J. Chem. Soc.*, 4397 (1956).
23. S. G. Cohen and C. H. Wang, *J. Amer. Chem. Soc.*, **75**, 5504 (1953).

24. S. G. Cohen and C. H. Wang, *J. Amer. Chem. Soc.*, 77, 2457 (1955).
25. S. W. Benson, "The Foundations of Chemical Kinetics," McGraw-Hill, New York, N.Y. 1960, p. 506-507.
26. Reference 3 page 454.
27. S. Solomon, C. H. Wang and S. G. Cohen, *J. Amer. Chem. Soc.*, 79, 4104 (1957).
28. M. Page, H. O. Pritchard and A. F. Trotman-Dickenson, *J. Chem. Soc.*, 3878 (1953).
29. W. A. Pryor and K. Smith, *J. Amer. Chem. Soc.*, 89, 1741 (1967), 89, 5403 (1970).
30. A. Oberlinner and C. Rüchardt, *Tetrahedron Letters*, 4685, (1967).
31. C. Rüchardt, private communication.
32. C. G. Overberger, M. T. O'Shaughnessy and H. Shalit, *J. Amer. Chem. Soc.*, 71, 2661 (1949).
33. C. G. Overberger and M. B. Berenbaum, *J. Amer. Chem. Soc.*, 73, 2618 (1951).
34. S. G. Cohen, S. J. Groszos and D. B. Sparrow, *J. Amer. Chem. Soc.*, 72, 3947 (1950).
35. C. G. Overberger, W. H. Hale, M. B. Berenbaum and A. B. Finestone, *J. Amer. Chem. Soc.*, 76, 6185 (1954).
36. C. G. Overberger, H. Biltech, A. B. Finestone, J. Litker and J. Herbert, *J. Amer. Chem. Soc.*, 75, 2078 (1953).
37. J. Hinz and C. Rüchardt, *Tetrahedron Letters*, 3095 (1970).



38. S. E. Scheppele and S. Seltzer, *J. Amer. Chem. Soc.*, 90, 358, (1968).
39. B. Strehlke, Ph.D. Thesis, 1971, Univ. of Alberta.
40. D. J. Steven and E. M. Kosower, *J. Amer. Chem. Soc.*, 91, 1710 (1969).
41. P. D. Bartlett and C. Rüchardt, *J. Amer. Chem. Soc.*, 82, 1756 (1960).
42. C. G. Swain, W. H. Stockmayer and J. T. Clark, *J. Amer. Chem. Soc.*, 72, 5426 (1950).
43. D. Swain, "Organic Peroxides", Vol. 1, Wiley Interscience, New York, 1970, Chapter 4.
44. D. B. Denny and D. G. Denny, *J. Amer. Chem. Soc.*, 79, 4806 (1957).
45. C. Overberger and H. Biltech, *J. Amer. Chem. Soc.*, 73, 4880 (1951).
46. (a) D. R. Blackmore and Sir Cyril Hinshellwood, *Proc. Roy. Soc.*, A268, 21 (1962).  
(b) D. R. Blackmore and Sir Cyril Hinshellwood, *Proc. Roy. Soc.*, A271, 34 (1963).  
(c) D. R. Blackmore and Sir Cyril Hinshellwood, *Proc. Roy. Soc.*, A268, 36 (1962).
47. (a) G. R. Freeman, C. J. Danby and Sir Cyril Hinshellwood, *Proc. Roy. Soc.*, A245, 28 (1958).  
(b) C. J. Danby and G. R. Freeman, *Proc. Roy. Soc.*, A245, 40, 68 (1958).  
(c) G. R. Freeman, *Proc. Roy. Soc.*, A245, 49, 75 (1958).

48. (a) F. W. Birss, C. J. Danby and Sir Cyril Hinshellwood, Proc. Roy. Soc., A239, 154 (1957).  
(b) G. Archer and Sir Cyril Hinshellwood, Proc. Roy. Soc., A239, 154 (1957).
49. J. R. E. Smith and C. N. Hinshellwood, Proc. Roy. Soc., A18,
50. J. R. E. Smith and C. N. Hinshellwood, Proc. Roy. Soc., A183, 33 (1944).
51. F. J. Stubbs and Sir Cyril Hinshellwood, Proc. Roy. Soc., A200, 458 (1950).
52. J. Jach, F. J. Stubbs and Sir Cyril Hinshellwood, Proc. Roy. Soc., A224, 283 (1954).
53. B. G. Gowenlock, Progr. Reaction Kinetics 3, 17 (1965).
54. A. F. Trotman-Dickenson, "Gas Kinetics", Butterworth, London, 1955, Chapter 3.
55. J. G. Calvert, S. S. Thomas, P. L. Hanst, J. Amer. Chem. Soc., 82 1 (1960).
56. B. G. Gowenlock and J. Kay, J. Chem. Soc., 2880 (1962).  
B. G. Gowenlock and J. Kay, Z. Elektrochem., 65, 713 (1961).
57. M. I. Christie, Proc. Roy. Soc., A249, 258 (1959).
58. H. T. J. Chilton and B. G. Gowenlock, J. Chem. Soc., 3232 (1953).
59. B. G. Gowenlock and J. Trotman, J. Chem. Soc., 4190 (1955).
60. L. Batt and B. G. Gowenlock, Trans. Faraday Soc., 56, 682 (1960).

61. G. L. Prott and J. H. Purnell, *Trans. Faraday Soc.*, 60, 371 (1964).
62. E. Bamberger, *Ber.*, 51, 634 (1918).
63. J. F. Brown, Jr., *J. Amer. Chem. Soc.*, 79, 2480 (1957).
64. M. I. Christie, *Proc. Roy. Soc. (London)*, A249, 248 (1958).
65. B. G. Gowenlock and M. J. Healey, *J. Chem. Soc.*, (B), 1014 (1968).
66. B. A. Gingras and W. A. Waters, *J. Chem. Soc.*, 1920 (1954).
67. B. Bromberger and L. Phillips, *J. Chem. Soc.*, 5302 (1961).
68. D. E. Hoare, *Can. J. Chem.*, 40, 2012 (1962).
69. A. Maschke, B. S. Shapiro and F. W. Lampe, *J. Amer. Chem. Soc.*, 85, 1876 (1963).
70. S. Seltzer, *J. Amer. Chem. Soc.*, 83, 2625 (1961); 85, 14 (1963).
71. E. A. Halevi in "Progress in Physical Organic Chemistry", Vol. 1, Interscience Publishers Inc., New York, N.Y., 1963.
72. A. A. Zavitas and S. Seltzer, *J. Amer. Chem. Soc.*, 86, 1265 (1964).
73. R. J. Crawford and D. M. Cameron, *Can. J. Chem.*, 45, 691 (1967).
74. R. J. Crawford and L. H. Ali, *J. Amer. Chem. Soc.*, 89, 3908 (1967).
75. B. H. Al-Sader and R. J. Crawford, *Can. J. Chem.*, 46, 3301 (1968).
76. T. Koenig and R. Cruthoff, *J. Amer. Chem. Soc.*, 91, 2562 (1969).

77. T. Koenig and R. Wolf, *J. Amer. Chem. Soc.*, 91, 2574 (1969).
78. T. Koenig, J. Huntington and R. Cruthoff, *J. Amer. Chem. Soc.*, 92, 5413 (1970).
79. K. Humski, R. Malojčić, S. Borčić and D. E. Sunko, *J. Amer. Chem. Soc.*, 92, 6534 (1970).
80. K. M. McMichael, *J. Amer. Chem. Soc.*, 89, 2943 (1967).
81. S. Seltzer, *J. Amer. Chem. Soc.*, 87, 1534 (1965).
82. K. W. Egger, D. M. Golden and S. W. Benson, *J. Amer. Chem. Soc.*, 86, 5420 (1964).
83. P. Nangia and S. W. Benson, *J. Amer. Chem. Soc.*, 86, 2773 (1964).
84. S. W. Benson, A. N. Bose and P. Nangia, *J. Amer. Chem. Soc.*, 85, 1388 (1963).
85. G. S. Hammond and C. H. DeBoer, *J. Amer. Chem. Soc.*, 86, 899 (1964).
86. H. R. Gerberich and W. D. Walters, *J. Amer. Chem. Soc.*, 83, 4884 (1961).
87. R. J. Ellis and H. M. Frey, *J. Chem. Soc.*, 959 (1964).
88. M. C. Flowers and H. M. Frey, *J. Chem. Soc.*, 3953 (1959).
89. E. Vogel and R. Sunderman, Ph.D. Dissertation, Koln (1966).
90. D. W. Setser and B. S. Rabinovitch, *J. Amer. Chem. Soc.*, 86, 564 (1964).
91. M. R. Willcott and V. Cargle, Unpublished results quoted in "thermal - unimolecular rearrangements" compiled by M. R. Willcott and R. L. Cargill.

92. R. J. Ellis and H. M. Frey, *J. Chem. Soc.*, 5578 (1964).
93. M. C. Flowers and H. M. Frey, *Proc. Roy. Soc.*, (London) A257, 121 (1960).
94. J. A. Berson and E. J. Walsh, Jr., *J. Amer. Chem. Soc.*, 90, 4730 (1968).
95. C. H. Mortimer, "Reaction Heats and Bond Strengths," Pergamon Press, New York, N.Y., 1962, p. 129.
96. R. J. Crawford and A. Mishra, *J. Amer. Chem. Soc.*, 88, 3963 (1966).
97. M. Szwarc and A. H. Schon, *J. Chem. Phys.*, 18, 237 (1950).
98. J. A. Kerr, R. Spencer and A. F. Trotman-Dickenson, *J. Chem. Soc.*, 6652 (1965).
99. J. B. Homer and F. P. Lossing, *Can. J. Chem.*, 44, 2211 (1966).
100. D. J. Ruzicka and W. A. Bryce, *Can. J. Chem.*, 38, 827 (1960).
101. W. K. Besfield and K. J. Ivin, *Trans. Faraday Soc.*, 57, 1044 (1961).
102. D. M. Golden, N. A. Gac and S. W. Benson, *J. Amer. Chem. Soc.*, 91, 2136 (1969).
103. D. M. Golden, A. S. Rodgers and S. W. Benson, *J. Amer. Chem. Soc.*, 88, 3196 (1966).
104. R. J. Akers and J. J. Throssell, *Trans. Faraday Soc.*, 63, 124 (1967).
105. M. Szwarc, B. N. Ghosh and A. H. Schon, *J. Chem. Phys.*, 18, 1142 (1950).

106. C. Vogelenang, *Rec. trav. Chim.*, 65, 789 (1946).
107. C. G. Bergstrom and S. Siegel, *J. Am. Chem. Soc.*, 74, 254 (1952).
108. R. D. Schultz and F. W. Millard, *J. Org. Chem.*, 24, 297 (1959).
109. J. Curtius and F. Rauterberg, *J. Prak. Chem.*, [2]44, 194 (1891).
110. L. I. Smith, K. L. Howard, "Organic Syntheses", Coll. Vol. 3, 351.
111. P. A. S. Smith, J. M. Clegg and J. Lakritz, *J. Org. Chem.*, 23, 1595 (1958).
112. W. D. Emmons, *J. Am. Chem. Soc.*, 79, 6522 (1957).
113. T. E. Stevens, *J. Org. Chem.*, 26, 2531 (1961).
114. R. C. Weast, "Handbook of Chemistry and Physics", 49th Edition, The Chemical Rubber Co., Cleveland, Ohio, 1968, p. B-4.
115. A. Cornu and R. Massot, "Compilation of Mass Spectral Data", Heyden & Son Limited, London (1966).
116. A. Mishra, Ph.D. Thesis, University of Alberta, 1965.
117. (a) A. Loewenstein and T. M. Connor, *Ber. Bunsen Gesellschaft Phys. Chem.*, 67, 280 (1963).  
(b) H. E. A. Kramer and R. Gompper, *Z. phys. Chem. (Frankfurt)*, 43, 292 (1964).  
(c) J. C. Breliere and J. M. Lehn, *Chem. Comm.*, 426 (1965).
118. (a) C. D. Hund and S. C. Lui, *J. Amer. Chem. Soc.*, 57, 2656 (1935).  
(b) I. Tabushi, K. Takagi, M. Okano and R. Oda, *Tetrahedron*, 23, 2621 (1967).

119. J. W. Kraus and J. G. Calvert, *J. Amer. Chem. Soc.*, 79, 5921 (1957).
120. A. F. Trotman-Dickenson, "Gas Kinetics", Academic Press, New York, N. Y., 1955, p. 236.
121. N. V. Sidgwick, "The Organic Chemistry of Nitrogen," The Clarenton Press, Oxford, 1949, p. 213.

## VITA

Kunihiko Takagi was born in Nagoya, Japan, on March 20, 1941 and attended school up to the ninth grade in Hajima City, Gifu Prefecture. He then attended the Asahigaoka High School in Nagoya. In 1959 he entered the Faculty of Technology at Kyoto University and graduated in 1963. He received his M. Tech. degree in 1965 from the Department of Industrial Chemistry after working with Prof. R. Oda and I. Tabushi on vinyl diazomethane cycloadditions.

For three years after his M. Tech. he worked with Nippon Rayon Co. Ltd. in Osaka (now Unitika Co. Ltd.) and then entered the Faculty of Graduate Studies at the University of Alberta in August 1968. In 1968-69 he was a graduate teaching assistant, and was a research assistant in 1969-70. He held a University of Alberta Graduate Research Assistantship during the year 1970-71.